SYNTHESIS AND INVESTIGATION OF TRANSITION METAL COMPLEXES WITH SMALL PENDANT ARM MACROCYCLES

Norman Munro Macdonald (B.Sc.)

A thesis submitted to the University of Glasgow for the degree of Doctor of Philosophy

Department of Chemistry

University of Glasgow

June 1994

ProQuest LLC.
789 East Eisenhower Parkway
P.O. Box 1346
Ann Arbor, MI 48106 – 1346

To Mum & Dad

ACKNOWLEDGEMENTS

I owe a great deal to my supervisor Dr. Robert D. Peacock whose knowledge and encouragement was invaluable. Many thanks to Dr. Louis Farrugia for his crystallographical skills and Mr Jim M^{c}Iver for technical assistance.

Thanks to Dr. Andrew Glidle for electrochemistry; Dr. L. Yellowlees (Edinburgh) - EPR and Prof. K. Wieghardt & Dr. P. Chaudhuri (Bochum) - Magnetochemistry.

I thank SERC for financial assistance.

Cheers to Paul Lovatt for slaving over a "hot" word processor.

To my family for all their support during my academic career.

Last, but by no means least, to all my friends and colleagues who have helped to make the past three years so enjoyable.

ABBREVIATIONS.

Abs	absorbance
B.pt.	boiling point
CD	circular dichroism
CPL	circularly polarised light
d	doublet
DIEN	diethylene triamine
DMF	dimethyl formamide
DMSO	dimethyl sulphoxide
en	ethylene diamine
EPR	electron paramagnetic resonance
HEEN	2-(2-aminoethylamino)ethanol
IR	infra-red
LFSE	ligand field stabilisation energy
m	multiplet
MeCN	acetonitrile
M.pt.	melting point
NHE	normal hydrogen electrode
NMR	nuclear magnetic resonance
ODEN	bis (2-aminoethyl)ether
PEM	photo-elastic modulator

PPL	plane polarised light
ppm	parts per million
q	quartet
tosyl (Ts)	p-tolyl sulphonyl
TP	trigonal prismatic
UV	ultra-violet
vis	visible
μ_B	Bohr magneton

LIGANDS

9-aneN_3, TACN	1,4,7-triazacyclononane
9-aneN_2O	1-oxa-4,7-diazacyclononane
TAETACN	N,N',N''-tris(2-aminoethyl)-1,4,7-triazacyclononane
TCTA	N,N',N''-tris(-carboxymethyl)-1,4,7-triazacyclononane
THETACN, L^3H_3	N,N',N''-tris(2-hydroxyethyl)-1,4,7-triazacyclononane
TPTACN	N,N',N''-tris(2-pyridylmethyl)-1,4,7-triazacyclononane
L^1H_3	(R) and (S) N,N',N''-tris(2-hydroxypropyl)-1,4,7-triazacyclononane
L^2H_3	N,N',N''-tris(2R-hydroxy-3-methylbutyl)-1,4,7-triazacyclononane
L^4H_2	N,N'-di(2R-hydroxy-3-methylbutyl)-1-oxa-4,7-diazacyclononane
L^5H_3	N,N',N''-tris(2R-hydroxypropyl)-1,4,7-triazacyclodecane

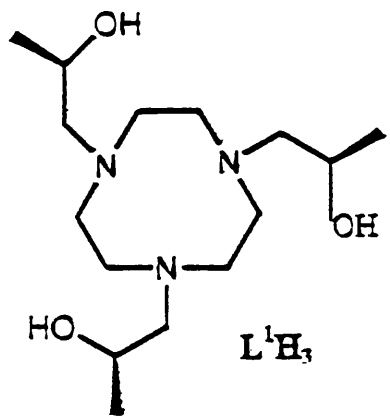

L^1H_3

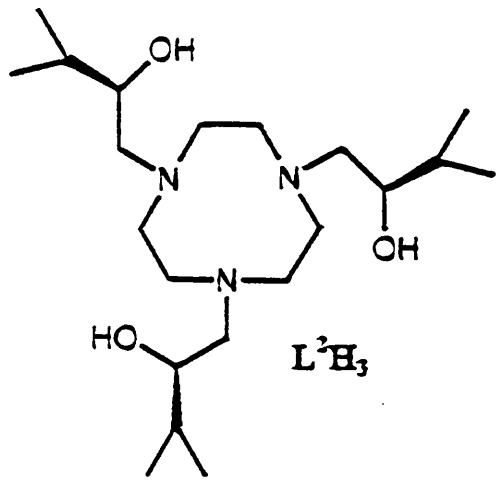

L^2H_3

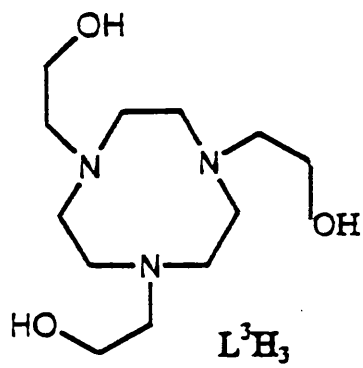

L^3H_3

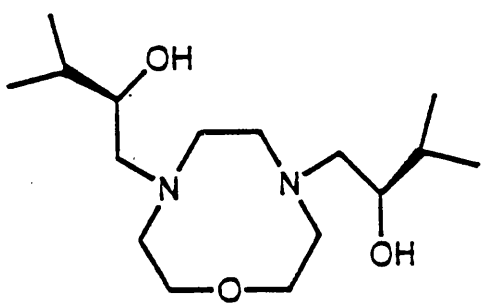

L^4H_2

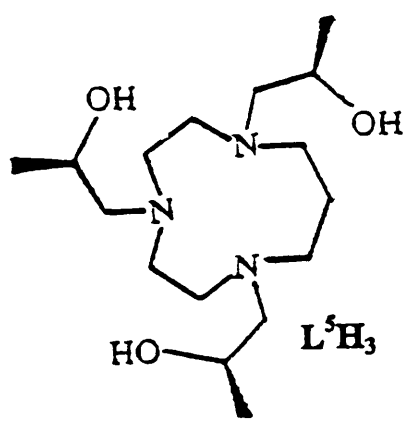

L^5H_3

SUMMARY

This work is centred upon the first row transition metal complexes formed with pendant arm macrocycles.

The pendant arms in question are alkyl chains containing hydroxyl functions, they are substituted at the 2 position with either methyl or isopropyl groups there by creating a chiral centre on each arm. The ligand L^1H_3 has three tertiary nitrogen and three alcohol functions, it is thus potentially hexadentate (N_3O_3). The chromophores of the resulting complexes exhibit varying degrees of trigonal distortion and are highly suitable for investigation using absorption and circular dichroism spectroscopy.

The donor properties of the pendant hydroxyl groups are pH dependant. At low pH values they remain protonated acting as alcohol ligators; increasing the pH leads to deprotonation forming alkoxide donors.

L^1H_3 is able to stabilise many different oxidation states. It forms extremely stable complexes with V(IV), Cr(III) and Mn(IV).

In the presence of low (divalent) oxidation levels the pendant groups, in neutral solution, remain protonated and monomeric complexes of the form $[ML^1H_3]^{2+}$ predominate. With higher oxidation states, e.g. Mn(IV) the superior Lewis acid properties of the metal leads to an increase in the acidity of the hydroxyl protons. Even in neutral conditions, deprotonation occurs yielding a tris alkoxide species $[ML^1]^+$.

This unit forms strong hydrogen bonds with protonated species, e.g. $[ML^1H_3]^{2+}$ resulting in dimer formation: $[ML^1H_3L^1M]^{3+}$ where the metal ions are in +2/+4 or +3/+3 oxidation states.

Dimer formation is prevented by increasing the steric bulk about the O,O',O'' face. This is achieved by replacing the pendant arm methyl substituents as on L^1H_3 for isopropyl groups i.e. L^2H_3. A monomeric complex $[Mn(IV)L^2]^+$ is formed under aerobic conditions.

Modified "parent" macrocycles are discussed where one nitrogen donor is replaced by a neutral oxygen group -O-, creating an N_2O ring system. Placing pendant alcohol groups on the remaining nitrogen donors creates a potentially pentadentate N_2O_3 ligand L^4H_2. Spectroscopic studies on complexes with this ligand are presented.

CONTENTS

CHAPTER 1

INTRODUCTION

INTRODUCTION

1.1 Macrocycles: an historical account.

Prior to 1960 the most important examples of synthetic macrocyclic compounds comprised entirely of phthalocyanine and its derivatives. Discovered accidentally in 1928 by ICI, phthalocyanines were of great importance to the colourings industry where they were used primarily as dyestuffs and pigments

The basic definition of a macrocycle is a ring compound, comprising nine or more atoms, of which, at least three are donor groups i.e. Lewis bases (NH, O, S etc.).

Naturally occurring complexes incorporating macrocyclic ligands have been known for many years; examples include porphyrins and corrins which, in the form of heme and chlorophyll, play an essential part in the biological processes of oxygen transport in mammals and photosynthesis in plants respectively. During the past three decades there has been an explosion in the synthesis and investigation of macrocycles and their complexes. Tetra-aza macrocycles of various ring sizes and degrees of unsaturation, were among the first nitrogen based ligands synthesised using a template type process pioneered by Curtis (**1**).

Research into cyclic ligands broadened in the late 1960's with the discovery by Pedersen of crown ethers (**2**) and the subsequent work carried out by Lehn and co-workers into cryptands (**3**). These ligands, as a result of their oxygen donor functions, prefer to complex alkali and alkaline earth metals, as opposed to the transition metals favoured by aza-macrocycles, in effect opening up a whole new area of macrocyclic chemistry. Particular emphasis has been paid to modelling the biological role of ions such as lithium, sodium and potassium.

Without doubt, the increased understanding of bioinorganic chemistry has fuelled the growing interest in macrocyclic chemistry and vice-versa; design and preparation of model systems gives a clearer insight into the biological processes being investigated, which invariably leads to an improved awareness of the coordination chemistry of many different combinations of metals and donor atoms.

In more recent years, with the advent of supramolecular chemistry, concepts such as molecular recognition and signalling have opened up a particularly exciting dimension to macrocyclic chemistry (**4**); that of nano-engineering, the prospect of assembling and operating "intelligent" systems on a purely molecular level.

1.2 Synthesis of Triazamacrocycles.

The first report of 1,4,7-triazacyclononane (TACN) came as early as 1937 by Peacock and Gwan (**5**); they proposed the ditosylate of TACN as a by-product from the reaction (scheme 1.1) between N,N'-di(p-tolylsulphonyl)-N,N'-bis(β-chloroethyl)ethylene diamine and alcoholic ammonia.

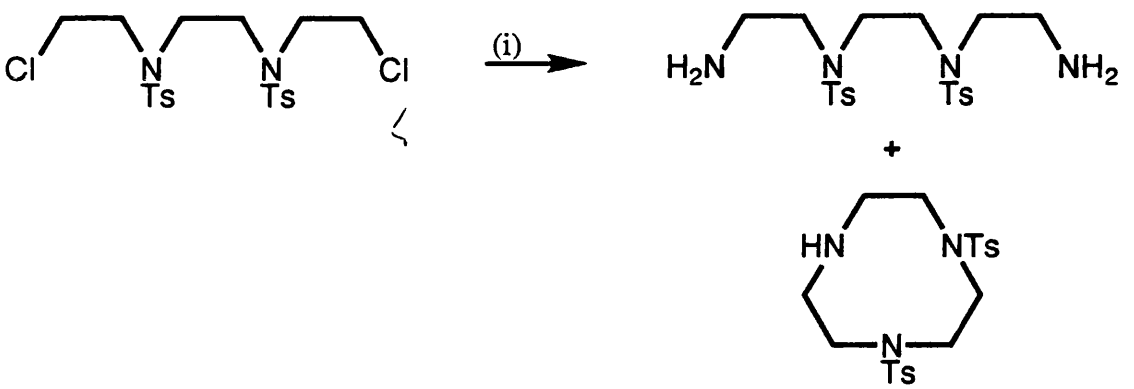

Scheme 1.1. *Proposed route to 1,4-ditosyl-TACN. (i) NH_3/EtOH*

By 1972 the first synthesis of 1,4,7-triazacyclononane was published by Koyama and Yoshino (**6**). They presented a high dilution route to triazamacrocycles, via the cyclisation of tritosyl triamines and dibromosubstituted alkanes in dimethyl formamide (scheme 1.2).

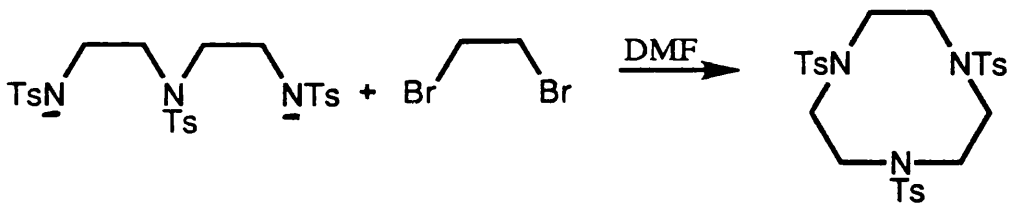

Scheme 1.2. *High dilution synthesis of 1,4,7-tritosyl-TACN.*

Some two years later Richman and Atkins (7) modified, low dilution, method presented a simple and general route to the preparation of TACN (scheme 1.3). Their strategy utilised sulphonate ester leaving groups as opposed to the previous halide moieties.

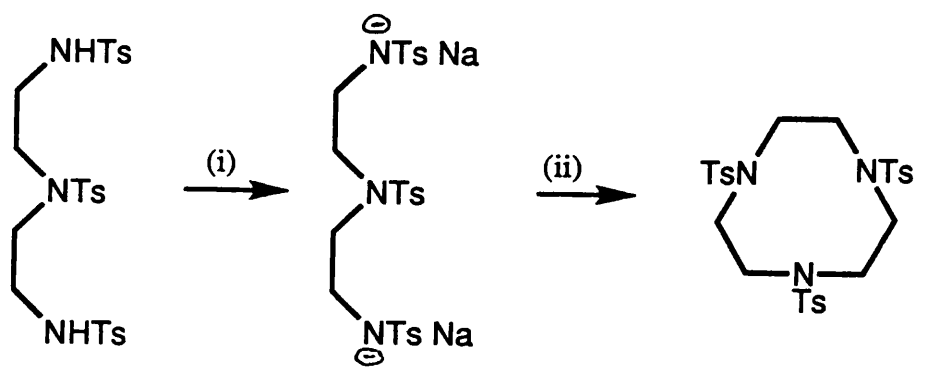

Scheme 1.3. *Richman-Atkins sequence.*
(i) NaH, DMF (ii) $TsO(CH_2)_2OTs$, 110°C.

The hydrolysis of these tosylated cyclic triamines may be achieved using one of two main routes.

(1) A reductive cleavage mechanism on refluxing the amine in a mixture of hydrobromic acid and glacial acetic acid to yield the trihydrobromide amine salt. This can be converted to the corresponding trihydrochloride by recrystallisation from concentrated hydrochloric acid.

(2) Alternatively concentrated sulphuric acid may be used, to yield, after refluxing for two days, the hygroscopic polysulphate salt which, again, may be easily converted to the trihydrochloride salt.

1.3 Chemistry of Triazacyclononane.

On comparing the protonation constants of TACN with those of its linear counterpart DIEN, $H_2N(CH_2)_2NH(CH_2)_2NH_2$, it has been observed that the successive constants measured are quite dissimilar. As indicated by the first protonation constant of approximately 10.6 for TACN (**8**) and 9.7 for DIEN (**9**), TACN is more basic than its non-cyclic congener. This effect is due to the lone pairs of the three amine functions "pointing-in" towards the cavity, effectively creating an electron rich hole which increases the rate of uptake of the first proton. The three donors are thought to bind the proton in a cooperative manner, as observed in the crystal structure of Me_3TACN (**10**) (fig 1.1) in which all the donor atoms coordinate the hydrogen atom. The second and third constants, however, are lower for the cyclic species, believed to be a

consequence of the increased repulsion towards an incoming proton by the one or two ammonium functions present.

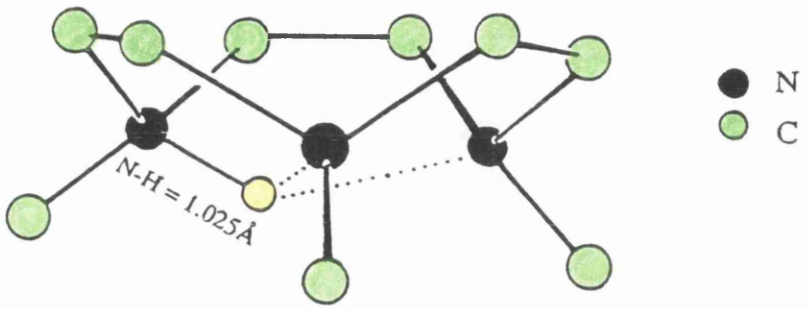

Fig 1.1. *Crystal Structure of [$Me_3$9-aneN_3H][ClO_4].*

1.4 Transition metal complexes with Triazacyclononane.

It is now well established that 1,4,7-triazacyclononane is an excellent metal chelator. In common with other macrocycles, the transition metal complexes formed with TACN exhibit enhanced stabilities over their linear analogues; this increase has been attributed to the "macrocyclic effect". This expression was first coined by Cabbiness and Margerum (**11**), following their investigation of various tetra-aza Cu(II) systems which they discovered to be around 10,000 times more stable than analogous complexes with linear polyamines.

Much debate has since taken place as to the origins of this effect, whether it is entropy or enthalpy dominated or a combination of the two (**12**).

The entropic term arises from the simple fact that on complexation there are more species or individual elements on the right hand side of the equation (fig 1.2), giving an overall positive entropy value for the chemical reaction.

$$[M(NH_3)_6]^{2+} + 2L = ML_2 + 6NH_{3(aq)}$$

Fig 1.2. *General complexation reaction. L = macrocyclic ligand.*

In addition, because the macrocycle is preformed into a particular configuration, the loss of entropy on complexation is less than that experienced for a non-cyclic system (**13**). This rearrangement of a given linear system also helps, in part, to explain the enthalpic contribution to the overall decrease in Gibbs Free Energy, $\Delta G°$, for a complexation process (vide supra). The cyclic ligand expends less energy and experiences less steric resistance during complexation than its linear congener; the donor atoms of a macrocycle are already in roughly the desired position for the coordination.

Further hypotheses have been forwarded for the enthalpy contribution: Hinz and Margerum (**14**) suggested that the greater steric hindrance to solvation of

the macrocyclic nitrogen donors led to a reduction in the hydration of the ligand in aqueous solution; in essence there are less hydrogen bonds to be broken to achieve complex formation.

Busch *et al.* with their theory of "multiple juxta-positional fixedness" (**15**) suggested that the ordered and stable position of nitrogen donors in the macrocycle results in improved metal to nitrogen overlap; this effect being found to increase with decreasing ring size.

The presence of secondary amine donors in the ring, which are superior Bronsted bases to their primary counterparts, occurs without the concomitant increase in steric crowding observed for non-cyclic polyamines - another important factor in the strong metal nitrogen bonding interaction - hence the improved stability of the macrocyclic complex.

The initial work on transition metal complexes with TACN was performed by Koyama and Yoshino (**6**); they investigated the spectroscopic properties of Co(III) complexes with various macrocyclic ligands including TACN. They assigned the TACN complex as a sandwich type structure (vide infra). The cavity of TACN is too small to allow meridional binding, it therefore coordinates facially to the metal centre. In addition, they surmised, from various modelling experiments that the geometry of TACN in this coordination mode was almost strain free, with respect to bond lengths and angles. With this facial mode of binding there exists two possible structures comprising either MONO or BIS coordination of the macrocycle (fig 1.3).

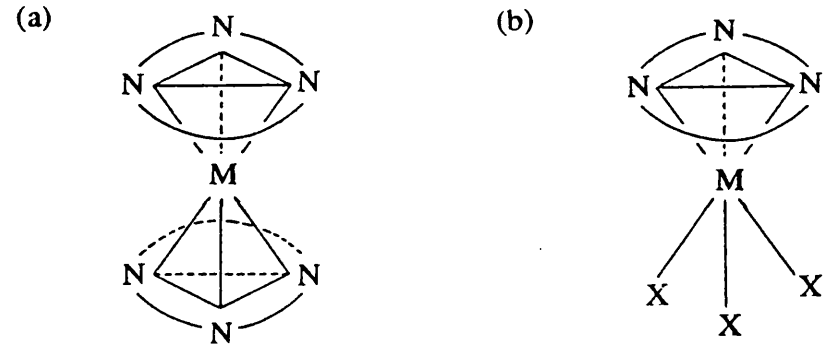

Fig 1.3. **(a)** *Bis complex of small triazamacrocycles.*
(b) *Mono coordination found for larger triazamacrocycles.*

From their investigations into the spectroscopic properties of the various complexes, Koyama and Yoshino were able to suggest the following spectrochemical series:-

$$[Co(NH_3)_6]^{3+} < [Co(10aneN_3)_2]^{3+} < [Co(en)_3]^{3+} < [Co(9aneN_3)_2]^{3+}$$

The series is arranged in order of increasing ligand field strength from left to right. Smaller rings result in higher 10Dq values and therefore, can stabilise higher oxidation states (smaller ions). Larger ring sizes give weaker ligand fields with a resultant lengthening of metal-ligand bonds.

Although the macrocyclic effect results in these compounds being more stable than analogous linear complexes, the stability of macrocyclic compounds varies, depending upon the ring size and the type of metal ion. In

general the size-match concept states that when the fit is good, the resulting formation constant will be high giving an extremely stable complex. When the metal ionic radius closely matches the ligand cavity then a good metal-nitrogen overlap results giving a high ligand field strength. This is demonstrated in the case of TACN which, in the form of TCTA is able to stabilise "unusual" oxidation states such as Ni(III) (**16**).

1.5 Pendant arm ligands.

One extremely useful feature of the secondary amine functions of 1,4,7-triazacyclononane is the relative ease of substitution of the proton with many alkyl functional groups. These appended moieties, known as pendant arms, modify the coordination properties and abilities of the ligand depending, of course, upon the nature of the pendant functionality. In essence they enable the macrocycle to incorporate additional ligating groups. A quite diverse array of pendant groups has been reported with triaza macrocycles ranging from alkyl donors through to phosphines, thiols and alcohols (Table 1.1).

Pendant Group	Reference
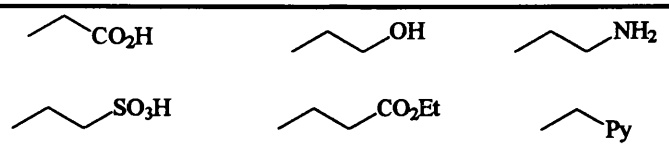	10
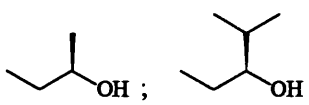	this work, 17
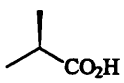	18
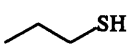	19
	20
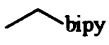	21
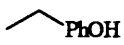	22
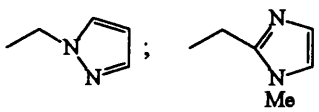	23
* Ph = C_6H_4	

Table 1.1. *Pendant arm types*

Various methods, outlined overleaf (scheme 1.4), have been employed to introduce these additional groups; they include nucleophilic attack at carbonyl groups, displacement of suitable leaving groups or ring opening reactions involving epoxides or aziridines.

(a) Nucleophilic attack at carbonyl carbon with reduction of resulting imine.

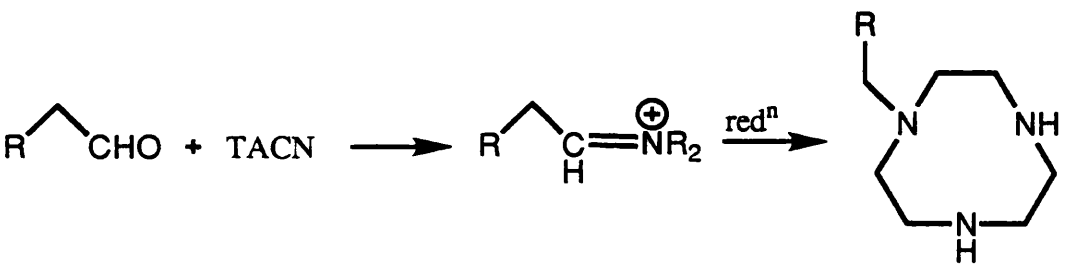

(b) Attack at secondary carbon with displacement of halide.

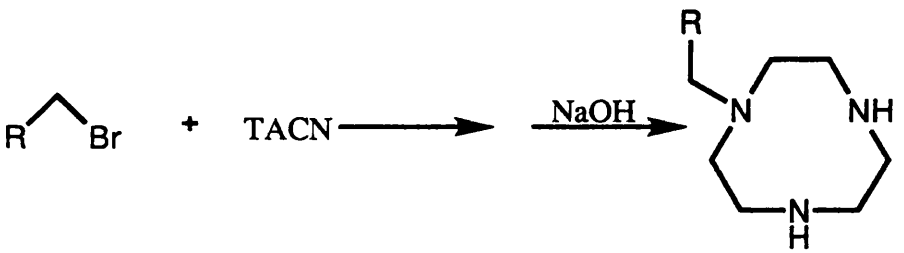

(c) Mannich type reaction.

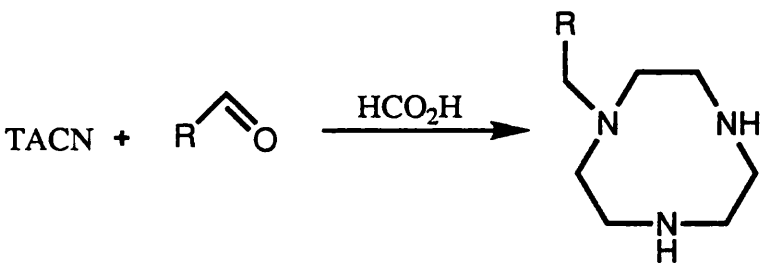

(d) Ring opening reaction.

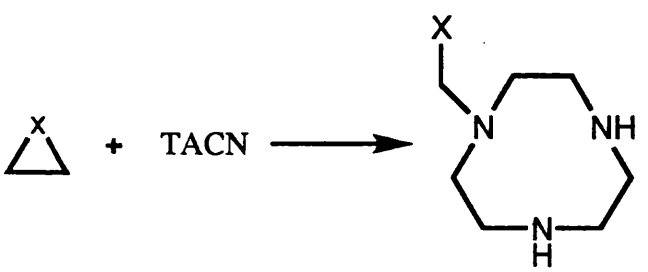

Scheme 1.4. *Methods of Pendant arm introduction.*

1.6 Geometry of Transition Metal Complexes: Octahedral vs. Trigonal Prismatic.

Octahedral symmetry for six coordinate metal complexes is extremely common and well known, less common are examples of trigonal prismatic and the rare bicapped tetrahedral geometries.

By regarding an octahedron as a trigonal antiprism it follows that a simple rotation of two opposite trigonal faces by 60° relative to each other, results in a lowering of the symmetry to D_{3h} i.e. trigonal prismatic coordination (fig 1.4).

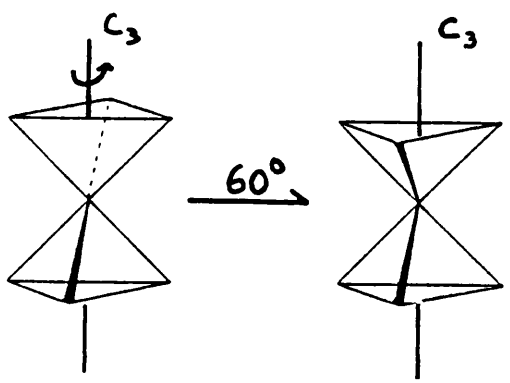

Fig 1.4. *Interconversion between octahedral and trigonal prismatic.*

The first trigonal prismatic stereochemistry was reported in 1923 (**24**) for the ionic lattice type structure of the metal sulphide MoS_2 and subsequently WS_2.

Bailar in 1958 (**25**) proposed that the isomerisation and racemisation of certain tris chelate octahedral complexes proceeded via a trigonal twist through a trigonal prismatic intermediate (fig 1.5).

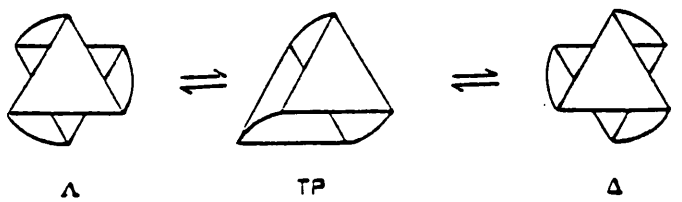

Fig 1.5. *Racemisation of O_h complexes.*

In 1965 the first trigonal prismatic tris chelate species, namely a rhenium dithiolato complex, was structurally characterised (**26**). Many more similar compounds involving both dithiolato and diselenato ligands have subsequently been characterised including $Mo(S_2C_2H_2)_3$ (**27**) and $V(S_2C_2Ph_2)_3$ (**28**).

A particular geometry results from the competing forces of inter-ligand repulsion and metal-ligand interactions; in other words acquiring the maximum metal-ligand and intra-ligand bonding interactions whilst ensuring any ligand-ligand repulsions are minimised.

It has been shown that with trigonal prismatic geometry (**29**) metal ligand bonding is increased, in comparison with simple octahedral compounds. Inter-ligand repulsion however, also increases - this has a significant destabilising effect, cancelling out the increased stability imparted by stronger metal-ligand bonding. When six unidentate ligators are present

octahedral geometry is favoured, this argument does not make any account for π-bonding interactions. In the case of higher denticity ligands the overall geometry will be determined by the stereochemical preferences of the metal versus the conformational requirements of the ligand.

The distortion of a six coordinate complex about the three fold symmetry axis is defined by the twist angle ϕ (fig 1.6).

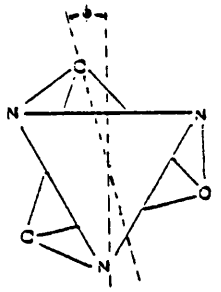

Fig 1.6. *Twist angle:* $\phi=0°$ (O_h) *and* $\phi=60°$ (T.P).

Many research groups have investigated the relationship of d-orbital energy with varying twist angle. Three main methods have been employed (a) extended Hückel calculations (**30**), (b) ionic models (**31**) and (c) angular overlap model (**32**).

Hoffmann *et al.* (**30**), showed the effect on d-orbital energies when twisting from octahedral to trigonal prismatic (fig1.7). The t_{2g} and e_g (O_h) levels transform into a_1' + e_1' and e'' (T.P) respectively. The reduction in orbital splitting results in a decrease of the LFSE value in the trigonal prismatic case compared with octahedral. This method, it must be stated, does not take into account metal-ligand orbital mixing.

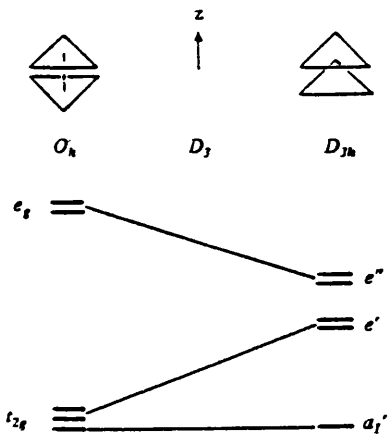

Fig 1.7. *Energy level order in O_h and T.P. ligand fields.*

The work of Gillum *et al.* (**31**), quantified the energy changes of the d-orbitals when transforming from O_h to T.P geometry. They calculated the changes in ligand field potentials between octahedral and trigonal prismatic symmetry, in the case of the T.P geometry the orbital energies are

$$E(e'') \equiv E(d_{xz,yz}) = \tfrac{5}{3}Dq$$
$$E(e_1') \equiv E(d_{x^2-y^2,xy}) = -\tfrac{2}{3}Dq$$
$$E(a_1') \equiv E(d_{z^2}) = -4Dq$$

It is worth noting that because the d-orbitals no longer lie on the normal Cartesian axes, the e_g set is labelled as $d_{xz}.d_{yz}$ thus the d_{z^2} level is almost unaffected by any trigonal twist (fig 1.8).

They concluded that, in general, the LFSE of a trigonal prismatic complex will be less than that of an octahedral one.

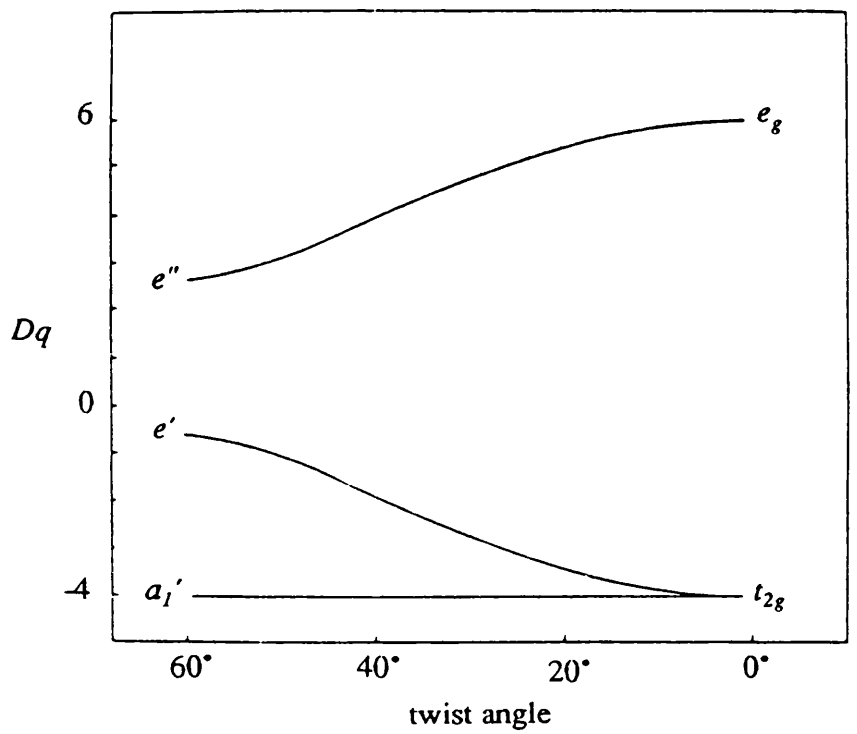

Fig 1.8. *d-orbital energy levels with varying twist angle.*

It can be seen that the choice between O_h and T.P will depend upon the stereochemical requirements of the metal to a large extent. When the metal has a significant amount of LFSE such as low spin d^6 (i.e. a high preference for O_h geometry), the overall structure will be octahedral, assuming of course that the ligand is able to accommodate pure octahedral symmetry. The preference of the metal may on the other hand be less strong, in which case an "equilibrium" geometry will result from the competition between the requirements of the metal and ligand. With no preference for O_h geometry

(metal ions with zero amount of LFSE - d^0, high spin d^5 and d^{10}) the ligand will determine the complex geometry.

In order to obtain a slightly more accurate model Wentworth (**33**) included the effects of electronic repulsion within the d-orbitals (Racah parameter B); for d^5 to d^{10} ions the following results were obtained:

d^5(H.S) : $E[(t_{2g})^3 (e_g^2)] - E[(a_1')^1(e_1')^2(e'')^2] = 0$

d^6(L.S) : $E[(t_{2g})^6] - E[(a_1')^2(e_1')^4] = {}^{-40}/_{3}Dq - 10B$

d^7(H.S) : $E[(t_{2g})^5(e_g)^2] - E[(a_1')^2(e_1')^3(e'')^2] = {}^{-10}/_{3}Dq + 3B$

d^8 : $E[(t_{2g})^6(e_g)^2] - E[(a_1')^2(e_1')^4(e'')^2] = {}^{-20}/_{3}Dq - 3B$

d^9 : $E[(t_{2g})^6(e_g)^3] - E[(a_1')^2(e_1')^4(e'')^3] = {}^{-10}/_{3}Dq$

d^{10} : $E[(t_{2g})^6(e_g)^4] - E[(a_1')^2(e_1')^4(e'')^4] = 0$

Octahedral symmetry is highly favoured for d^6(LS) and d^8 species, whilst the stability of the d^7(HS) ion is negated by the increase in electron repulsion, in other words Co(II) (high spin) should show no overall preference for octahedral symmetry. This is verified by the almost perfect trigonal prismatic stereochemistry encountered for the d^7 Co(II) complexes of $[Co(py)_3tach]^{2+}$ (**31**) and $[\{Co(III)(OCH_2CH_2NH_2)_3\}Co(II)]^{2+}$ (**34**).

Some recent examples of trigonal prismatic geometry include compounds with the tris(catecholyamide) system TRENCAM. This ligand was found to coordinate Fe(III) in a trigonal prismatic manner (**35**). This particular

ligand's preference for T.P stereochemistry was initially attributed to the strong intramolecular hydrogen bonding between the amide group and catecholate oxygen functions. This strong interaction however, has been observed in analogous complexes which display pseudo-octahedral coordination.

Raymond and co-workers (**36**), have proposed that a π-bonding interaction between the ligand and metal may be a primary stabilising factor, since this π interaction is maximised when trigonal prismatic geometry is present.

1.7 Optical Activity and Circular Dichroism. (Ref.37)

A material which is optically active is one which possesses the ability to rotate the plane of polarised light. The characteristics of such a material were discovered and investigated by Pasteur, van't Hoff and Le Bel. The compound in question must be chiral, it must possess no mirror planes, improper axes of rotation or a centre of symmetry, it is thus said to be dissymmetric.

In the case of metal complexes the sources of this dissymmetry may arise from either configurational or conformational isomerism. The compound $[Co(en)_3]^{3+}$ is a classical example of a molecule which displays both types:

the configurational element is observed as twist of the propeller blades when viewed down the C_3 axis (fig 1.9).

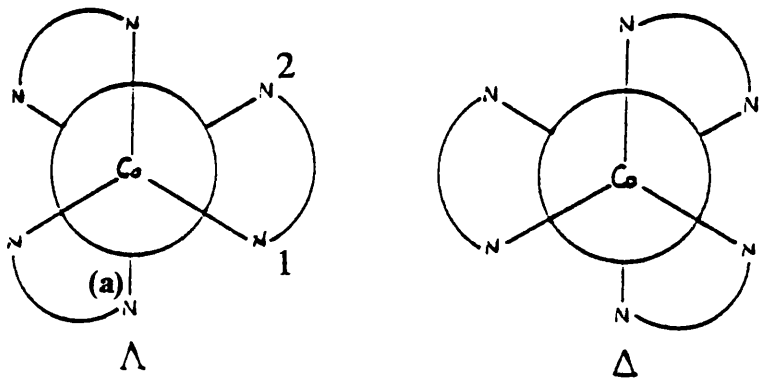

Fig 1.9. *Configurational isomerism in* $[Co(en)_3]^{3+}$.

If the connection between the front (1) and rear (2) nitrogens is to the right of atom A then the Λ configuration is present. On the other hand, if this connection is to the left of the nitrogen, Δ symmetry results. The conformational aspect of the chirality results from the "puckering" of the smaller chelate rings formed by the ethylene diamine units. Using the 1970 IUPAC convention, if the carbon-carbon bond forms a right handed helix in relation to the nitrogen-nitrogen distance, this is defined as the δ conformer. The opposite λ conformation results if the helix described by the carbon-carbon bond is left handed with respect to the nitrogen-nitrogen bond (fig 1.10).

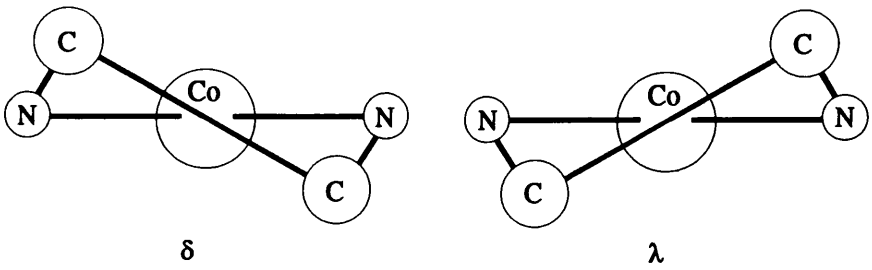

Fig 1.10. *Conformational isomers of ethylene diamine chelate rings.*

Additionally, the chirality displayed by a given metal complex may arise through an intrinsic property of the ligand, such as the presence of a dissymmetric carbon or nitrogen function giving a chiral centre.

One extremely useful property of a chiral molecule is its propensity to rotate the plane of plane polarised light. Chiral compounds exist in one of two enantiomeric forms and any imbalance in the distribution of these enantiomers will result in a rotation: if the left handed form predominates then any rotation will be to the left and vice versa. It is desirable now to define the nature of plane polarised light .

"Ordinary" light may be regarded as consisting of many electromagnetic waves which vibrate in all possible orientations about the direction of propagation of the light rays. With plane polarised light (PPL) these waves vibrate only in one particular plane (the electric and magnetic vectors are at 90° to each other but concentrating on just the electric component the ray can be considered planar). Plane polarised light comprises of two superimposed circularly polarised (CPL) components which spiral around the

direction of propagation (fig 1.11); it is these CPL components which interact with the chiral molecule(s). Such an interaction results in either the left or right handed component being retarded with respect to the other. The two waves will thus be out of phase by an angle ϕ, in general the component which has the strongest interaction with the chiral medium will be retarded most (its refractive index, n, will be larger). On recombining, the waves form plane polarised light which is rotated from its original position by an angle α (fig 1.12).

If the left component is retarded, as in figure 1.12, the rotation of the resultant PPL is to the right.

In 1895 Cotton (**38**) discovered the phenomenon which arose from the relationship between rotary power and light absorption in optically active molecules. The Cotton Effect consists of the two helical (R and L) components having differing refractive indices and additionally, within the absorption band of a complex, differing molar extinction coefficients (ε). Overall the linearly polarised light is transformed into elliptically polarised light - an example of circular dichroism. If a compound near an absorption band absorbs left CPL more strongly than right CPL then $\varepsilon_R > \varepsilon_L$. Also if we assume that $n_R > n_L$ the R component will be retarded to a greater extent than L, giving elliptically polarised light (fig 1.13).

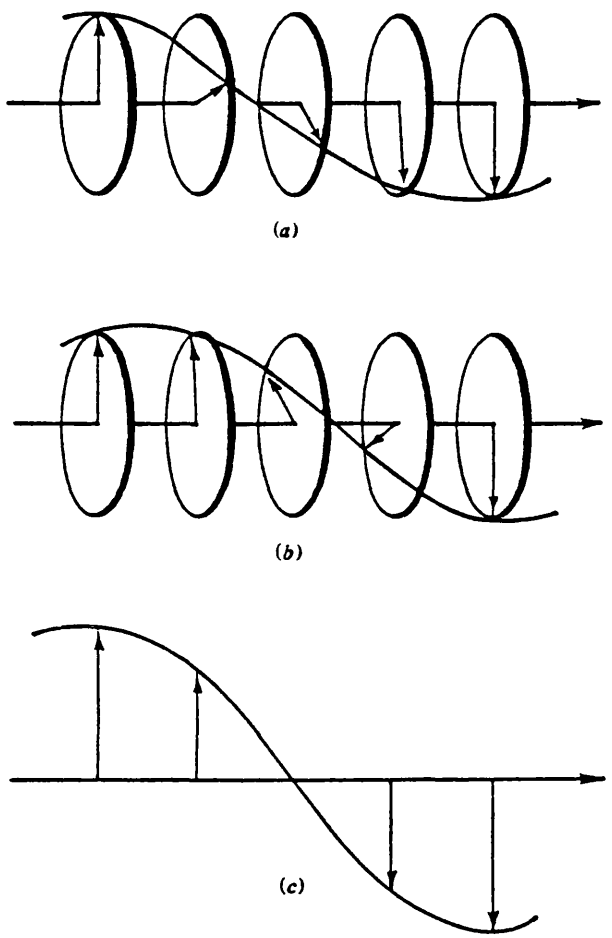

Fig 1.11.(a) *Right handed CPL* **(b)** *Left handed CPL* **(c)** *Resultant PPL.*

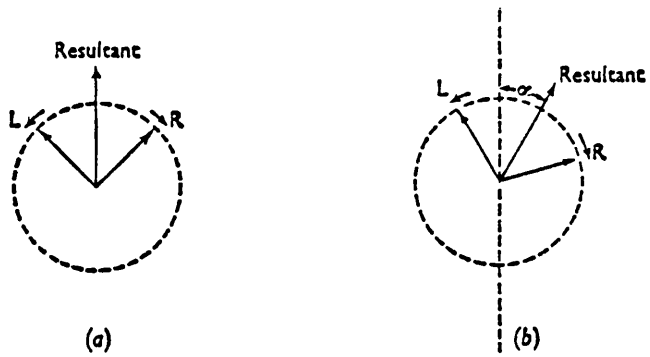

Fig 1.12. *Left and right CPL and plane polarised resultant (a) before and (b) after passing through an optically active medium ($n_L > n_R$).*

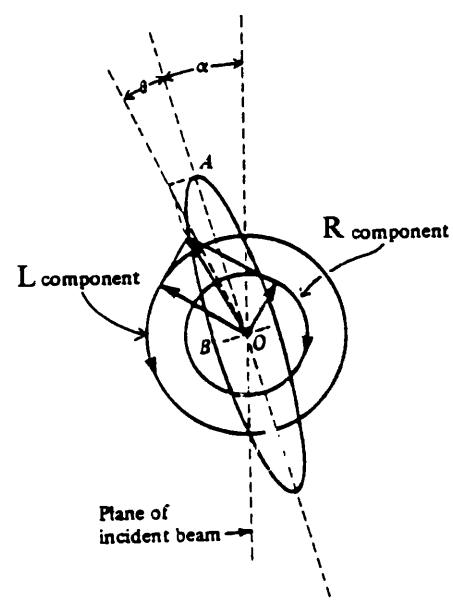

Fig 1.13. *Production of elliptically polarised light when $n_R > n_L$ and $\varepsilon_L > \varepsilon_R$.*

The ellipticity is given by the angle ψ which is related to the specific ellipticity using the equation

$$[\psi] = \frac{\psi}{lpd}$$

l = path length (cm); d = density; p = fraction of optically active material.

Once the specific ellipticity has been derived the molecular ellipticity is defined.

$$[\theta] = \frac{[\psi]M}{100}$$

M = molecular weight of optically active material.

Finally [θ] may be given in terms of the extinction coefficients

$$[\theta] = 3300(\varepsilon_L - \varepsilon_R)$$

The CD spectrum now consists of a plot of Δε or $(\varepsilon_L - \varepsilon_R)$ against wavelength.

1.8 Spectroscopy of Selected Transition Metals.

The spectroscopic characteristics of some first row transition metal ions and their macrocyclic complexes will be discussed in the following chapters. It is

therefore appropriate to outline the electronic spectroscopy of the relevant metal ions. Octahedral labels are used for simplicity.

The V(IV) species with its d^1 configuration is probably the simplest example, with normally only one absorption expected for the $^2T_{2g} \rightarrow {}^2E_g$ transition. The circular dichroism spectrum yields a single band pertaining to this transition; splitting of the $^2T_{2g}$ state into $^2A_1$ and $^2E_2$ can occur on distorting from O_h to T.P.

Mn(IV) and Cr(III) are both d^3 species; in the majority of cases two transitions are observed in the visible region, a third spin allowed band is normally hidden under charge transfer absorptions. In order of increasing energy the $^4A_{2g} \rightarrow {}^4T_{2g}$ ($d_{xy} \rightarrow d_{x^2-y^2}$) and $^4A_{2g} \rightarrow {}^4T_{1g}$ (F) ($d_{xy} \rightarrow d_{z^2}$) bands are usually seen, whilst the $^4A_{2g} \rightarrow {}^4T_{1g}$(P) transition is quite often hidden (vide supra). Any lowering of the symmetry (i.e. trigonal distortion) results in the T states splitting into A and E levels. Thus the T_{2g} state becomes A_1 + E and T_{1g} transforms into A_2 + E. When dealing with CD spectroscopy any A and E states originating from a T state have oppositely signed bands.

A typical CD spectrum of Cr(III) or Mn(IV) consists of, at lower energy the single $^4A_2 \rightarrow {}^4E$ ($^4T_{2g}$) and $^4A_2 \rightarrow {}^4A_1$ ($^4T_{2g}$) transitions. The $^4A_2 \rightarrow {}^4A_2$ transition is, of course, symmetry forbidden. In some cases spin forbidden transitions may also be observed as sharp low energy bands ($^4A_2 \rightarrow {}^2T_1$ and $^4A_2 \rightarrow {}^2E$).

The spectrum of Mn(II) or Fe(III) high spin ions will be very weak as a result of the ^6S ground state arising from the five parallel spins of the d^5 configuration. Any transitions are symmetry and spin forbidden, as they require a change of the spin state.

Octahedral Ni(II) complexes (d^8 ion), display three bands due to transitions between the $^3A_{2g}$ ground state to three excited triplet states $^3T_{1g}(P)$, $^3T_{1g}(F)$ and $^3T_{2g}(F)$. In common with the Cr(III) and Mn(IV) case, trigonal distortion results in T state splitting. Transitions to the first two excited levels $^3T_{1g}(P)$ and $^3T_{1g}(F)$ have symmetry $A_1 + E$ (forbidden), those of symmetry $A_2 + E$ from the $^3T_{2g}$ state have oppositely signed bands in the circular dichroism spectrum. The lowest energy $^3A_{2g} \rightarrow {}^3T_{2g}$ band is sometimes split by spin orbit coupling into $^3F_4$, $^3F_3$ and $^3F_2$ states as a result of its zero order magnetic dipole.

1.9 Complexes of Pendant Arm Ligands.

The first pendant arm triazamacrocycle was N,N',N''-tris(-carboxy methyl)-1,4,7-triazacyclononane TCTA (fig 1.14), synthesised by Takamoto and co-workers (**39**). This potentially hexadendate N_3O_3 donor was found to form extremely stable complexes with Co(III) and Cr(III) (**40**). Many examples of divalent metal compounds with TCTA have been reported (**10**).

The high stability of these complexes may be attributed, in part, to the efficient binding of the pendant carboxylate groups to the various metal ions. This may be observed from the crystal structure of $[H_3O][Ni(TCTA)]$ (**16**) (fig 1.15).

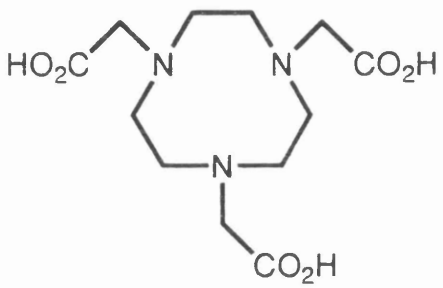

Fig 1.14. *N,N',N''-tris(-carboxy methyl)-1,4,7-triazacyclononane (TCTA).*

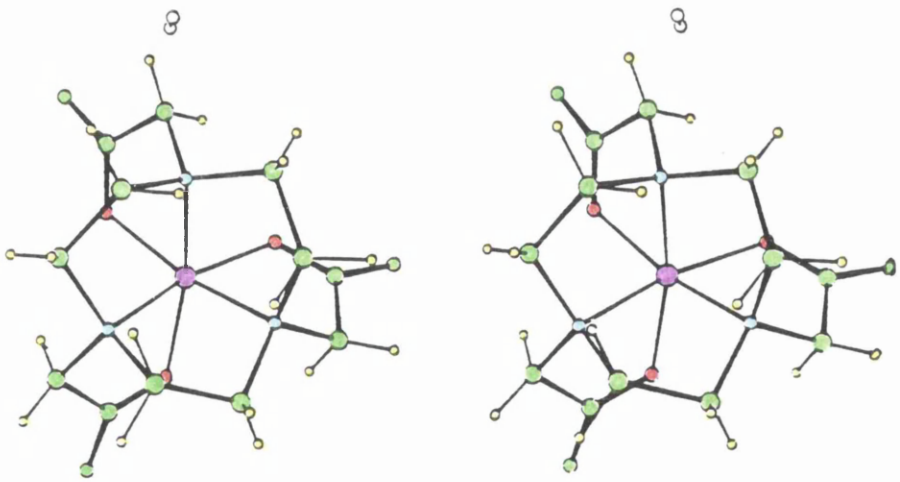

Fig 1.15. *Stereo view of complex* $[H_3O][Ni(II)(TCTA)]$.

The proton is present as a hydronium ion whilst the carboxylate groups remain deprotonated and bound to the metal. Protonation would probably result in a detachment of one of these acid functions, the free site being taken by a less sterically efficient water molecule, leading to an overall increase in the length of the metal-nitrogen bonds and hence a destabilisation of the complex.

The crystal structures of complexes with TCTA and other similar hexadentate ligands show the geometries to lie almost anywhere in the range from octahedral to trigonal prismatic.

The reported complexes of TCTA vary in the degree of trigonal twist around the metal centre, the main determinant of the geometry being the magnitude of LFSE required by the metal ion; since the ligand is the same in all cases. The table below lists the change in twist angle for various TCTA complexes.

Metal Ion	d^n	Twist Angle ϕ	Geometry	Ref.
Cr(III)	n=3	11.0°	pseudo-octahedral	42
Ni(II)	n=8	12.0°	pseudo-octahedral	41
Cu(II)	n=9	33.4°	pseudo-trigonal prismatic	42
Fe(III)	n=5	35.0°	pseudo-trigonal prismatic	42

Table 1.2. *Twist angles for TCTA complexes.*

The all nitrogen donor ligand, N,N',N''-tris(2-aminoethyl)-1,4,7-triazacyclononane (TAETACN) (fig 1.16) was first prepared by Hammershoi and Sargeson (**43**). They synthesised the Co(III) complex and from ^{1}H and ^{13}C NMR data, assigned a C_3 geometry. On the basis of additional evidence from electronic and circular dichroism spectroscopy the overall configuration of Δ was attributed to the molecule. This was subsequently verified by X-ray crystallographic analysis (**44**), the geometry around the Co(III) centre was found to be pseudo-octahedral.

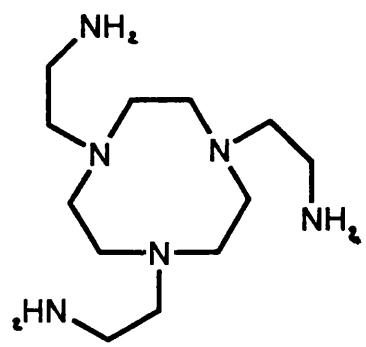

Fig 1.16. *N,N',N''-tris(2-aminoethyl)-1,4,7-triazacyclononane (TAETACN).*

An alcohol appended triazamacrocycle, namely N,N',N''-tris(2-hydroxy ethyl)-1,4,7-triazacyclononane THETACN (fig 1.17), was synthesised by Hancock and co-workers in 1983 (**45**). They explored its chemistry with Cu(II) and Zn(II), protonation studies on the ligand showed the pk_1^K value was greater for THETACN than for that measured for TACN. This was unusual due to the electron withdrawing nature of the hydroxyl functions,

which would suggest a lower pk_1 value for the pendant arm macrocycle. The second protonation constant, however, was in keeping with the expected behaviour i.e. the electron withdrawing alcohol groups would decrease the basicity of the ring donors. The anomalous result for the first constant was attributed, by the authors, to a hydrogen bonding interaction between the incoming proton and the hydroxyl moieties. As the pH fell this behaviour broke down leading to much lower values for the second and third constants.

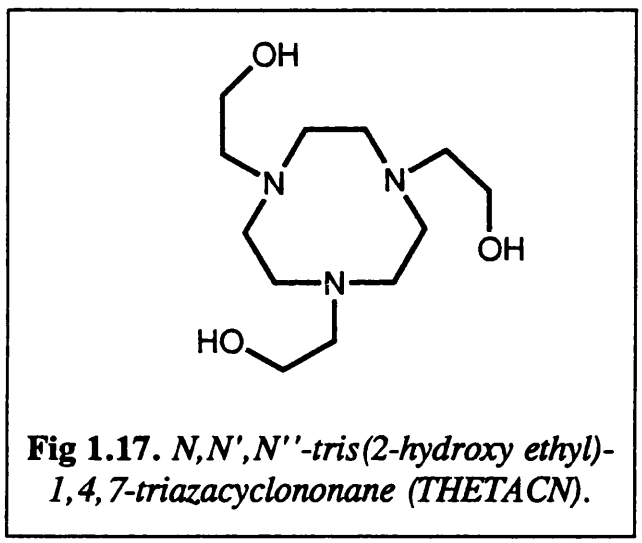

Fig 1.17. *N,N',N''-tris(2-hydroxy ethyl)-1,4,7-triazacyclononane (THETACN).*

Stability measurements on both the Cu(II) and Zn(II) compounds indicated that THETACN formed complexes which were just as stable as those with the parent macrocycle TACN. This they suggested was good evidence that all six donor atoms were coordinated to the metal.

The ligand N,N',N''-tris(2-pyridyl methyl)-1,4,7-triazacyclononane (TPTACN) (fig 1.18), was prepared independently by two groups Christiansen *et al.* (**46**) and Wieghardt *et al.* (**47**). The former reported the crystal structure of $[Fe(TPTACN)][ClO_4]_2$, the geometry was distorted from

octahedral by 11.1°; the ligand was designed to promote trigonal prismatic stereochemistry. This result was rationalised on the basis that an Fe(II) low spin d^6 species would be expected to exhibit a strong preference for octahedral coordination.

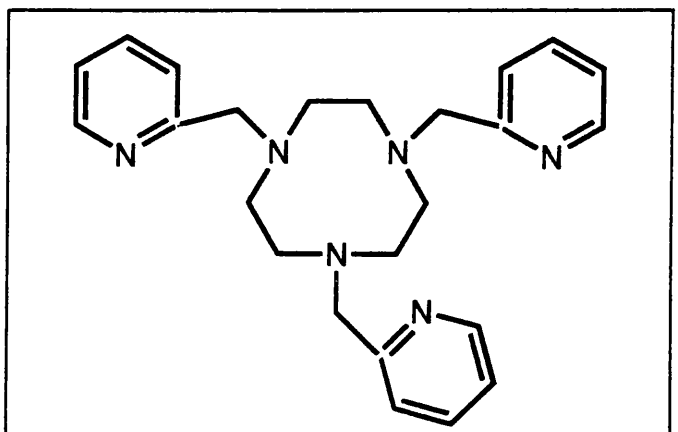

Fig 1.18. *N,N',N''-tris(2-pyridyl methyl)-1,4,7-triazacyclononane (TPTACN).*

Wieghardt *et al.*obtained structural data for the Mn(II) and Ni(II) complexes. The Mn(II) centre was found to be in a pseudo-trigonal prismatic environment, twist angle $\phi=40.4°$ expected for a high spin d^5 ion which should have no overall preference for octahedral geometry. The nickel structure was almost octahedral with a trigonal twist of 13.2°. These results, however, are somewhat unusual in that a ligand, initially thought to be quite rigid and inflexible should distort to such a degree, highlighting the powerful driving force of LFSE on the overall complex geometry.

1.10 Chemistry of 1-oxa-4,7-diazacyclononane: 9-aneN_2O.

The tosylated form of this ligand (scheme 1.5), was first synthesised by Vögtle and co-workers in 1976 (**48**). The method of cyclisation was based loosely upon the Richman-Atkins procedure (vide supra), resulting in various ring sizes incorporating the mixed N, O donor set including 9-aneN_2O.

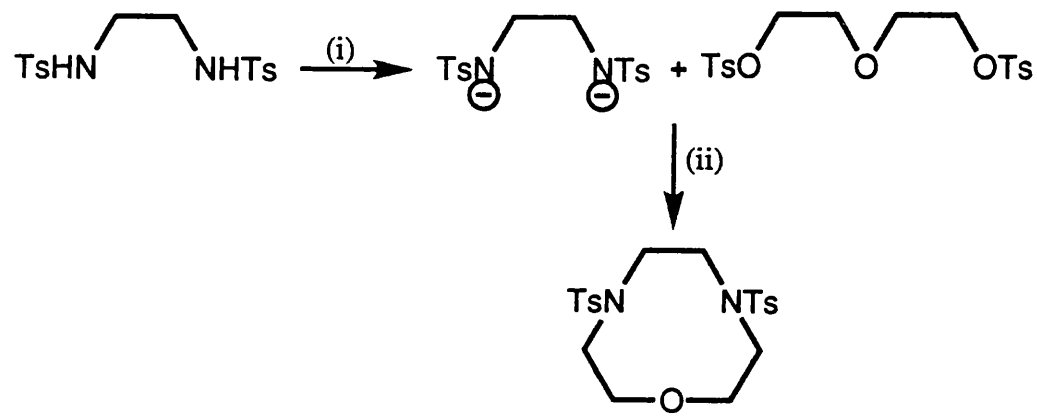

Scheme 1.5. *Preparation of ditosyl- 1-oxa-4,7-diazacyclononane. (I) KOBu^t/DMF (ii) DMF/ 6h/Δ.*

The amine N',N''-ditosyl ethylene diamine was converted to its dianionic form using potassium tert butoxide in DMF. Ditosyl diethylene glycol was added slowly, in situ, and following a suitable work up the ditosylated macrocycle was obtained in approximately 32% yield. Improved yields may be obtained using slightly modified procedures (**49**). These higher yields are to a certain extent compromised due to the relative difficulty in

detosylating the macrocycle. A hydrolytic method, utilising conc. H_2SO_4, as employed for the analogous 9-aneN_3 gave quite poor yields, due to acid catalysed ether cleavage processes. Use of a mixture of HBr in glacial acetic acid (**6**) works slightly better, while a reductive alkaline detosylation strategy (**50**) operates very efficiently.

Unlike TACN, the successive protonation constants for 9-aneN_2O do not differ greatly from those of its open chain congeners - ODEN and HEEN (table 1.3).

SPECIES	pk_1 (K_1)	pk_2 (K_2)	
9-aneN_2O	9.59[a] 9.677[b]	5.32[a] 5.45[b]	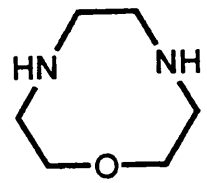
HEEN	9.59[c]	6.60[c]	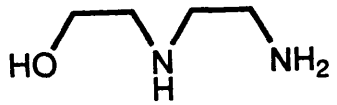
ODEN	9.75[c]	8.90[c]	

(a) Ref. 51 (b) Ref. 52 (c) Ref. 9

Table 1.3. *Protonation constants for 9-aneN_2O and analogues.*

This similarity in the protonation values may be attributed to a reduction in synergic internal hydrogen bonding in comparison with the all aza donor TACN. This is primarily due to the hydrogen bonding ability of the various

donor atoms where N >> O > S (in order of decreasing H-bonding ability) (**53**). Thus by replacing one nitrogen donor with an oxygen, the extent of internal hydrogen bonding, which stabilises the first coordinated proton, is of a much lower magnitude.

It has also been established that, like TACN, the $pk_2^{K_2}$ values for the macrocyclic system are much lower than for analogous linear molecules. The higher $pk_2^{K_2}$ for ODEN (8.90) is a consequence of the distance between the two nitrogen donors; the repulsion towards the second incoming proton is thus smaller.

One interesting point, concerning the open chain ligands, is the almost identical $pk_2^{K_2}$ values of DIEN $H_2N(CH_2)_2NH(CH_2)_2NH_2$ and ODEN $H_2N(CH_2)_2O(CH_2)_2NH_2$, suggesting that inductive effects do not affect the basicity of the amine functions: a phenomenon which is believed to extend through to cyclic ligands.

1.11 Transition Metal Complexes with 9-aneN_2O.

Much speculation has reigned as to whether the replacement of nitrogen donors, with neutral oxygen groups affects the overall stability of a complex. Early investigations (**54, 55**) indicated a fall in stability, however the chosen

systems were found not to be accurate models of the first row transition metal complexes with small macrocyclic ligands.

Hancock and Thom (**51**) examined Cu(II), Ni(II) and Zn(II) complexes with 9-aneN_2O, they found the stability constants for these compounds were markedly different to those with ODEN; suggesting the macrocyclic effect towards the overall stability is maintained. Although, it must be noted that the stability constants were less than for equivalent TACN compounds.

Cabral *et al.* (**52**) in addition examined the stability of the Co(II) complex.

		9-aneN_3		9-aneN_2O	
METAL ION	SPECIES	K log k^a	K log k^b	K log k^c	K log k^d
Co(II)	ML	11.2	-	6.33	-
	ML_2	7.8	-	5.30	-
Ni(II)	ML	13.6	16.2	8.05	8.59
	ML_2	11.8	-	7.85	-
Cu(II)	ML	15.1	15.5	10.80	10.85
	ML_2	12.01	-	8.80	-
Zn(II)	ML	11.7	11.6	6.40	6.32
	ML_2	10.0	-	5.70	-

a&c - taken from ref. 52 b - taken from ref. 56 d - taken from ref. 51

Table 1.4. *Stability of 9-aneN_2O complexes vs. 9-aneN_3 complexes.*

The groups observed that although the stabilities measured for 9-aneN_2O complexes were less than for 9-aneN_3 the rate of formation of compounds increased.

1.12 Electronic Spectroscopy of Simple 9-aneN_2O Complexes.

The spectroscopic properties of bis-9-aneN_2O complexes indicate a reduction in the ligand field splitting, in comparison with analogous 9-aneN_3 compounds. The complex $[Ni(9\text{-ane}N_2O)_2]^{2+}$ comprises a nickel ion surrounded by four equatorially coordinated nitrogen atoms and two apical oxygen functions in an almost perfect octahedral geometry (**57**).

A 10Dq value of 11,900cm^{-1} has been calculated (**58**) for this complex; the ligand field splitting of the non-cyclic compound $[Ni(HEEN)_2]^{2+}$ was measured at 11,250cm^{-1} - an overall decrease in splitting of 650cm^{-1} between the two. The equivalent all aza donor compounds $[Ni(TACN)_2]^{2+}$ (12,200cm^{-1}) and $[Ni(DIEN)_2]^{2+}$ (11,200cm^{-1}) differ by 1000cm^{-1}. These results have been attributed to the change from primary to secondary amine groups; the latter are superior Bronsted bases. This leads to an increased metal-ligand bonding interaction (i.e. shorter bonds). With cyclic systems this transformation to secondary donors does not seem to incur the same increase in steric strain as experienced by linear ligands.

In the case of 9-aneN_2O, the change from alcohol to ether donation, on cyclisation does not result in the same increase in basicity thus explaining the

smaller increase in ligand field splitting in the mixed N, O donor compounds.

The difference in 10Dq between the complexes of the precursors $[Ni(HEEN)_2]^{2+}$ (11,250cm^{-1}) and $[Ni(ODEN)_2]^{2+}$ (10,200cm^{-1}) exemplifies the effect of donor groups on ligand field strength. HEEN exerts a stronger ligand field because of the superior base properties of its alcohol and secondary amine groups leading to a more intimate metal-ligand contact. Stability measurements also indicate that HEEN complexes with Cu(II), Ni(II) and Zn(II) are more stable than equivalent ODEN compounds (**9**).

Reinen *et al.* (**50**) investigated the electronic spectra of $[Co(9\text{-ane}N_2O)_2]^{2+}$; the reflection spectra at 298 and 5K, suggested the metal lay in a tetragonally distorted octahedron which had D_{4h} symmetry. They calculated the ligand field splitting at approximately 12,800cm^{-1}, the authors believed the distortion was necessary to stabilise the low spin d^7 ground state of the metal ion.

Nonoyama and Ishida (**59**) prepared Co(III), Ni(II) and Cu(II) complexes with 9-aneN_2O. Examination of the electronic spectra of $[Ni(TACN)_2]^{2+}$ and $[Ni(9ane N_2O)_2]^{2+}$ showed a marked difference between the two not only in terms of ligand field strengths. These differences the authors attributed to a lowering of the overall symmetry to D_{4h} on substituting a nitrogen for the oxygen. To obtain CD spectra they prepared a derivative of 9-aneN_2O containing a chiral carbon substituted onto the ring namely (R)-5-methyl-1-

oxa-4,7-diazacyclononane. They found the CD limit corresponding to the $^3A_{2g} \rightarrow {}^3T_{2g}$ transition to be much weaker than for the (R)-MeTACN complex. The authors suggested the weaker Ni-O bond (relative to Ni-N bond) would result in a more flexible conformation of the chelate rings, thus reducing the overall chirality of the molecule.

1.13 Pendant Arm Compounds.

In common with TACN, the nitrogen donors of 9-aneN_2O present the opportunity to increase the denticity and coordinating abilities of the ring by introducing pendant functional groups. This area has been less extensively studied than with 9-aneN_3.

Cabral *et al.* (52) obtained protonation data and stability measurements for the carboxylate derivative N-ac$_2$[9]-aneN_2O (fig 1.19).

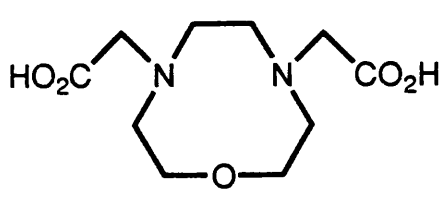

Fig 1.19. *N,N'-di(2-carboxy methyl)-1-oxa-4,7-diazacyclononane.*

Using potentiometric and ^1H NMR techniques, they evaluated successive protonation constants for the ligand (table 1.5).

	K_1	K_2	K_3	K_4
	pk_1	pk_2	pk_3	pk_4
N-ac_2[9]-aneN_2O	10.57 ± 0.01	4.02 ± 0.03	1.8 ± 0.3	<1

Table 1.5. *Protonation studies of diacetate 9-aneN_2O.*

The first value (pk_1), they attributed to the protonation of one nitrogen donor, stabilisation of this group occurring via hydrogen bonding to the carboxylate functions. The second measurement is consistent with the protonation of a carboxylate group bonded to an unprotonated nitrogen. The third figure suggested protonation of the remaining carboxylate. The final constant (pk_4) is in the view of the authors indicative of the second nitrogen being protonated, the recorded value is very low because of the repulsion effects of the other ammonium function. This ligand shows similar behaviour to TCTA (section 1.9), in that the nitrogen donors are less basic than the carboxylate donors. Using a slightly different method, Ewin and Hill (**60**) obtained a pk_1 value of 10.8 which compares favourably with the values indicated above.

Thermodynamic data on the stability of N-ac_2[9]-aneN_2O complexes has been obtained by Cabral *et al.* (**52**) (table 1.6).

ION	SPECIES	K log k (T=25°C)
Mn(II)	ML	7.73 ± 0.01
Fe(II)	ML	9.70 ± 0.01
Co(II)	ML	11.48 ± 0.02
Ni(II)	ML	11.89 ± 0.02
Cu(II)	ML	13.37 ± 0.09
Zn(II)	ML	12.53 ± 0.01

Table 1.6. *Stability measurements of diacetate 9-aneN_2O complexes.*

From the table it may be seen that the most stable complex results, when the fit between metal radius and ligand cavity is close. The best fit for 9-aneN_3 ring has been calculated at 1.4Å [Ni(II)] (**61**), thus the marginally larger cavity of 9-aneN_2O, in addition to its greater flexibility, atoms such as Cu(II) and Zn(II) would be expected to form a closer size-match relationship.

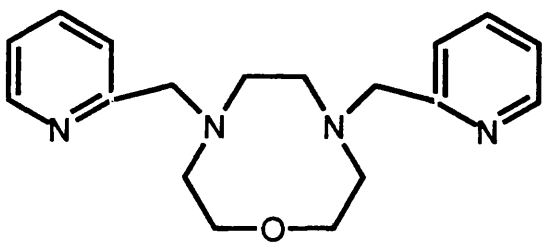

Fig 1.20. *N,N'-dipicolyl-1-oxa-4,7-diazacyclononane.*

A 4,7-dipicolyl derivative of 9-aneN_2O (fig 1.20) was synthesised by Busch and co-workers (**62**) to study the catalytic behaviour of the Fe(II)

complex with regard to the hydrogen peroxide/superoxide process. Suitable crystals were obtained for X-ray analysis which showed the overall geometry was midway between octahedral and trigonal prismatic (fig 1.21), the twist angle ϕ was measured at 29°. The Fe(II) ion in this complex is high spin d^6 and thus would be expected to have a relatively low preference for O_h coordination.

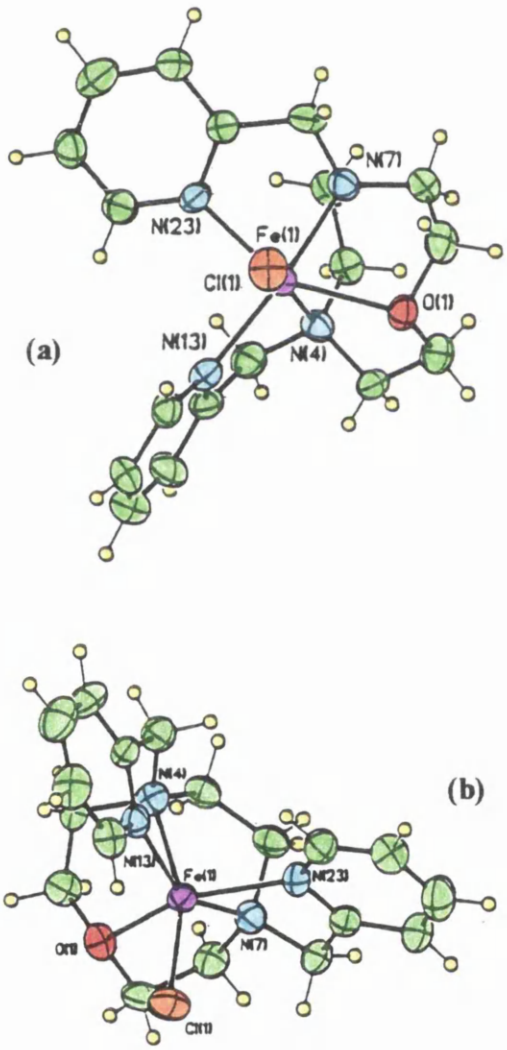

Fig 1.21. *Crystal structure of [Fe(II){bis(2-picolyl)-1-oxa-4,7-diazacyclononane}Cl][PF_6] (a) down Cl-Fe-N axis (b) down C_3 axis.*

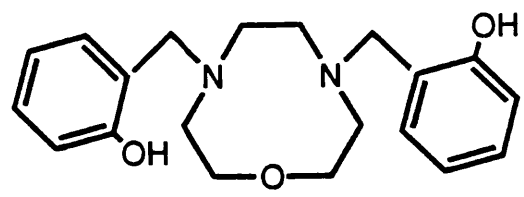

Fig 1.22. *N,N'-di(2-hydroxybenzyl)-1-oxa-4,7-diazacyclononane.*

The chemistry of the above ligand (fig 1.22) has been explored to a limited extent by Flassbeck *et al.* (**63**). The structure of the Zn(II) compound was determined, it comprised a dimer held together by 2 hydrogen bridges in conjunction with a μ-hydroxyl moiety. Each zinc ion was in an octahedral environment, Zn(II) would be expected to display no overall preference for octahedral symmetry - it must be assumed that the dimeric nature of the complex confers octahedral coordination about each metal centre. The oxygen donor of the ring coordinates the metal ion with a Zn-O bond length of 2.310Å indicative of a bonding interaction.

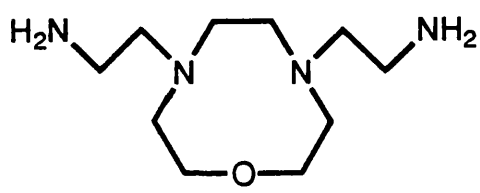

Fig 1.23. *N,N'-di(2-aminoethyl)-1-oxa-4,7-diazacyclononane.*

The 9-aneN_2O equivalent of TAETACN (fig 1.23), was prepared by Beveridge *et al.* (**49**) as a precursor in the metal template style synthesis of a larger bicyclic ligand. A Cu(II) ion was used as the template, coordinated with bis (aminoethyl)- 9-aneN_2O followed by reaction with glyoxal to effect a ring closure to yield a larger 4 donor; 14 membered ring fused to a smaller 3 donor 9 membered macrocycle. The crystal structure of the template intermediate showed the Cu(II) ion in a trigonal bipyramidal environment, the oxygen of the 9-aneN_2O segment assumed the apical position with a Cu-O distance of 2.275Å suggesting a strong bonding interaction between the two.

1.14. Objectives.

The chemistry of macrocyclic ligands and their transition metal complexes is currently an area of great interest. Many different ring sizes and donor types have been employed. The coordination chemistry of triazamacrocycles with pendant ligating groups, however, has still to be fully investigated. Especially ring systems involving pendant alcohol arms.

Triazamacrocycles, due to their size, generally impose "strained" geometries upon metal ions. The potential range of coordination geometries and

characteristic spectroscopic properties of the N_3O_3 chromophore make ligands like L^1H_3 especially interesting to the coordination chemist.

An important feature of the pendant arms is their chiral centre which enables circular dichroism spectroscopy to be used in the investigation of complexes.

Some tris and di alcohol arm substituted triaza and oxa-diaza macrocycles have been prepared, with the aim of examining the complexes they form with transition metal ions particularly in respect of their physical and spectroscopic properties.

References

(1) N.F.Curtis, *J.Chem.Soc.*, 1960, 4409.

(2) C.J.Pedersen, *J.Am.Chem.Soc.*, 1967, **89**, 7017.

(3) B.Dietrich, J.M.Lehn and J.P.Sauvage, *Tetrahedron Lett.*, 1969, **34**, 2885.

(4) J.M.Lehn, *Angew.Chem.,Int.Ed.Engl.*, 1988, **27**, 89.

(5) D.H.Peacock and Y.S.Gwan., *J.Chem.Soc.*, 1937, 1468.

(6) H.Koyama and T.Yoshino, *Bull.Chem.Soc.Jpn.*, 1972, **45**, 481.

(7) J.E.Richman and T.J.Atkins, *J.Am.Chem.Soc.*, 1974, **96**, 2268.

(8) E.Kimura, *Top.Curr.Chem.*, 1985, **128**, 113.

(9) A.E.Martell and R.M.Smith, *Critical Stability Constants*; Plenum, New York, 1975, Vol.2. (Amines).

(10) P.Chaudhuri and K.Wieghardt, *Prog.Inorg.Chem.*, 1987, **35**, 329.

(11) D.K.Cabbiness and D.W.Margerum, *J.Am.Chem.Soc.*, 1969, **91**, 6540.

(12) L.Fabbrizzi, P.Paoletti and R.M.Clay, *Inorg.Chem.*, 1978, **17**, 1042.

(13) G.J.McDougall, R.D.Hancock and J.C.A.Boeyens, *J.Chem.Soc.,Dalton Trans.*, 1978, 1438.

(14) F.P.Hinz and D.W.Margerum, *Inorg.Chem.*, 1974, **13**, 2941.

(15) D.H.Busch, K.Farmery, V.Goedken, V.Katovic, A.C.Melnyk, C.R.Sperati and N.Tokel, *Adv.Chem.Ser.*, 1971, **100**, 44.

(16) M.J.van der Merwe, J.C.A.Boeyens and R.D.Hancock, *Inorg.Chem.*, 1983, **22**, 3489.

(17) I.Fallis, L.J.Farrugia, N.M.Macdonald, and R.D.Peacock, *J.Chem.Soc., Dalton Trans.*, 1993, 2759.

(18) R.C.Matthews, D.Parker, G.Ferguson, B.Kaitner, A.Harrison and L.Royle, *Polyhedron*, 1991, **10**, 1951.

(19) D.A.Moore, P.E.Fanwick and M.J.Welch, *Inorg.Chem.*, 1990, **29**, 672.

(20) E.Cole, D.Parker, G.Ferguson, J.F.Gallagher and B.Kaitner, *J.Chem.Soc., Chem. Commun.*, 1991, 1473.

(21) N.W.Alcock, F.McLaren, P.Moore, G.A.Pike and S.M.Roe, *J.Chem.Soc., Chem. Commun.*, 1989, 629.

(22) U.Auerbach, U.Eckert, K.Wieghardt, B.Nuber and J.Weiss, *Inorg.Chem.*, 1990, **29**, 938.

(23) G.de Martino Norante, M.Di Vaira, F.Mani, S.Mazzi and P.Stoppioni, *J.Chem.Soc., Dalton Trans.*, 1992, 361.

(24) R.G.Dickinson and L.Pauling, *J.Am.Chem.Soc.*, 1923, **45**, 1466.

(25) J.C.Bailar, *J.Inorg.Nucl.Chem.*, 1958, **8**, 165.

(26) R.Eisenberg and J.A.Ibers, *J.Am.Chem.Soc.*, 1965, **87**, 3776.

(27) A.E.Smith, G.N.Schrauzer, V.P.Mayweg and W.Heinrich, *J.Am.Chem.Soc.*, 1965, **87**, 5798.

(28) R.Eisenberg, E.I.Stiefel, R.C.Rosenberg and H.B.Gray, *J.Am.Chem.Soc.*, 1966, **88**, 2874.

(29) R.Hultgren, *Phys.Rev.*, 1932, **40**, 891.

(30) R.Hoffmann, J.M.Howell and A.R.Rossi, *J.Am.Chem.Soc.*, 1976, **98**, 2484.

(31) W.O.Gillum, R.A.D.Wentworth and R.F.Childers, *Inorg.Chem.*, 1970, **9**, 1825.

(32) E.Larsen, G.N.La Mar, B.E.Wagner, J.E.Parks and R.H.Holm, *Inorg.Chem.*, 1972, **11**, 2652.

(33) R.A.D.Wentworth, *Coord. Chem. Rev.*, 1972, **9**, 171.

(34) J.A.Bertrand, J.A.Kelley and E.G.Vassian, *J.Am.Chem.Soc.*, 1969, **91**, 2394.

(35) T.J.McMurry, M.W.Hosseini, T.M.Garrett, F.E.Hahn, Z.E.Reyes and K.N. Raymond, *J.Am.Chem.Soc.*, 1987, **109**, 7196.

(36) T.B.Karpishin, T.D.P.Stack and K.N.Raymond, *J.Am.Chem.Soc.*,1993, **115**, 182.

(37) S.F.Mason, *Molecular Optical Activity and the Chiral Discriminations*; Cambridge University Press, Cambridge, 1982.

(38) A.Cotton, *Comptes Rendus de L'Academie des Science*, 1895, **120**, 989.

(39) T.Arishima, K.Hamada and S.Takamoto, *Nippon Kagaku Kaishi*, 1973, 1119.

(40) M.Takahashi and S.Takamoto, *Bull.Chem.Soc.Jpn.*, 1977, **50**, 3413.

(41) M.J. van der Merwe, J.C.A.Boeyens and R.D.Hancock, *Inorg.Chem.*, 1985, **24**, 1208.

(42) K.Wieghardt, U.Bossek, P.Chaudhuri, W.Herrmann, B.C.Menke and J.Weiss, *Inorg.Chem.*, 1982, **21**, 4308.

(43) A.Hammershoi and A.M.Sargeson, *Inorg.Chem.*, 1983, **22**, 3554.

(44) S.G.Taylor, M.R.Snow and T.W.Hambley, *Aust.J.Chem.*, 1983, **36**, 2359.

(45) B.A.Sayer, J.P.Michael and R.D.Hancock, *Inorg.Chim.Acta.*, 1983, **77**, L63.

(46) L.Christiansen D.N.Hendrickson, H.Toftlund, S.R.Wilson and C.L.Xie, *Inorg. Chem.*, 1986, **25**, 2813.

(47) K.Wieghardt, E.Schoffmann, B.Nuber and J.Weiss, *Inorg.Chem.*, 1986, **25**, 4877.

(48) W.Rasshofer, F.Wehner and F.Vogtle, *Liebigs Ann.Chem.*, 1976, 916.

(49) K.A.Beveridge, A.McAuley and C.Xu, *Inorg.Chem.*, 1991, **30**, 2074.

(50) D.Reinen, A.Ozarowski, B.Jakob, J.Pebler, H.Stratemeier, K.Wieghardt and I.Tolksdorf, *Inorg.Chem.*, 1987, **26**, 4010.

(51) R.D.Hancock and V.J.Thom, *J.Am.Chem.Soc.*, 1982, **104**, 291.

(52) M.F.Cabral, J.Costa, R.Delgado, J.J.R.F.da Silva and M.F.Vilhena, *Polyhedron*, 1990, **9**, 2847.

(53) S.M.Hart, J.C.A.Boeyens, J.P.Michael and R.D.Hancock, *J.Chem.Soc., Dalton Trans.*, 1983, 1601.

(54) H.K.Frensdorff, *J.Am.Chem.Soc.*, 1971, **93**, 600.

(55) L.F.Lindoy, H.C.Lip, J.H.Rea, R.J.Smith, K.Henrick, M.McPartlin and P.A.Tasker, *Inorg.Chem.*, 1980, **19**, 3360.

(56) R.Yang and L.J.Zompa, *Inorg.Chem.*, 1976, **15**, 1499.

(57) J.C.A.Boeyens, R.D.Hancock and V.J.Thom, *J.Crystallogr.Spec.Res.*, 1984, **14**, 261.

(58) V.J.Thom, M.S.Shaikjee and R.D.Hancock, *Inorg.Chem.*, 1986, **25**, 2992.

(59) M.Nonoyama and T.Ishida, *Transition Met.Chem., (Weinheim,Ger),* 1984, **9**, 367.

(60) G.Ewin and J.O.Hill, *J.Chem.Res.(S),* 1985, 334; *(M),* 1985, 3501.

(61) R.D.Hancock, S.M.Dobson and J.C.A.Boeyens, *Inorg.Chim.Acta.*, 1987, **133**, 221.

(62) W.S.Sulbinski, P.R.Warburton, D.H.Busch and N.W.Alcock, *Inorg.Chem.*, 1993, **32**, 297.

(63) C.Flassbeck, K.Wieghardt, E.Bill, C.Butzlaff, A.X.Trautwein, B.Nuber and J.Weiss, *Inorg.Chem.*, 1992, **31**, 21.

CHAPTER 2

EXPERIMENTAL

2.1 INSTRUMENTATION.

The N.M.R. spectra were recorded using either Perkin Elmer RS32 and Varian EM390, 90MHz continuous wave spectrometers or a Bruker AM 200, 200MHz FT-NMR apparatus; utilising the Bruker Dis-NMR suite of programs. All samples were internally referenced to the relevant solvent resonances. Deuterated solvents were stored over 4Å molecular sieves, under a nitrogen atmosphere.

Infra-red spectra were measured on a Philips FT-IR spectrometer. The samples were prepared as 8mm KBr discs using 300mg of KBr and a press force of 10 tons.

UV-visible spectra were obtained using a Perkin Elmer Lambda 9 spectrophotometer. Both reference and sample spectra were recorded in a TSL 1cm semi-micro far-UV. quartz cuvette. Corrected spectra were produced by sample - reference subtraction using the Perkin-Elmer PECSS suite of programs.

Melting points were recorded in air using a Gallenkamp melting point apparatus and were uncorrected.

2.2 X-RAY CRYSTALLOGRAPHIC DATA COLLECTION.

Crystallographic data ~~was~~ were obtained by Dr Louis Farrugia; crystals were mounted on a glass fibre and data collected at ambient temperature on an Enraf-Nonius CAD4F automated diffractometer in the $\theta/2\theta$ scan mode, using graphite monochromated X-radiation (λ = 0.71069Å).

Unit cell dimensions were determined using the SET 4 routine by refinement of the setting angles ($11 < \theta < 13$) averaging angles from four diffracting positions. All calculations were performed on a MICROVAX 3600 computer using the Glasgow GX suite of programs.

2.3 CIRCULAR DICHROISM SPECTROSCOPY.

Circular dichroism measurements were obtained using a spectrometer (fig2.1) centered around a JOBIN-YVON 0.6m monochromator. The light from a 150W Xenon arc lamp is focused with a parabolic reflector before passing through the monochromator. A quartz Rochon prism polarises this light in the vertical plane, it is circularly polarised on passing through a photo-elastic modulator.

The photo-elastic modulator (PEM) is vital to the operation of the spectrometer. It consists of a series of transducers (quartz piezoelectric elements) bonded to a bar shaped crystal of calcium fluoride. When the transducers are excited, by the modulator power supply, at the resonant frequency of the crystal (50kHz), the vibrations induce a birefringence which causes an overall phase difference between the x and y electric vector components of light passing through the crystal. The modulation frequency is such that the left and right components are alternatively retarded by a quarter wave (90°). This 90° difference is maintained as the monochromator scans through light of decreasing wavelength by varying the frequency of modulation. The light then enters the sample and the resulting signal is collected by a photomultiplier tube. Phase sensitivity is obtained using a lock-in amplifier (referenced to the power supply of the photo-elastic modulator), which detects the periodic difference in light intensity due to the

presence of an optically active sample. The lock-in output is plotted on a chart recorder as the monochromator is scanned in wavelength. The resulting spectrum comprises, the fractional circular dichroism absorbance (ΔA) varying with wavelength (λ).

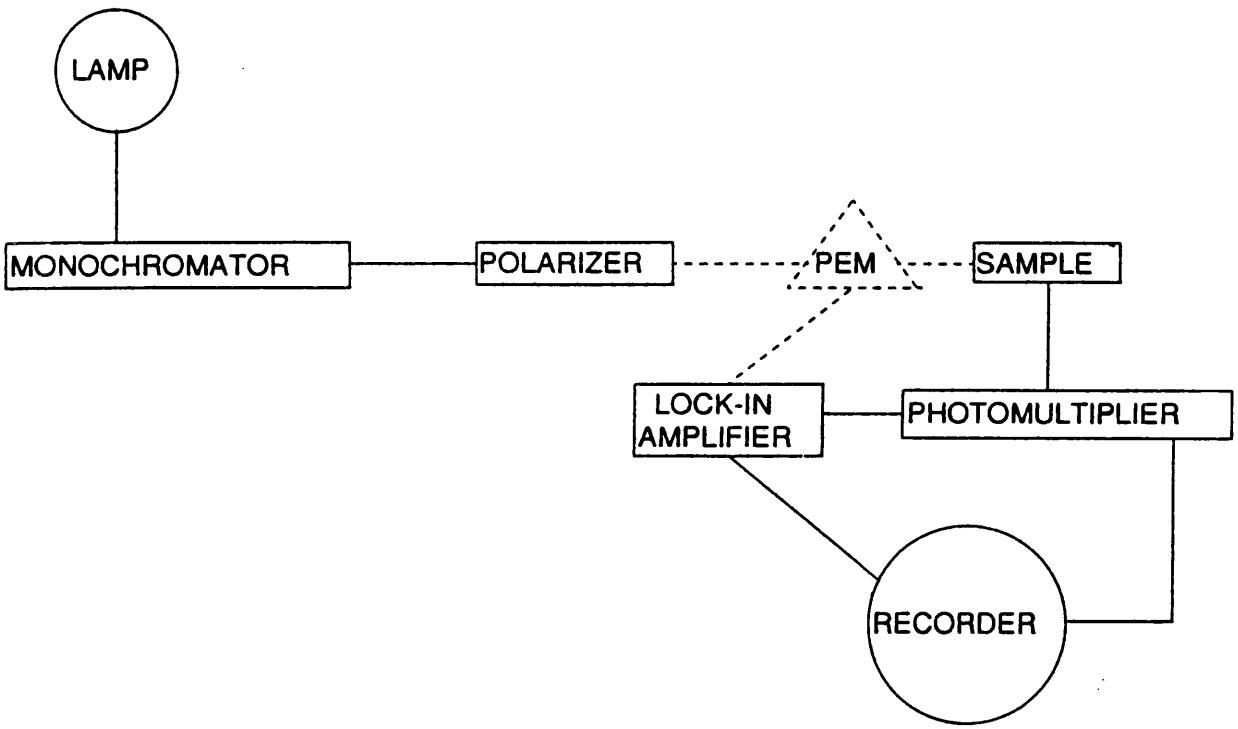

Fig. 2.1. *Circular dichroism apparatus*

2.4 CHEMICALS AND SOLVENTS.

Chemicals, their suppliers and purity used in preparative work are listed in table 2.1. Solvents and purification methods are listed in table 2.2.

Table 2.1 Chemicals and suppliers.

(S)-Alanine (Lancaster)	99%
Ammonium hexafluorophosphate (Fluka)	98+%
Bis(2-hydroxyethyl)ether (Lancaster)	99%
Calcium hydride (Aldrich)	95+%
Chromic chloride.$6H_2O$(Aldrich)	99%
Cobaltous nitrate.$6H_2O$ (Hopkin & Williams)	99%
Cupric Sulphate.$5H_2O$ (Aldrich)	98+%
1,2-Diamino ethane (BDH)	99%
Diethylenetriamine (BDH)	99%
Ethane-1,2-diol (BDH)	99+%
Lithium aluminium hydride (Aldrich)	95%
Manganous chloride.$4H_2O$ (BDH)	99%
Nickel Nitrate.$6H_2O$ (Aldrich)	99+%
(*S*)-Propylene oxide (Fluka)	99%
Sodium in liquid paraffin (Fisons)	99+%

Sodium carbonate (BDH)	99.9%
Sodium chloride (Koch Light)	99+%
Sodium hydride (BDH)	60% dispersion in oil
Sodium hydrogen carbonate (Prolabo)	99%
Sodium nitrite (BDH)	97+%
Sodium sulphate (Aldrich)	99%
Triethylamine (Prolabo)	99%
p-Toluene sulphonyl chloride (Lancaster)	98%
Vanadyl chloride.$2H_2O$ (BDH)	99%
Zinc nitrate.$6H_2O$ (Hopkin & Williams)	99+%
Zinc granules (20 mesh) (Hopkin & Williams)	99%

Table 2.2. Solvents and purification methods.

Absolute Ethanol	Twice distilled from magnesium turnings and iodine, under N_2; stored over 4Å sieves.
Acetonitrile	Distilled from calcium hydride under N_2.

Di-n-butyl ether	Analytical grade.
Dichloromethane	Distilled from calcium hydride under N_2.
Diethyl ether	Distilled from sodium benzophenone under N_2.
Dimethyl formamide	Distilled from calcium hydride in vacuo. Stored over 4Å sieves.
Methanol	Stored over activated 3Å sieves.
40-60°C Petroleum Ether	Distilled under N_2 from sodium/potassium alloy.
Pyridine	Distilled from potassium hydroxide
Tetrahydrofuran	Distilled under N_2 from sodium benzophenone.

Toluene	Distilled from sodium under N_2 and stored over 4Å molecular sieves.

All other solvents used were of technical grade and no further purification was carried out.

2.5 EXPERIMENTAL PROCEDURES.

2.5.1 1,4,7-TRIAZACYCLONONANE AND ITS PRECURSORS.

The preparations outlined below are based upon the Richman & Atkins (1) and Searle & Geue(2) procedures.

(1) N,N',N''-tris(p-tolylsulphonyl)diethylene triamine.

$TsHN(CH_2)_2NTs(CH_2)_2NHTs$

A 2L beaker equipped with mechanical stirrer and dropping funnel was charged with diethylene triamine (15.45g, 0.15mol) and sodium hydroxide (18g, 0.45mol) dissolved in distilled water (600mL). The solution was stirred vigorously and p-toluene sulphonyl chloride (95.25g, 0.5mol) dissolved in diethyl ether (600mL) was added dropwise over a period of 2h. Stirring must be vigorous to ensure complete mixing of the two phases. After a total reaction time of 3h most of the ether had evaporated off. Addition of methanol (250mL) precipitated the ditosylate product, this was filtered, washed with water and methanol then air dried.

Yield 56g, 66%.

Found: C 53.1% H 5.6% N 7.25% Calc. for $C_{25}H_{31}N_3O_6S_3$ C 53.1% H 5.5% N 7.4%.

^{1}H NMR (90MHz, $CDCl_3$, δ): 7.45 (12H, m, Ar-H); 3.10 (4H, m, N-CH_2); 2.97 (4H, m, N-CH_2); 2.58 (6H, s, Ar-CH_3); 2.40 (3H, s, Ar-CH_3).

M.pt. 173-174°C.

(2) 1,2-bis[(p-tolylsulphonyl)oxy]ethane.

$TsO(CH_2)_2OTs$

In a 1L beaker with mechanical stirring and cooling was placed 1,2-dihydroxyethane (15.5g, 0.25mol) in dry pyridine (80mL) the temperature was maintained at 0°C and p-toluene sulphonyl chloride (143g, 0.75mol) was added portionwise over 2h. The mixture was stirred for a further 4h before being poured into ice water (500mL) with vigorous stirring. The solid was filtered, washed with distilled water and dried in air. Recrystallisation from methanol gave the pure ditosylate.

Yield 55g, 60%.

Found: C 51.75% H 4.8% Calc. for $C_{16}H_{18}O_6S_2$ C 51.9% H 4.9%.

^{1}H NMR (200MHz, $CDCl_3$, δ): 7.60 (8H, dd, Ar-H); 4.43 (4H, s, -CH_2-); 2.50 (6H, s, Ar-CH_3).

M.pt. 124-126°C.

(3) N,N',N''-tris(p-tolylsulphonyl)-1,4,7-triazacyclononane.

A 5L three necked round bottomed flask was fitted with a nitrogen inlet/outlet, magnetic stirring bar, thermometer and an oil bath. The flask was purged with nitrogen and charged with N,N',N''-tris(p-tolylsulphonyl)diethylene triamine (84.75g, 0.15mol) dissolved in dry dimethyl formamide (1650mL). Sodium hydride (60% suspension in oil, 24g, 0.6mol) was added in small portions over a period of 1h. Once hydrogen evolution had ceased the temperature was raised to 70°C and maintained for 1h (during this period a 5L three necked round bottom flask was equipped with a nitrogen inlet, a large filter funnel - with a pad of celite 535 - and an adapter fitted to a water aspirator). The warm solution was filtered with suction, the initial reaction flask was cleaned, dried and equipped with a stirring bar, a 1L dropping funnel, a nitrogen inlet/outlet, an oil bath and a thermometer. The filtered solution was re-transferred under a strong flow of nitrogen and heated to 110°C. 1,2-bis[(p-tolylsulphonyl)oxy]ethane (55.57g, 0.15mol) dissolved in dry dimethylformamide (600mL) was added dropwise over a period of 3h. The solution was stirred for a further 3h maintaining heating throughout. The solution was allowed to cool and then reduced in volume to approximately 600mL on the rotary evaporator. The solution was added slowly to ice water (2L) whilst stirring, the solid was filtered and washed with water

(4x300mL), methanol (3x150mL) and diethyl ether (3x150mL). Once dry the product was recrystallised from the minimum volume of hot chloroform followed by addition of three volumes of cold ethanol. The solution was cooled to 0°C, crystallisation commenced after 1h and was completed by refrigeration overnight. The product was collected by filtration and washed with ice cold ethanol (2x100mL) and ether (4x100mL). The product was recrystallised twice more.

Yield 49.6g, 56%.

Found: C 54.5% H 5.35% N 7.0% Calc. for $C_{27}H_{33}N_3O_6S_3$ C 54.8% H 5.6% N 7.1%.

^{1}H NMR (200MHz, $CDCl_3$, δ): 7.31 (12H, dd, Ar-H); 3.20 (12H, s, N-CH_2); 2.18 (9H, s, Ar-CH_3).

M.pt. 216-219°C.

(4a) 1,4,7-triazacyclononane.

A 500mL three necked round bottomed flask was equipped with a magnetic stirring bar, a nitrogen inlet/outlet and an oil bath. The flask was charged with conc. sulphuric acid (200mL) and purged with nitrogen for 15 minutes. N,N',N''-tris(p-tolylsulphonyl)-1,4,7-triazacyclononane (77g, 0.13mol) was added to the flask with stirring. The mixture was heated to 115-120°C for 48h whilst maintaining a nitrogen atmosphere. The flask was allowed to cool

and the reaction mixture was added dropwise with stirring to a cooled beaker containing ethanol (750mL). The 1,4,7-triazacyclononane polyhydrosulphate salt was precipitated as a white solid, diethyl ether (500mL) was added and the solution refrigerated overnight. The precipitated grey/brown solid was filtered off (glass microfibre paper) and washed with ether (3x100mL). The solid was dissolved in the minimum volume of distilled water and the solution basified to pH > 12 with 5M aqueous sodium hydroxide. The solution was extracted with chloroform (3x250mL) discarding the aqueous phase. The organic layer was dried ($MgSO_4$), filtered and solvent removed on a rotary evaporator to yield the required product as a viscous yellow oil. This was transferred rapidly to a small Schlenk tube for storage. The oil solidified to form a crystalline mass which was best kept refrigerated.

Yield 12.5g, 75%.

^{1}H NMR (200MHz, $CDCl_3$, δ): 2.28 (12H, s, -C$\underline{H_2}$-).

(4b) 1,4,7-triazacyclononane trihydrobromide.

An analogous procedure to that for 1,4,7-triazacyclononane was employed except that once the polyhydrosulphate salt was dissolved in water, an equivalent volume of 48% hydrobromic acid was added, this produced almost immediately a precipitate. Crystallisation was completed by storing in a refrigerator for 24h. The solid material was filtered and washed with small

amounts of cold 48% hydrobromic acid, ethanol and ether. The product was air dried.

(4c) 1,4,7-triazacyclononane trihydrochloride.

The dry 1,4,7-triazacyclononane trihydrobromide was dissolved in the minimum volume of boiling 36% hydrochloric acid. The solution was cooled slowly and refrigerated overnight. The solid product was filtered, washed with cold 36% hydrochloric acid, ethanol and ether then dried in air. This recrystallisation procedure was normally performed twice more.

^{1}H NMR (200MHz, D_2O, δ): 3.35 (12H, s, -C$\underline{H}_2$-).

^{13}C NMR (D_2O, δ):41.67 (-$\underline{C}H_2$-).

M.pt. 260-264°C.

2.5.2 PENDANT ARM PRECURSORS.

The synthesis of enantiomerically pure (S)-2-chloroalkanols and subsequent pendant arm precursors [(R)-alkyl oxiranes] was based upon the method of Koppenhoefer and Schurig (3).

(1) (S)-2-chloropropanoic acid.

In a 5L three necked flask, equipped with magnetic stirring bar, 1000mL dropping funnel and thermometer, was placed (S)-alanine (178.2g, 2mol) dissolved in 5M hydrochloric acid (2600mL). The mixture was cooled to 0°C in an ice/salt bath and a pre-cooled solution of sodium nitrite (220g, 3.2mol) in water (800mL) was added dropwise, at a rate of 2mL per min, with vigorous stirring and efficient cooling to keep the temperature below 5°C. After 5h the bath was removed and the reaction was allowed to stand overnight at room temperature.

The contents of the flask were light yellow in colour and under reduced pressure on a water aspirator the unreacted oxides of nitrogen were removed over a period of 4h, leaving the solution clear and colourless.

With vigorous stirring sodium carbonate (200g, 1.9mol) was carefully added in small portions. The reaction mixture was extracted with portions of diethyl ether (8x400mL). The combined ether layers were concentrated to 400mL on a rotary evaporator (bath temp 40-55°C) at atmospheric pressure.

The solution was washed with saturated brine (100mL) which was thereafter re-extracted with diethyl ether (6x100mL). The combined ethereal solutions were dried overnight over calcium chloride. The ether was stripped off using a rotary evaporator (atmospheric pressure) and the oily residue was transferred into a distillation flask and fractionally distilled under reduced pressure. The main fraction boiled at 75-77°C (10mmHg) to give 129g (60%) of a clear oil, this process was carried out once more to produce an overall yield of 257g.

^{1}H NMR (200MHz, $CDCl_3$, δ): 11.97 (1H, s, $CO_2\underline{H}$); 4.41 (1H, q, -C$\underline{H}$CH_3); 1.67 (3H, d, -C$\underline{H}_3$).

^{13}C NMR ($CDCl_3$, δ): 176.5 ($\underline{C}O_2H$); 52.04 ($\underline{C}H$); 21.19 ($\underline{C}H_3$).

(2) (S)-2-Chloro-3-methyl butanoic acid.

The same procedure was used as for (S)-2-chloropropanoic acid. (S)-valine (93.73g, 0.8mol) was dissolved in 5M hydrochloric acid (1900mL). The neutralisation stage required 80g of sodium carbonate and the product distilled at 143-145°C (15mmHg).

Yield 66.4g, 60%.

^{1}H NMR (200MHz, $CDCl_3$, δ): 11.31 (1H, broad, $CO_2\underline{H}$); 4.16 (1H, d, C$\underline{H}$ClCH$(CH_3)_2$); 2.32 (1H, m, C$\underline{H}(CH_3)_2$); 1.04 (6H, m, CH$(C\underline{H}_3)_2$).

^{13}C NMR ($CDCl_3$, δ): 175.65 ($\underline{C}O_2H$); 63.66 ($\underline{C}HClCO_2H$); 32.41 ($\underline{C}H(CH_3)_2$); 19.53 ($\underline{C}H_3$); 17.71 ($\underline{C}H_3$).

(3) (S)-2-chloropropanol.

Into a 2L three necked flask, fitted with magnetic stirring bar, 250mL dropping funnel, nitrogen inlet and condenser (with calcium chloride drying tube), was placed lithium aluminium hydride (10g, 0.26mol) and dry diethyl ether (410mL) added with caution. The slurry was cooled in an ice bath and a solution of (S)-2-chloropropanoic acid (23.9g, 0.22mol) in dry diethyl ether (160mL) was added dropwise with vigorous stirring over a 10min period. After a total reaction time of 15min, the drying tube was removed and distilled water (20mL) was added drop by drop with efficient stirring and cooling. The precipitate was dissolved by addition of 2M sulphuric acid (600mL). The layers were separated out and the aqueous portion was extracted with diethyl ether (2x200mL). The combined ether layers were washed with water (50mL), sodium carbonate (50mL) and sodium bicarbonate (50mL) solutions, each aqueous layer was quickly re-extracted with portions of diethyl ether (2x50mL). The combined ethereal layers were concentrated on a rotary evaporator at atmospheric pressure to approximately 300mL, dried over sodium sulphate and further concentrated to give an oily residue. Fractional distillation afforded 10.5g, 51%.

^{1}H NMR (200MHz, $CDCl_3$, δ): 4.0 (1H, m, C<u>H</u>Cl); 3.59 (2H, m, C<u>H</u>$_2$-OH); 3.48 (1H, s, O<u>H</u>); 1.39 (3H, d, C<u>H</u>$_3$).

^{13}C NMR ($CDCl_3$, δ): 68.1 (<u>C</u>H_2OH); 59.4 (-<u>C</u>H(CH_3)); 21.04 (-CH(<u>C</u>H_3)).

B.pt. 140-142°C.

(4) (S)-2-Chloro-3-methyl butan-1-ol.

The method was similar to that for (S)-2-chloropropan-1-ol. (S)-2-chloro-3-methyl butanoic acid (27.3g, 0.2mol) was reacted with lithium aluminium hydride (9.1g, 0.24mol) for 30 minutes. The addition of distilled water (20mL) was followed by neutralisation using 2M sulphuric acid (60g conc. H_2SO_4 and 540g ice). Distillation yielded a clear oil at 109-111°C (95mmHg).

Yield 16.9g, 69%.

^{1}H NMR (200MHz, $CDCl_3$, δ): 3.85 (1H, m, C<u>H</u>Cl); 3.73 (2H, m, C<u>H</u>$_2$OH); 2.03 (1H, m, C<u>H</u>(CH_3)$_2$); 0.97 (6H, m, CH(C<u>H</u>$_3$)$_2$).

^{13}C NMR ($CDCl_3$, δ): 71.50 (<u>C</u>HCl); 65.26 (<u>C</u>H_2OH); 31.20 (<u>C</u>H(CH_3)$_2$); 19.91 (<u>C</u>H_3); 17.80 (<u>C</u>H_3).

(5) (R)-2-methyl oxirane.

(caution: Oxiranes are suspected carcinogens and as such must be handled with care and this process performed in a well ventilated fume cupboard).

This procedure required specially adapted distillation apparatus (Fig 2.2). The chlorohydrin prepared above undergoes a cyclisation reaction in the presence of base, the oxirane was distilled as it was formed in situ to overcome problems of alkaline hydrolysis of the cyclic product.

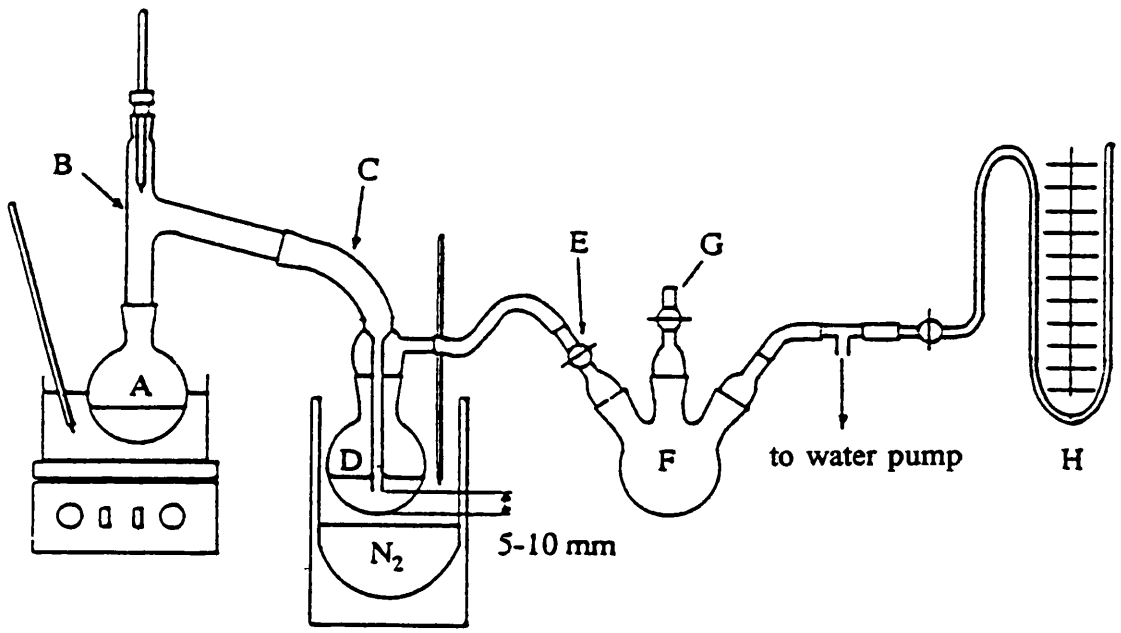

Fig 2.2. *Epoxide still apparatus.*

A narrow necked (B14) 100mL round bottom flask (A) was equipped with a Teflon coated stirring bar, and a Claisen stillhead (B) fitted with a thermometer and connected to a modified receiver adapter (C). A small (50mL) round bottom flask (D) acted as a trap for the oxirane. The specially prepared receiver adapter was designed so that the end of the receiver pipe was 5-10 mm from the bottom of the receiver flask; to prevent any clogging of the receiver inlet and maintain efficient trapping of the product. The vacuum outlet of flask D was connected by means of a stopcock (E) to a 50mL three necked round bottomed flask (F), equipped with a flexible (plastic) pipe carrying a flat pipe clamp (G). The third neck of the flask was fitted via a T-connector to a manometer (H) and a water aspirator.

Flask A was charged with (S)-2-chloropropan-1-ol (14g, 0.15mol) and immersed in an ice bath supported on a stirrer/hotplate and labjack. A low temperature (alcohol) thermometer was positioned at the same height as flask D. Once assembled stopcock E was closed and flask D air-cooled to -80°C by placing it in a Dewar flask partially filled with liquid nitrogen, the top of this flask was insulated with glass wool. The temperature of D was controlled by adjusting the height of the Dewar flask with a labjack.

Pipe clamp G was tightened to give a pressure of 100mmHg. The thermometer was briefly removed from the stillhead and a pre-cooled solution of potassium hydroxide (14.5g, 0.26mol) in water (14mL) was

introduced rapidly to flask A. The thermometer was replaced immediately and efficient cooling of A was maintained throughout. The solution was stirred vigorously to ensure adequate mixing of the two phases in flask A.

Stopcock E was opened carefully for short periods of time (~5 seconds) until the pressure in the system was constant at 100mmHg, whilst A was maintained at 0°C. The ice bath was replaced with a water bath at 15-20°C. As the flask warmed up, the cyclisation commenced with a white precipitate of potassium chloride being formed.

Approximately once every minute stopcock E was opened carefully for 3-5 seconds to maintain a gentle distillation of the oxirane. After about 10 minutes, the temperature of the water bath was raised gradually to 30°C. At all times during the reaction the manometer reading was noted, if water pressure varied at the aspirator the pressure in flask F might rise above 100mmHg. If stopcock E was opened, oxirane in D would be blown back into the reaction vessel. In the event of any pressure increase clamp G was tightened to reduce the pressure in F to 100mmHg.

After an overall reaction time of 40 minutes, stopcock E was closed and pipe clamp G was opened fully. The stillhead thermometer was removed, admitting air into the system. Flask D was allowed to warm gradually to 0° C. The apparatus was dismantled cleaned and reassembled for redistillation of the oxirane.

With stopcock E closed and flask D at room temperature the oxirane was placed in flask A and cooled in an ice bath to 0°C. With the stillhead thermometer removed, calcium hydride (powdered) was added in small portions over 2-4 h, until hydrogen evolution had ceased. The pressure in F was reduced to 100mmHg and the Claisen head thermometer replaced. Flask D was cooled to -80°C and the oxirane was distilled as described previously. Care was taken to ensure the oxirane did not boil too vigorously. Trap D was then allowed to warm to 10°C. The final anhydrous oxirane was collected as a clear mobile liquid, and stored in an air tight bottle in the refrigerator.

Yield 5.1g, 60%.

^{1}H NMR (200MHz, $CDCl_3$, δ): 2.88 (1H, m, -CH_2-C<u>H</u>(CH_3)O-); 2.65 (1H, m, -<u>H</u>-CH-CH(CH_3)O-); 2.33 (1H, m, <u>H</u>-CH-CH(CH_3)O-); 1.21 (3H, d, -C<u>H</u>$_3$).

(6) (R)-2-isopropyl oxirane.

This followed the same method as utilised for (R)-2-methyl oxirane. To (S)-2-chloro-3-methyl butan-1-ol (16.8g, 0.14mol) was added potassium hydroxide (13.6g, 0.24mol) dissolved in distilled water (13.5mL). The bath

temperature was raised to 50°C. After approximately 40 minutes reaction time the pressure was reduced (50mmHg) for a further 5 minutes. Redistillation from calcium hydride was performed by repeating this procedure.

Yield 10g, 85%.

^{1}H NMR (200MHz, $CDCl_3$, δ): 2.60 (2H, m, pr^i $CHC\underline{H}_2O$); 2.41 (1H, m, pr^i $C\underline{H}CH_2O$); 1.37 (1H, m, $C\underline{H}(CH_3)_2$); 0.93 (3H, d, $H_3CCHC\underline{H}_3$); 0.86 (3H, d, $\underline{H}_3CCHCH_3$).

^{13}C NMR ($CDCl_3$, δ): 57.37 ($\underline{C}HCH_2O$); 45.82 ($CH\underline{C}H_2O$); 30.64 ($\underline{C}H(CH_3)_2$); 18.82 ($\underline{C}H_3$); 17.93 ($\underline{C}H_3$).

2.5.3 1-OXA-4,7-DIAZACYCLONONANE AND ITS PRECURSORS.

(1) N,N'-di-(p-tolylsulphonyl)ethane-1,2-diamine.

$TsHN(CH_2)_2NHTs$

In a 2L round bottom flask equipped with mechanical stirrer and dropping funnel was placed 1,2-diaminoethane (13.4mL, 0.2mol) and sodium hydroxide (16g, 0.4mol) dissolved in distilled water (400mL). The solution was stirred vigorously for 2h during which p-toluene sulphonyl chloride

(76.2g, 0.4mol), in diethyl ether (500mL), was added dropwise. The mixture was stirred for a further 2h at room temperature after which addition of methanol (300mL) precipitated the solid ditosylate. Finally the product was washed with water and methanol, then air dried.

Yield 59g, 80%.

Found: C 52.2% H 5.5% N 7.6% Calc. for $C_{16}H_{20}N_2O_4S_2$ C 52.1% H 5.5% N 7.6%.

^{1}H NMR (200MHz, $CDCl_3$, δ): 7.7 (4H, d, Ar-H); 7.3 (4H, d, Ar-H); 4.9 (2H, t, N-H); 3.05 (4H, m, -CH_2-CH_2-); 2.43 (6H,s, Ar-CH_3).

M.pt. 157-160°C.

(2) Ditosyl 2,2'-oxydiethanol.

$TsO(CH_2)_2O(CH_2)_2OTs$

A 2L round bottom flask equipped with mechanical stirrer and dropping funnel was charged with 2,2'-oxydiethanol (26.63g, 0.25mol) and p-toluene sulphonyl chloride (95.25g, 0.5mol) in acetone (200mL). To this mixture was added, dropwise, sodium hydroxide (31g, 0.75mol) in distilled water (95mL, cooled to room temperature), keeping the temperature below 12°C for 6h. After the last addition efficient stirring was maintained until the solution was cold. The mixture was then poured into ice water (500mL), with good mechanical stirring, the white precipitate was filtered off and

dried at 90°C for 12h. Recrystallisation from the minimum amount of hot ethanol gave white needles of pure ditosylate.

Yield 72g, 70%.

Found: C 52.2% H 5.3% Calc. for $C_{18}H_{22}O_7S_2$ C 52.2% H 5.35%.

^{1}H NMR (90MHz, $CDCl_3$, δ): 7.45 (8H, m, Ar-H); 4.3 (4H, m, CH_2OCH_2); 3.65 (4H, m, -CH_2OTs); 2.5 (6H, s, Ar-CH_3).

M.pt. 97-98°C.

(3) N,N'-di(p-tolylsulphonyl)-1-oxa-4,7-diazacyclononane.

To ditosyl-1,2-diamino ethane (36.83g, 0.1mol) in dimethyl formamide (1000mL), under a nitrogen atmosphere, was added sodium hydride (3.84g, 0.1mol), on cessation of hydrogen gas evolution the temperature was raised to 70°C for 1h, excess sodium hydride was removed by filtration. The temperature was raised immediately to 120°C and ditosyl 2,2'-oxydiethanol (41.43g, 0.1mol) in dimethyl formamide (500mL) was added dropwise over 5-6h. The mixture was stirred overnight at 120°C and on cooling sodium hydride (5g, 0.15mol) was added and the temperature was increased slowly to 70°C for 1h. The removal of excess sodium hydride was followed by an increase in temperature to 120°C for a further 4h before cooling. The volume of solvent was reduced to 250mL on a rotary evaporator and then

poured slowly into ice water (1.5L) with vigorous stirring. The crude ditosylate was filtered off, washed with water, ethanol and diethyl ether then recrystallised from the minimum amount of boiling methanol.

Yield 16g, 37%.

Found: C 54.7% H 6.0% N 6.4% Calc. for $C_{20}H_{26}N_2O_5S_2$ C 54.8% H 6.0% N 6.4%.

^{1}H NMR (200MHz, $CDCl_3$, δ): 7.6 (4H, dd, Ar-H); 7.35 (4H, dd, Ar-H); 3.9 (4H, t, O-CH_2); 3.46 (4H, s, NCH_2CH_2N); 3.25 (4H, t, NCH_2CH_2O); 2.43 (6H, s, ArCH_3).

M.pt. 197-199°C.

(4) 1-oxa-4,7-diazacyclononane.

This procedure was based on the method employed by Wieghardt and co-workers (4).

Butan-1-ol (140mL) and di-n-butyl ether (93mL) were placed in a 2L round bottom flask equipped with thermometer, stirrer, condenser and drying tube. The cyclic ditosylate (20g, 0.05mol) was added and the mixture heated to 125°C. Sodium metal (18g, 0.78mol) was cut into small pieces (stored under N_2) each lump was allowed to dissolve before the next was added. After completion of the addition stirring was maintained for 18h and the temperature raised slowly to 135°C. On cooling to room temperature, 36%

hydrochloric acid (80mL) was added slowly ensuring that the solution temperature did not exceed 80°C. To assist stirring portions of water (2x10mL) were added, the mixture was stirred overnight at room temperature (the pH of the aqueous phase was kept below 3). The supernatant (organic phase) was separated and solvent removed using a rotary evaporator, the residue was dissolved by refluxing with distilled water. When cool the solution was treated with sodium hydroxide (9g) and filtered. To this aqueous phase was added dry toluene (70mL), and the water was removed using Dean-Stark apparatus. When no more water distilled over, more sodium hydroxide (2g) was added and the solution filtered. The residue was suspended in hot dry toluene (70mL) and filtered, this was repeated twice more and the combined toluene filtrates were reduced to 15mL by rotary evaporation and placed in a 100mL bulb of vacuum apparatus. During the distillation toluene escaped first and at 108°C (76mmHg) a clear/slightly yellow liquid distilled over.

Yield 2g, 34%.

^{1}H NMR (200MHz, $CDCl_3$, δ): 3.83 (4H, m, -OC$\underline{H}_2$-); 3.55 (4H, s, NC$\underline{H}_2$C$\underline{H}_2$N); 3.30 (4H, m, -NC$\underline{H}_2$CH_2O-).

2.5.4 N-SUBSTITUTED MACROCYCLES.

The introduction of pendant groups via reaction with epoxides was based upon the method of Hancock and co-workers (**5**).

[Note on the preparation of ligands]

The solution containing mixture of macrocycle and epoxides was initially allowed to stand in the refrigerator overnight. It was subsequently discovered that yields improved as well as purity of the desired product if a longer reaction time of 6-7 days was employed. Additionally the reaction was allowed to proceed at room temperature. Unfortunately as a consequence of their highly hygroscopic nature elemental analyses of these ligands was not possible.

(1) N,N',N''-tris[(2S)-2-hydroxypropyl]-1,4,7-triazacyclononane (L^1H_3).

In a 100mL round bottom flask 1,4,7-triazacyclononane trihydrochloride (5.71g, 24mmol) was dissolved in a minimum volume of water (5mL). Sodium hydroxide (2.88g, 72mmol) was added slowly to this solution with cooling. On addition of all the sodium hydroxide, dry ethanol (20mL) was added and the solution refrigerated overnight. The precipitated sodium chloride was filtered off and washed with a small portion of cold ethanol.

The solvents were removed to give 1,4,7-triazacyclononane as a cloudy oil (presence of residual NaCl). This was taken up in dry absolute ethanol and cooled (5°C) by means of an ice bath. To this solution was added, in dropwise fashion, (S)-propylene oxide (4.15g, 71mmol) which was previously stored at 5°C. The reaction vessel was stoppered and placed in the refrigerator overnight. The solution was then allowed to stand at room temperature for a further 6 days. Solvent removal was undertaken (avoiding excessive heating) to yield a tacky mass of N,N',N''-tris(2S)-2-hydroxypropyl-1,4,7-triazacyclononane which was recrystallised from a small volume of isopropyl alcohol to yield the required product.

Yield 4.5g (62%).

^{1}H NMR (200MHz, $CDCl_3$, δ): 3.80 (3H, m, -C<u>H</u>(CH_3)); 2.24-2.14 (18H, m, -C<u>H</u>$_2$-N) 1.03 (9H, d, -C<u>H</u>$_3$).

^{13}C NMR ($CDCl_3$, δ): 66.65 (<u>C</u>H_2, arm); 63.50 (<u>C</u>HCH_3, arm); 52.98 (<u>C</u>H_2, ring, b); 19.99 (<u>C</u>H_3, arm).

(2) N,N',N''-tris[(2R)-2-hydroxypropyl]-1,4,7-triazacyclononane (L^1H_3).

In a 25mL round bottom flask was placed 1,4,7-triazacyclononane (2g, 16mmol) dissolved in dry absolute ethanol (10mL). The solution was cooled to 5°C and (R)-2-methyl oxirane (2.73g, 47mmol) was added dropwise and the flask securely stoppered. The flask was allowed to stand at room

temperature for 7 days. The solvent was removed to afford the required product as a viscous slightly yellow oil. It was found that upon refrigeration this oil crystallised to a solid although no sharp melting point was obtained. Yield 2.6g, 54%.

(3) N,N',N''-tris[(2R)-2-hydroxy-3-methylbutyl]-1,4,7-triazacyclononane L^2H_3.

A similar procedure to that for L^1H_3 was employed. In this case 1,4,7-triazacyclononane (0.65g, 5mmol) was reacted with (1.29g, 15mmol) of 2-(R)-isopropyl oxirane. The mixture was kept at room temperature for 7 days. Removal of solvent gave the product as a solid with no sharp melting point. Yield 1.06g, 55%

^{1}H NMR (200MHz, $CDCl_3$, δ): 5.47 (3H, s, -O<u>H</u>); 3.33 (3H, m, -C<u>H</u>-OH); 2.82-2.33 (18H, m, N-C<u>H</u>$_2$); 1.53 (3H, m, -C<u>H</u>$(CH_3)_2$); 0.83 (18H, m, CH$(C\underline{H}_3)_2$).

^{13}C NMR ($CDCl_3$, δ): 71.87 (-<u>C</u>H-OH); 62.53 (N-<u>C</u>H_2); 53.11 (N-<u>C</u>H_2); 31.96 (-<u>C</u>H$(CH_3)_2$); 18.40 (<u>C</u>H_3); 18.08 (<u>C</u>H_3).

(4) N,N'-Di-[(2R)-2-hydroxy-3-methyl butyl]-1-oxa-4,7-diazacyclononane L^4H_2.

A 50mL round bottomed flask was charged with a solution of 1-oxa-4,7-diazacyclononane (0.5g, 3.85mmol) in absolute ethanol (10mL). To this solution (R)-isopropyl oxirane was added, with stirring, the flask was sealed and left at room temperature for 5 days. The solvent was stripped off under reduced pressure to yield a viscous oil which required no further purification.

Yield 0.64g, 55%.

^{1}H NMR (200MHz, $CDCl_3$, δ): 3.75 (4H, m, ring $C\underline{H}_2OC\underline{H}_2$); 3.4 (4H, m, $NC\underline{H}_2CH_2O$); 2.3-3.0 (6H, m, arm $C\underline{H}_2$ & $NC\underline{H}_2C\underline{H}_2N$); 1.62 (1H, m, $C\underline{H}(CH_3)_2$); 1.27 (1H, t, $CH_2C\underline{H}C(CH_3)_2$); 1.01 (12H, dd, $C\underline{H}_3$).

^{13}C NMR ($CDCl_3$, δ): 75.2 ($\underline{C}H_2O\underline{C}H_2$ ring); 72.68 (O$\underline{C}$HCH arm); 63.18 ($NCH_2\underline{C}H_2O$); 57.62 ($N\underline{C}H_2CH_2O$); 55.91 ($N\underline{C}H_2\underline{C}H_2$); 32.26 ($\underline{C}H(CH_3)_2$); 18.49 ($\underline{C}H_3$); 18.28 ($\underline{C}H_3$).

2.5.5 COMPLEXES WITH L^1H_3 AND L^2H_3.

(1) $[Cr(III)L^1H_3L^1Cr(III)][PF_6]_3$.

Chromium chloride hexahydrate (0.26g, 0.97mmol) was dissolved in dimethyl sulphoxide (30mL) the temperature was raised to 170°C to dehydrate the chromium salt. On cooling to 70°C, L^1H_3 (0.3g, 0.97mmol) in ethanol (10mL) was added, the resulting mixture was taken to 160°C for 30min, cooled then stoppered and left overnight. The complex was obtained by column chromatography (SP Sephadex cation exchange resin and 0.1M sodium chloride solution as eluent). Recrystallisation from acetonitrile gave small purple prisms suitable for structural determination.

Yield 125mg.

Found: C 31.8% H 5.55% N 7.6% P 8.3% Calc. for $C_{30}H_{63}Cr_2F_{18}N_6O_6P_3$ C 31.5% H 5.5% N 7.4% P 8.1%.

IR (KBr): ν=841cm^{-1} (P-F).

Crystal data for $C_{30}H_{63}Cr_2F_{18}N_6O_6P_3$: M=1142.76; space group $P2_13$ (N^{o} 198, T^4); a=16.406(3)Å; V=4416(2)Å^3; Z=4; $\rho_{calc.}$=1.72g/cm^3; $\mu(MoK_\alpha)$=7.10cm^{-1}; R(Rw)=0.029(0.035).

(2) $[Fe(III)L^1H_3L^1Fe(III)][PF_6]_3$.

To an aqueous solution of ferric chloride hexahydrate (88mg, 0.33mmol) was added L^1H_3 (0.1g, 0.33mmol) also in distilled water. The resulting mixture was acidified with a small amount of conc. hydrochloric acid and the temperature raised to 80°C for 30min. On cooling excess ammonium hexafluorophosphate was added giving a yellow precipitate which was collected.

Yield 162mg, 43%.

Found: C 30.9% H 5.2% N 7.2% P 8.05% Calc. For $C_{30}H_{63}Fe_2F_{18}N_6O_6P_3$ C 31.3% H 5.5% N 7.3% P 8.1%.

IR (KBr): $\nu = 839cm^{-1}$ (P-F).

(3) $[Mn(II)L^1H_3L^1Mn(IV)][PF_6]_3$.

To a solution manganous chloride hexahydrate (0.23g, 1mmol) in distilled water (10mL), was added a solution of L^1H_3.HCl (0.34g, 1mmol) also in distilled water (10mL) and the pH of the solution was adjusted to 8 with sodium hydroxide. The solution, which was initially colourless, slowly darkened, becoming deep red after about 12h. Solid ammonium hexafluorophosphate was added to the solution and the precipitated $[PF_6]^-$

salt was filtered off and recrystallised from boiling acetonitrile to give small dark red prisms.

Yield 350mg, 65%.

$C_{30}H_{63}F_{18}Mn_2N_6O_6P_3$

Found: C 31.3% H 5.5% N 7.2% P 8.0% Calc. for C 31.3% H 5.6% N 7.3% P 8.1%.

Crystal data for $C_{30}H_{63}F_{18}Mn_2N_6O_6P_3$: M=1149.6; space group R3; a=10.427(1)Å; c=36.637(7)Å; V=3479(4)Å^3; Z=3; $\rho_{calc.}$=1.65g/cm^3; $\mu(MoK_\alpha)$=7.4cm^{-1}; R(Rw)=0.038(0.049).

(4) $[Zn(II)L^1H_3L^1V(IV)][PF_6]_3$.

An aqueous vanadyl chloride solution (57mg, 0.33mmol) was reduced with zinc amalgam and the resulting mixture reacted with an aqueous solution of L^1H_3 (0.1g, 0.33mol). The temperature was raised to 90°C for 30min and on cooling ammonium hexafluorophosphate salt was added. A mixture of yellow and purple solids were obtained and separated by differential solubility in acetone. The purple compound was satisfactorily recrystallised from acetonitrile giving small cubic shaped single crystals.

Yield 72mg, 20%.

Found: C 31.4% H 5.75% N 7.35% Calc. for $C_{30}H_{63}F_{18}N_6O_6P_3VZn$ C 31.2% H 5.5% N 7.3%.

Crystal data for $C_{30}H_{63}F_{18}N_6O_6P_3VZn$: M=1155.1; space group R3; a=10.430(1)Å; c=36.852(2)Å; V=3471.8(5)Å^3; Z=3; $\rho_{calc.}$=1.66g/cm^3; $\mu(MoK_\alpha)$=9.44cm^{-1}; R(Rw)=0.074(0.075).

(5) [Mn(IV)L^2][PF$_6$].H$_2$O.

Into a 25mL beaker was placed $MnCl_2.4H_2O$ (49.5mg, 0.25mmol) dissolved in distilled water (2mL). To this was added L^2H_3 (97mg, 0.25mmol), almost instantaneously a dark brown colour was produced. After evaporating slowly to dryness the residue was redissolved in H_2O (3mL) and solid ammonium hexafluorophosphate was added. A brown precipitate formed overnight and was filtered off, washed with a small portion of water and air dried. Recrystallisation was effected from the evaporation of an acetone solution to give the complex as lustrous black crystals.

Yield 78.3mg, 52%.

Found: C 42.3% H 7.5% N 7.0% F 18.8% Calc. For $C_{21}H_{44}F_6MnN_3O_4P$ C 41.9% H 7.4% N 7.0% F 18.9%.

IR (KBr): ν=3433, 1630cm^{-1}; ν=839cm^{-1} (P-F).

Crystal data for $C_{21}H_{44}F_6MnN_3O_4P$: M=602.5; space group $P2_1$ (N^o 4, C^2_2); a=8.4160(7)Å; b=11.992(1)Å; c=14.222(1)Å; V=1393.1(2)Å^3; Z=2; $\rho_{calc.}$=1.44g/cm^3; $\mu(MoK_\alpha)$=5.80cm^{-1}; R(Rw)=0.040.

2.5.6 COMPLEXES WITH L^4H_2.

(1) $[CoL^4H_2.H_2O][PF_6]_2$.

$CoCl_2.6H_2O$ (0.24g, 1mmol) was dissolved in absolute ethanol (10mL) and placed in a 50mL round bottomed flask equipped with a magnetic stirring bar. Addition of L^4H_2 (0.3g, 1mmol) in absolute ethanol (10mL) gave an immediate colour change, initially to red then after heating (50°C) for 1h to violet. On cooling the flask was stored at room temperature overnight. Removal of the solvent, yielded a very tacky violet residue which was taken up in acetonitrile. The addition of solid ammonium hexafluorophosphate precipitated a pink solid, leaving a purple coloured solution. The solid was filtered washed with a little cold acetonitrile and dried in vacuo.

Yield 80mg, 12%.

Found: C 30.1% H 5.95% N 4.5% Calc. For $C_{16}H_{26}CoF_{12}N_2O_4P_2$ C 28.7% H 5.4% N 4.2%.

IR (KBr): ν=3305, 1609cm^{-1} (H_2O); ν=839cm^{-1} (P-F).

(2) $[Ni(II)L^4H_2.H_2O][PF_6]_2$.

Into a 50mL round bottomed flask, equipped with a hotplate/stirrer and teflon stirring bar, was placed L^4H_2 (0.3g, 1mmol) in methanol (15mL). To

this solution was added $Ni(II)(H_2O)_6.SO_4$ (0.26g, 1mmol) dissolved in methanol (15mL) (heating was required to ensure complete dissolution). The resulting mixture turned bright blue almost immediately. Heating at 50°C was maintained in conjunction with stirring for 1h. After storing overnight at room temperature solid $[NH_4][PF_6]$ was added yielding a pale blue precipitate which was filtered and washed with a little cold methanol before being air dried.

Yield 0.134g, 20%

Found: C 28.4% H 5.6% N 7.8% P 8.6% Calc. for $C_{16}H_{44}F_{12}N_4NiO_4P_2$ C 27.3% H 6.25% N 7.95% P 8.8%.

{NB. These results were calculated assuming excess ammonium cations present i.e. $[NH_4PF_6]_2$}

IR (KBr): ν=3326, 1620cm^{-1} (H_2O); ν=840cm^{-1} (P-F).

(3) $Cu(II)L^4H_2.(NO_3)_2$.

A 25mL round bottomed flask was charged with $CuSO_4.5H_2O$ (0.1g, 0.4mmol) dissolved in absolute ethanol (5mL). To this solution was added, with stirring L^4H_2 (0.14g, 0.4mmol). The mixture turned deep blue almost instantaneously, the temperature was raised to 50°C for approximately 1h. The flask was stored overnight at room temperature. The solvent was removed under reduced pressure and the blue residue was taken up in the

minimum volume of distilled water (2mL). To this was added excess sodium nitrate in an attempt to precipitate the complex as a nitrate salt. On evaporation of the solution an amorphous blue solid was obtained.

Yield 45mg, 23%.

Found: C 38.2% H 7.55% N 11.2% Calc. for $C_{16}H_{34}CuN_4O_9$ C 37.8% H 7.1% N 11.0%.

IR (KBr): ν=3493cm^{-1} (H_2O); ν=1364cm^{-1} (N-O).

References

(1) J.E.Richman and T.J.Atkins, *J.Am.Chem.Soc.*, 1974, **96**, 2268.

(2) G.H.Searle and R.J.Geue, *Aust.J.Chem.*, 1984, **37**, 959.

(3) B.Koppenhoefer and V.Schurig, *Org.Synth.*, 1988, **66**, 151 & 160.

(4) D.Reinen, A.Ozarowski, B.Jakob, J.Pebler, H.Stratemeier, K.Wieghardt and I.Tolksdorf, *Inorg.Chem.*, 1987, **26**, 4010.

(5) B.A.Sayer, J.P.Michael and R.D.Hancock, *Inorg.Chim.Acta.*, 1983, **77**, L63.

CHAPTER 3

CHROMIUM COMPLEXES WITH L^1H_3.

3.1 CHROMIUM CHEMISTRY.

A well known feature of many Cr(III) complexes is their kinetic inertness. It is primarily this characteristic which has resulted in the relative lack of macrocyclic chromium(III) compounds. In spite of the synthetic difficulties, however, there are a few known complexes involving triazamacrocycles. Many of the reported compounds have been dimeric or trimeric species incorporating hydroxide bridges, including $[Cr_2(TACN)_2(OH)_2(CO_3)]I_2.H_2O$ (**1**); $[Cr_2(TACN)_2(OH)_3(H_2O)]I_3.3H_2O$ (**2**) and $[Cr_3(TACN)_3(OH)_5]I_4.5H_2O$ (**3**), all of which have been structurally characterised.

Of more relevance to this work are those complexes which involve pendant arm ligands. One such compound is [Cr (TCTA)] (**4**); the crystal structure indicates the metal to be in a pseudo-octahedral environment, with a trigonal twist of 11°; the short pendant groups of this ligand prevent a pure octahedral symmetry being adopted.

The electrochemistry of this species shows a reversible Cr^{III}/Cr^{II} wave at -1.17V (vs NHE), showing the $[Cr(II)TCTA]^-$ species to be highly reducing, thus indicating this particular ligand's preference for small metal ions. The complex $[Cr(THETACN)_2]_2[PF_6]_3$ has also been structurally determined (**5**). Assigned a dimeric structure with connecting hydrogen bridges, verified by magnetic susceptibility measurements the crystallographic analysis could not be sufficiently well refined due to the presence of a highly disordered counter-ion.

Compounds which have not been structurally investigated include $[Cr(TAETACN)]^{3+}$ (**6**) $[Cr(TPTACN)]^{3+}$ (**7**) and $[CrL^2H_3]$ (L^2H_3=N,N',N''-tris[(2R)-2-hydroxy-3-methylbutyl]-1,4,7-triazacyclononane (**8**). Like the analogous TCTA complex, the cyclic voltammogram of [Cr(TPTACN)] shows this ligand to have a strong preference for the smaller Cr(III) ion with a reversible one electron wave corresponding to the Cr(III)/Cr(II) couple at -1.32V (vs NHE). The chromium complexes with L^2H_3 (bulky arm) and chiral derivative of TCTA {(2S)-2-methyl-N,N',N''-tris(2-carboxymethyl)-1,4,7-triazacyclononane} will be discussed in section 3.4.2.

3.2 SYNTHESIS OF COMPLEX.

The initial starting material in the preparation of the chromium complex was hydrated chromium chloride $\{[CrCl_2.(H_2O)_4]Cl.2H_2O\}$ which is kinetically inert due to the inherent stability of the d^3 configuration of the Cr(III) centre. Therefore this starting product must be modified, in order to promote facile ligand replacement; this was achieved by dehydrating the chromium salt in DMSO at 170°C. The high temperature promotes ligand replacement of water with dimethyl sulphoxide; the product $CrCl_3.(DMSO)_3$ is more suitable for reaction with L^1H_3 due to the more labile nature of the DMSO ligands present. It must be noted, however, that even after ligand replacement the overall yield

for the subsequent complexation reaction is very low. Column chromatography, using SP Sephadex cation exchange resin and 0.1M NaCl as eluent, was required to isolate the desired complex. The material separated into 2 pink fast moving bands and 1 purple slower moving band. The pink bands were collected first, but analysis by CD spectroscopy indicated that no chiral species were present and they were discarded. The purple band was found to be optically active; an excess of ammonium hexafluorophosphate salt was added and a purple precipitate filtered off then recrystallised from acetonitrile giving crystals of suitable quality for X-ray crystallographic analysis.

3.3 STRUCTURAL ANALYSIS.

An immediate and striking feature of the structure (fig3.1) is the dimeric nature of the complex - hydrogen bridges connect and stabilise the two subunits. Each metal centre is coordinated facially by three nitrogen and three oxygen donors; the geometry at each centre is pseudo-octahedral. A twist angle of 15° has been calculated for each half of the dimer and thus the environment about each chromium atom is essentially the same. The degree of trigonal distortion is greater than measured for the isomorphous $[CoL^1H_3.L^1Co]^{3+}$ (**9**) complex (ϕ=10-11°) and the isoelectronic Mn(IV) complex $[MnL^1]^+$ (ϕ=11°). Overall, models indicate that the most stable dimeric configuration results when one

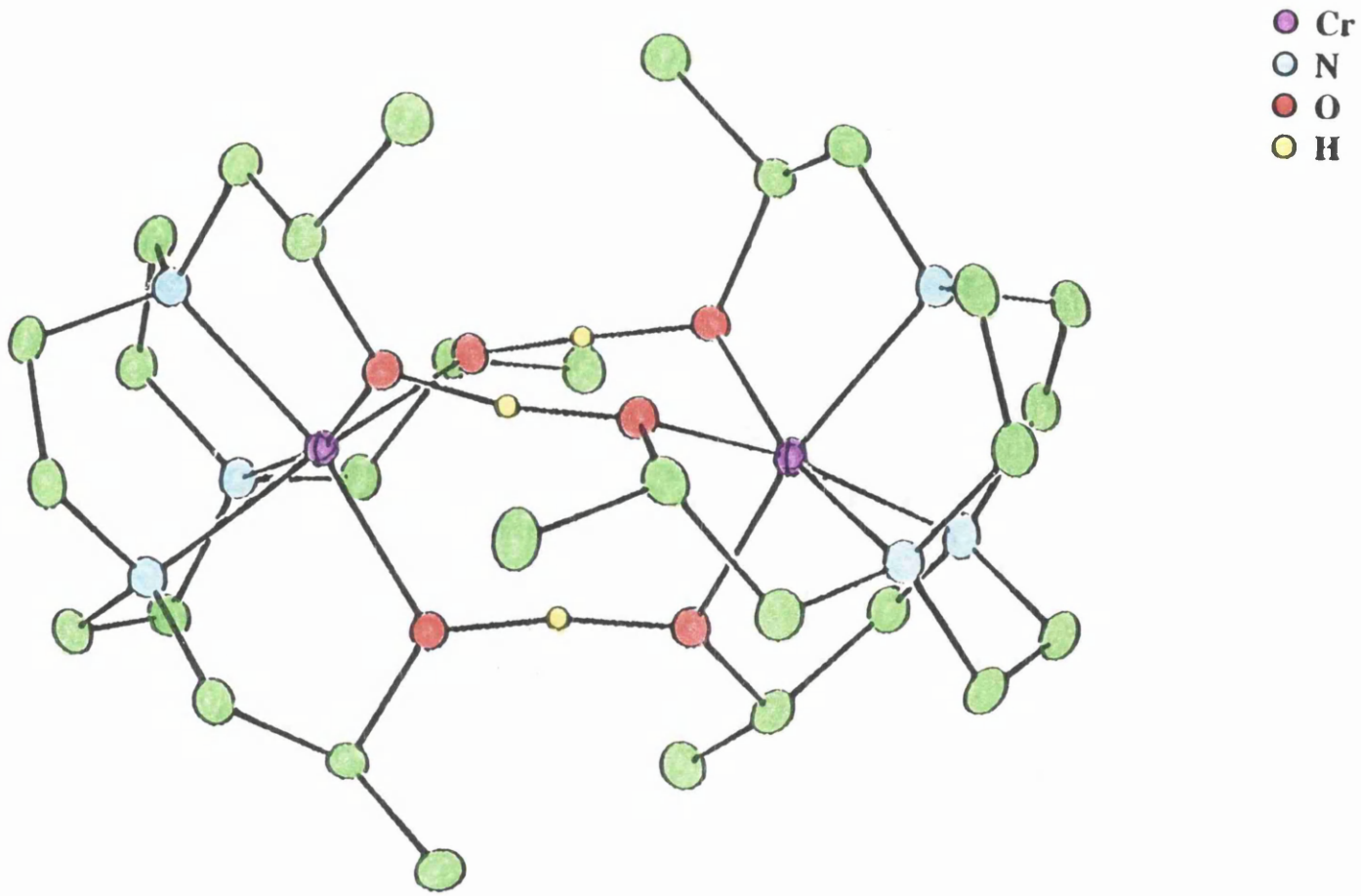

Fig. 3.1. *Crystal structure of* $[Cr(III)L^1H_3L^1Cr(III)]^{3+}$ *cation.*

subunit is trigonal prismatic and the other is pseudo-octahedral. The relatively large degree of twist (for a d^3 species) is believed to be a consequence of the two halves locking into the dimer structure. This suggests that the angle ϕ should be reduced in protonated or deprotonated monomers (vide infra). A selection of bond lengths and bond angles is presented in table 3.1.

Cr(1)-N(1)	2.071(3)	Cr(1)-O(1)	1.971(2)
Cr(2)-N(2)	2.070(3)	Cr(2)-O(2)	1.969(2)
O(1)-H(1)	1.22(5)	O(2)-H(1)	1.25(5)
N(1)-Cr(1)-N(1)	84.2(1)	O(1)-Cr(1)-O(1)	95.5(1)
N(2)-Cr(2)-N(2)	84.1(1)	O(2)-Cr(2)-O(2)	95.3(1)
O(1)-H(1)-)(2)	168.2(37)		

Table 3.1. *Selected bond lengths (Å) and bond angles (deg) for* $[Cr(III)L^1H_3.L^1Cr(III)]^{3+}$.

The $[CrL^1H_3.L^1Cr]^{3+}$ and $[CoL^1H_3.L^1Co]^{3+}$ species are isomorphous; both have a $\Delta(\lambda\delta)$ configuration. In the dimer there are six chiral carbons all of which have the S-configuration, there are also two distinct chelate rings; endocyclic and exocyclic. The endocyclic rings are defined as those formed by the parent macrocyclic ring and the metal centre, while the exocyclic rings are those described by the pendant arms. The endocyclic rings are fixed in the λ conformation; the exocyclic rings all being in the δ conformation. The sign of

the twist of these rings is primarily dictated by the chirality of the asymmetric carbon atom, although it is no determinant of the magnitude of such a twist. Examination of the crystal structure shows the twist around each chromium centre to be clockwise when viewed down the C_3 axis (fig3.2). Thus, the overall configuration of each half of the dimer is Δ, the symmetry of the complex is described as $[\Delta(\lambda\delta)]_2$.

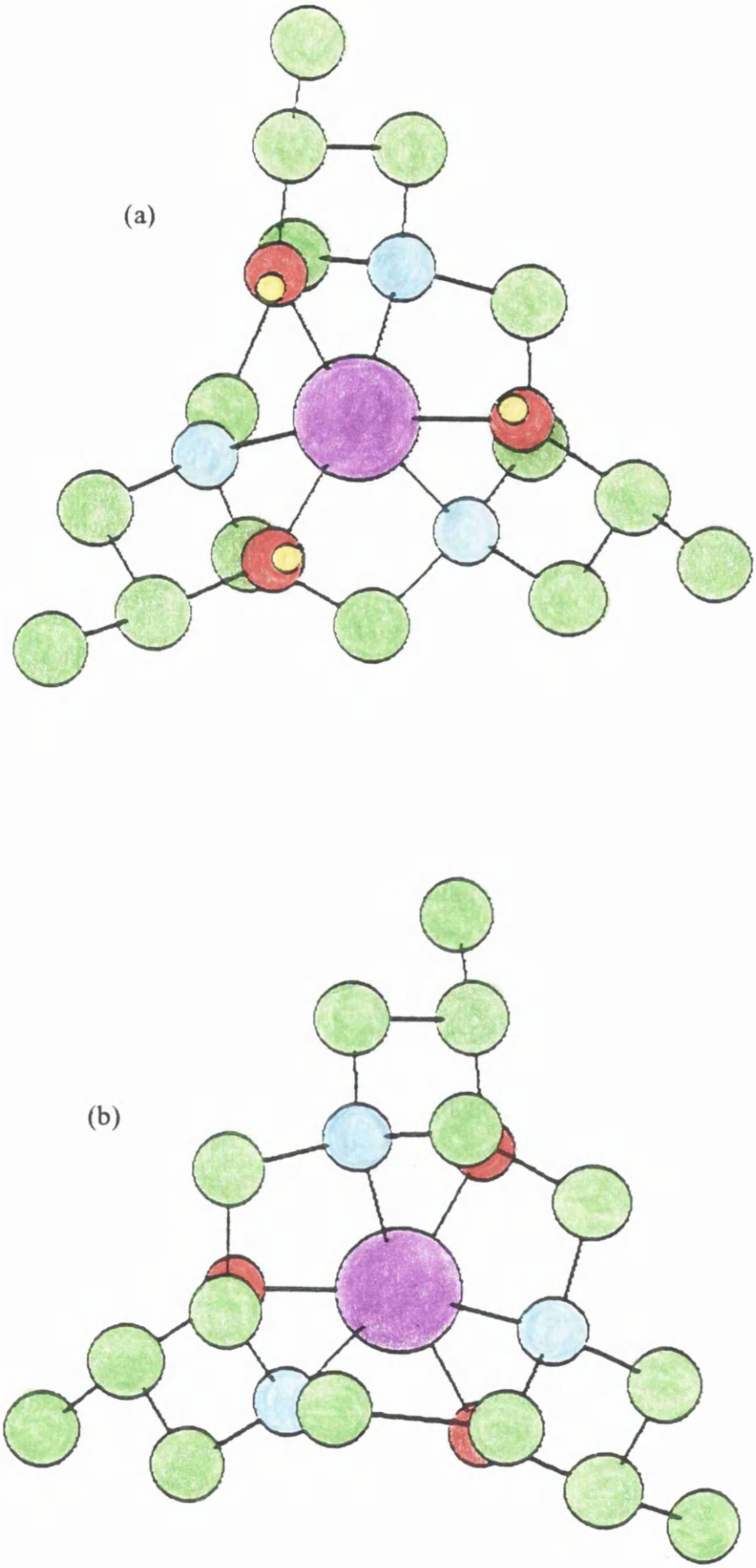

Fig. 3.2. *Views along C_3 axis. (a) towards O, O', O'' face (b) towards N, N'N'' face.*

3.4 ELECTRONIC SPECTROSCOPY

3.4.1 ABSORPTION SPECTRA.

The $[Cr(III)L^1H_3.L^1Cr(III)]^{3+}$ cation has some unusual acid/base properties: on acidification both components become protonated with a resultant dissociation into two monomeric $[Cr(III)L^1H_3]^{3+}$ subunits. With basification complete deprotonation occurs, leading to hydrogen bond rupture and ultimately dimer dissociation. At these higher pH levels the two components are thought to be $[Cr(III)L^1]$ species; these changes have been followed spectroscopically.

The absorption and circular dichroism spectrum of $[Cr(III)L^1H_3.L^1Cr(III)][PF_6]_3$ in acetonitrile is shown in figure 3.3. Acidification was performed by adding a few drops of trifluoroacetic acid to the MeCN solution, the resulting absorption and CD spectra are displayed in figure 3.4. Lastly basification of the initial neutral solution with a few drops of triethylamine, yields deprotonated monomers whose absorption and circular dichroism spectra are shown in figure 3.5. Although the overall symmetry of the complex is C_3 the microenvironment about the metal centre is such that octahedral labels will be used in assigning the various absorption bands.

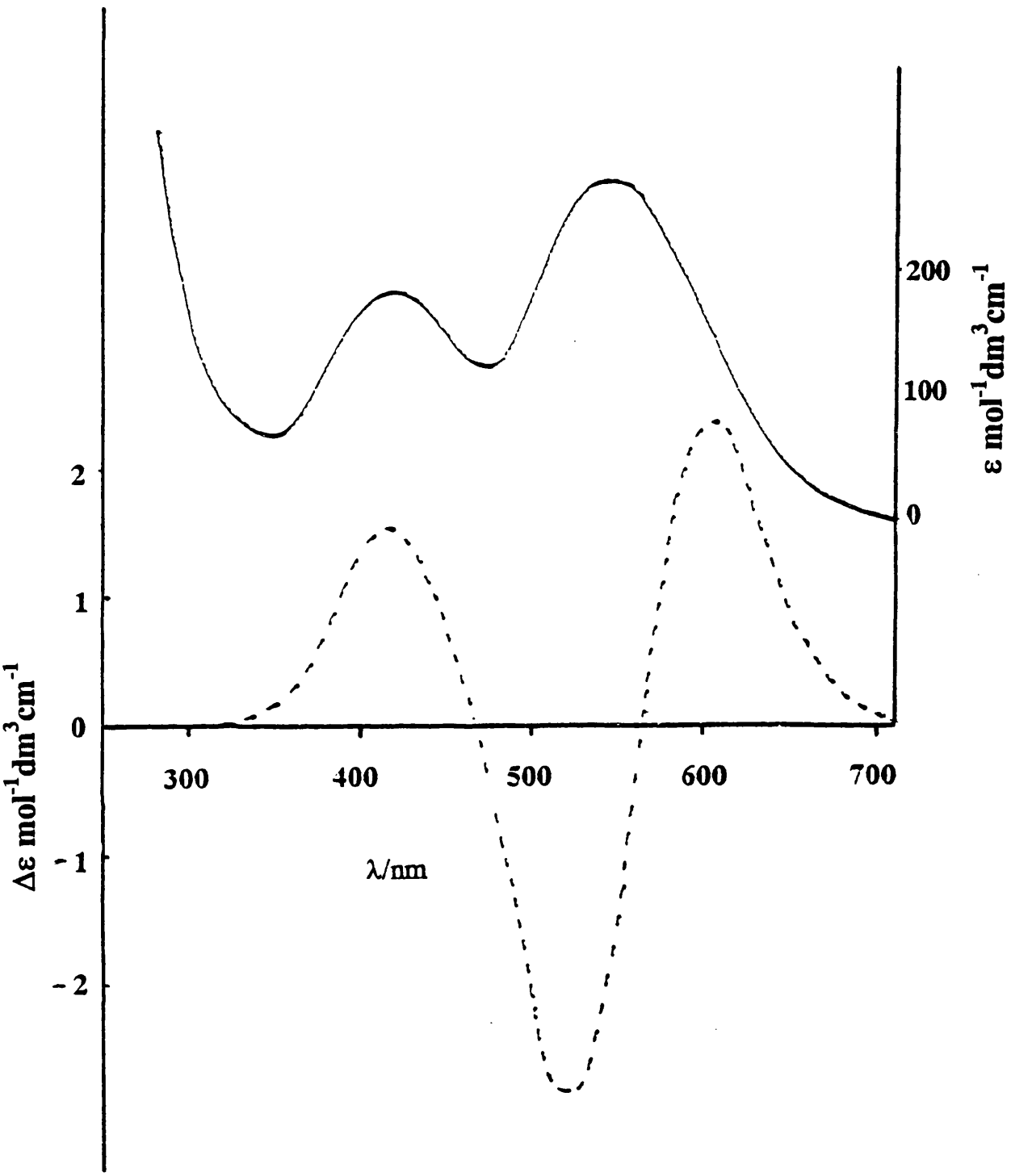

Fig. 3.3. *Absorption / CD spectra of* $[Cr(III)L^1H_3L^1Cr(III)]^{3+}$ *in MeCN.*

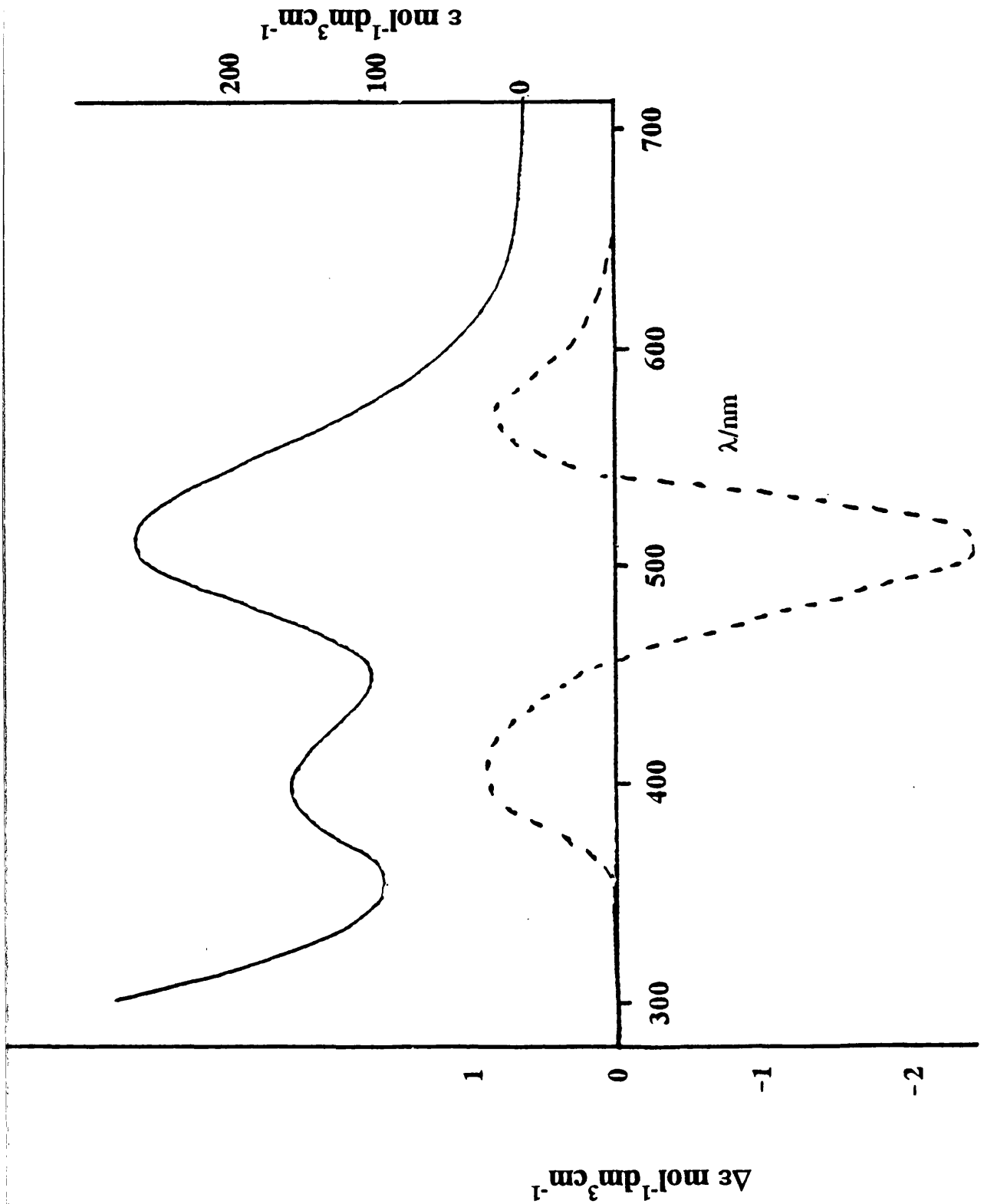

Fig. 3.4. *Absorption / CD spectra of* $[Cr(III)L^1H_3]^{3+}$ *(acidic medium).*

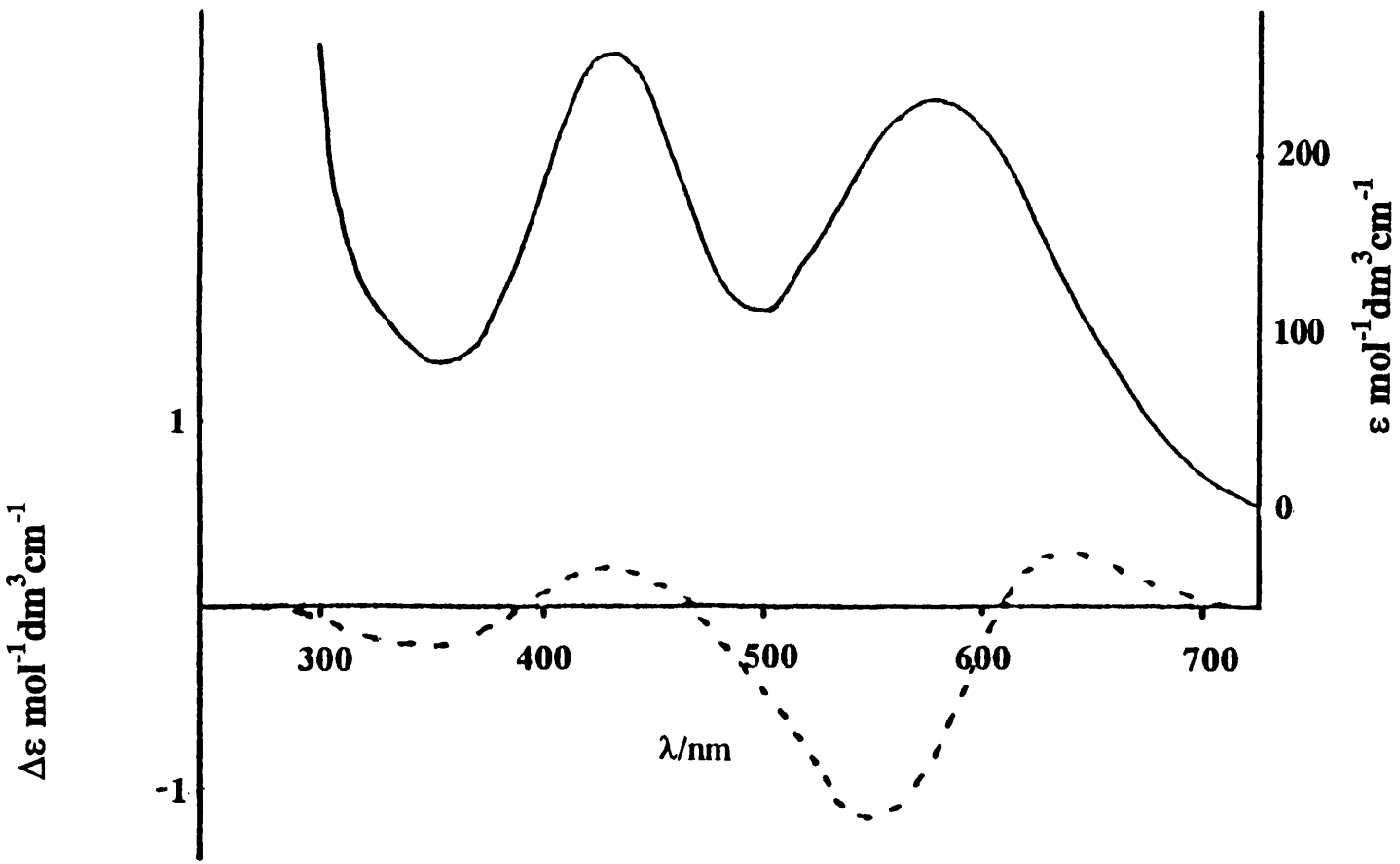

Fig. 3.5. *Absorption / CD spectra of* $[Cr(III)L^1H_3]^{3+}$ *(basic medium).*

The low energy $^4A_{2g} \rightarrow {}^4T_{2g}$ transition of the dimer (544nm) lies approximately midway between the analogous bands of the protonated and deprotonated forms at 516 and 576nm respectively. This may be rationalised by assigning the dimer a protonation level of approximately 1.5 per side. Thus the donor type per metal centre will be half-way between the all alcohol nature of the acidic monomer and the all alkoxide functions of the basic monomer.

The overall ligand field splitting may be calculated from the energy of the lowest ($^4A_{2g} \rightarrow {}^4T_{2g}$) transition. Thus $\Delta_o(cm^{-1})$ is 17,360 (Racah parameter $B=538cm^{-1}$) for the all alkoxide donor species (basic medium); 18,380 (Racah parameter $B=511cm^{-1}$) in the case of the hydrogen bridged dimer complex in "neutral" solution, and 19380 (Racah parameter $B=580cm^{-1}$) of the protonated (alcohol ligators) monomer in acid solution.

These results may be explained by examining the donor properties of each form of the ligand, L^1H_3.

Alkoxide ligators, have two p^{π} orbitals available for π-bonding and are thus good π donors. In general a p^{π}-d^{π} interaction is a repulsive process. Electron donation from the p^{π} orbitals of the ligand to the metal t_{2g} set, weakens the metal-nitrogen (σ) bonds, due to the greater covalency of the π bonds. Hence the smaller Δ_o value for the monomer $[Cr(III)L^1]$.

The interaction between the lone pairs of the oxygen and the t_{2g} set has a two fold effect. The lone pairs help to shield the d electrons from the positive

charge of the metal, in effect expanding the d-shell. The reverse process of transferring electron density back to the ligand also helps to reduce the magnitude of intra d-shell electronic repulsion. Thus bonds with a high degree of covalency help to reduce the effective charge experienced by the d-electrons. Overall a reduction in electronic repulsion is observed; the Racah parameter B, which is a measure of this repulsion, is reduced in value.

Alcohol donors are less able to partake in such a π-bonding interaction. Therefore the degree to which metal-nitrogen (σ) bonding is affected in $[Cr(III)L^1H_3]^{3+}$ is much reduced, hence the higher value of Δ_o.

The Racah B value is also greater due to the less covalent nature, overall, of the metal ligand bonds.

In the absorption spectra of Cr(III) complexes usually three transitions may be observed, in the visible region, they are $^4A_{2g}\rightarrow{}^4T_{1g}(P)$ and $^4A_{2g}\rightarrow{}^4T_{1g}(F)$ at higher energy and $^4A_{2g}\rightarrow{}^4T_{2g}(F)$ at lower energy. In the case of $[Cr(III)L^1H_3.L^1Cr(III)]^{3+}$ the highest energy $^4A_{2g}\rightarrow{}^4T_{1g}(P)$ absorption is masked by charge transfer bands. The transition $^4A_{2g}\rightarrow{}^4T_{2g}(F)$ has T_{1g} symmetry in the octahedral point group and as such, it possesses a zero order magnetic dipole. On the other hand the $^4A_{2g}\rightarrow{}^4T_{1g}(F)$ transition has T_{2g} symmetry and is magnetic dipole forbidden, the intensity of this band is therefore reduced.

3.4.2 CIRCULAR DICHROISM SPECTROSCOPY.

When the overall symmetry of a complex is reduced from octahedral to D_3, the triplet states lose their degeneracy, the $^4T_{1g}$ state splits into ^4E and $^4A_2$ with the $^4T_{2g}$ level transforming into ^4E and $^4A_1$. Therefore under the $^4A_{2g}\rightarrow{}^4T_{2g}$ (O_h) band lie two transitions $^4A_2\rightarrow{}^4E$ and $^4A_2\rightarrow{}^4A_1$, while under the $^4A_{2g}\rightarrow{}^4T_{1g}$ transition there are $^4A_2\rightarrow{}^4E$ and $^4A_2\rightarrow{}^4A_2$ bands, (the latter possesses no magnetic dipole and as such is forbidden). Overall in a D_3 or C_3 environment there should be three absorptions observed in the circular dichroism spectrum. The sign of the ^4E and ^4A components, in trigonally distorted symmetry, which originate from transitions to the "parent" (O_h) T states is opposite. Since for a chiral molecule with D_3 or C_3 symmetry the sense of chirality viewed down the C_3 axis is opposite to that observed along any of the C_2 axes. The overall effect is, the CD spectrum of a chromium complex with D_3 symmetry comprises a bisignate doublet at lower energy $\{^4A_2\rightarrow{}^4A_1,\ ^4A_2\rightarrow{}^4E\ (^4T_{2g})\}$ and a single band at higher energy $\{^4A_2\rightarrow{}^4E\ (^4T_{1g})\}$.

The intensity of CD bands is proportional to the product of the electric and magnetic dipole moments. As the $^4A_2\rightarrow{}^4A_1$ transition is magnetic dipole allowed and the $^4A_2\rightarrow{}^4A_2$ transition is magnetic dipole forbidden the intensity of bands arising from the latter transition will be considerably weaker. To gain

any intensity the $^4A_2 \rightarrow {}^4E$ ($^4T_{1g}$) transition must obtain magnetic dipole intensity by mixing with an allowed transition of similar symmetry such as $^4A_2 \rightarrow {}^4E$ ($^4T_{2g}$).

It is a combination of, in phase, left and right handed circularly polarised light which makes up plane polarised light. Any interaction with a chiral substance results in one of these circularly polarised components being preferentially absorbed, leading to a rotation of the plane of plane polarised light. In essence when light energy is absorbed, an electron is elevated to an excited state giving a change in dipole. Being subject to a chiral field the electron moves in a right or left handed manner, depending upon the nature of the field. In practice, the precise nature of this motion is extremely difficult to determine. Empirical methods may be used to predict the rotational direction. Peacock and Stewart (**10**) related the sign of the E component, originating from the $^4A_{2g} \rightarrow {}^4T_{2g}(F)$ transition, to an intra molecular angle ω. This is defined as the smallest angle measured between a ligator of the top set and one of the bottom set (fig3.6). Thus by using the author's procedure it may be stated that a positive angle ω gives rise to a negative E component and vice versa. It is not possible to relate the absolute configuration with the sign of a given CD transition, in the above example both the complexes have the same configuration but different ω angles and hence different CD spectra. It is possible merely to infer an overall configuration from CD data; it is only the sign of the twist angle between

ligators which may be related to the sign of the ^4E and $^4A_1$ transitions in the $^4A_{2g}\rightarrow{}^4T_{2g}(F)$ region. For instance in the complex $[Co(tmd)_3]^{3+}$ (**11**) a negative angle of twist ω (-55.7°) confers a negative rotational strength for the $^4A_2\rightarrow{}^4A_1(T_{2g})$ transition and conversely a positive value for the $^4A_2\rightarrow{}^4E$ component.

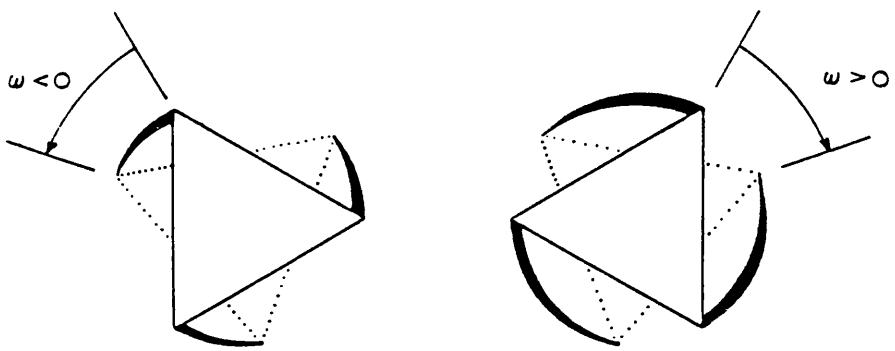

Fig. 3.6. *Measurement of angle ω, from ref.10.*

The complex $[Cr(III)L^1H_3.L^1Cr(III)]^{3+}$ has all its chiral centres in the same (S)-configuration;the overall absolute configuration of each half of the molecule is Δ. The angle of twist ω measured for this complex is positive and therefore the $^4A_2\rightarrow{}^4A_1(^4T_{2g})$ and $^4A_2\rightarrow{}^4E(^4T_{2g})$ transitions would be expected to have positive and negative rotational strengths respectively. As shown by the CD spectrum (fig3.3) for the dimeric species $[Cr(III)L^1H_3.L^1Cr(III)]^{3+}$ the $^4A_{2g}\rightarrow{}^4T_{2g}$ absorption comprises a positive and negative, higher energy,

couplet. From the symmetry arguments the positive band has been assigned to the $^4A_2 \rightarrow {}^4A_1(^4T_{2g})$ transition and thus has A symmetry; the negative band is therefore the $^4A_2 \rightarrow {}^4E(^4T_{2g})$ transition with resultant E symmetry. As expected the higher energy absorption band $^4A_{2g} \rightarrow {}^4T_{1g}(F)$ gives rise to a single transition namely $^4A_2 \rightarrow {}^4E(^4T_{1g})$ again the E symmetry of this results in a negative rotational strength.

3.4.3 COMPARISON WITH [Cr(III)(S)-MeTCTA] and $[Cr(III)L^2H_3]^{3+}$.

The observed CD spectrum (fig3.3) of the dimeric complex $[Cr(III)L^1H_3.L^1Cr(III)]^{3+}$ (neutral, MeCN solution) has, at lower energy, two bands $^4A_2 \rightarrow {}^4A_1$ $\{(^4T_{2g})$, positive$\}$ and $^4A_2 \rightarrow {}^4E$ $\{(^4T_{2g})$, negative$\}$. At higher energy is the positive $^4A_2 \rightarrow {}^4E(^4T_{1g})$ band which is less intense than the corresponding $^4A_2 \rightarrow {}^4E(^4T_{2g})$. The former arises from a magnetic dipole allowed "parent" transition whilst the later originates from a magnetic dipole forbidden band.

As the structure of the complex proceeds from a dimer to protonated monomer to deprotonated monomer, the intensity of each transition reduces. This is indicative of the degree of distortion (trigonal twist) in each species decreasing. The dimer has a trigonal distortion of 15° at each metal centre, on dissociation

it is conceivable that this angle decreases to a value in line with that found for other d^3 ions with similar ligands i.e. 10-11°. A reduction in the trigonal twist would, in effect, reduce the optical activity of the complex leading to a lower magnitude of rotational strength $\Delta\varepsilon$. The difference in $\Delta\varepsilon$ observed between the acidic and basic forms may be explained by a repulsive interaction between the hydroxyl protons of the O,O',O'' face. This would increase the trigonal distortion of the protonated (acidic) monomer compared with the deprotonated (basic) species. The g-factor measurements for all the CD transitions for this complex are of the order 10^{-2} and are consistent with d-d electronic transitions.

The complex [Cr (S)-MeTCTA] was prepared by Robb (**12**) and although not structurally characterised, the analogous [Cr TCTA] complex has a trigonal twist of almost 11°, a similar value would be expected for [Cr (S)-MeTCTA]. By simple analogy with (R)-MeTACN in which the endocyclic rings are in the λ conformation, those of (S)-MeTCTA would be expected to adopt the opposite δ conformation. The overall symmetry of the complex is therefore tentatively assigned as $\Lambda(\delta\lambda)$, with an anticlockwise (negative) ligator twist, ω. This compares favourably with the observed CD spectrum (fig3.7). The sign of the $^4A_2 \rightarrow {}^4A_1(^4T_{2g})$, $^4A_2 \rightarrow {}^4E(^4T_{2g})$ and $^4A_2 \rightarrow {}^4E(^4T_{1g})$ transitions are opposite to those found in the $[CrL^1H_3.L^1Cr]^{3+}$ species, further evidence that the twist, ω,is oppositely signed (negative compared to positive). The observed rotational strengths, $\Delta\varepsilon$, for the three bands are similar to those displayed in the

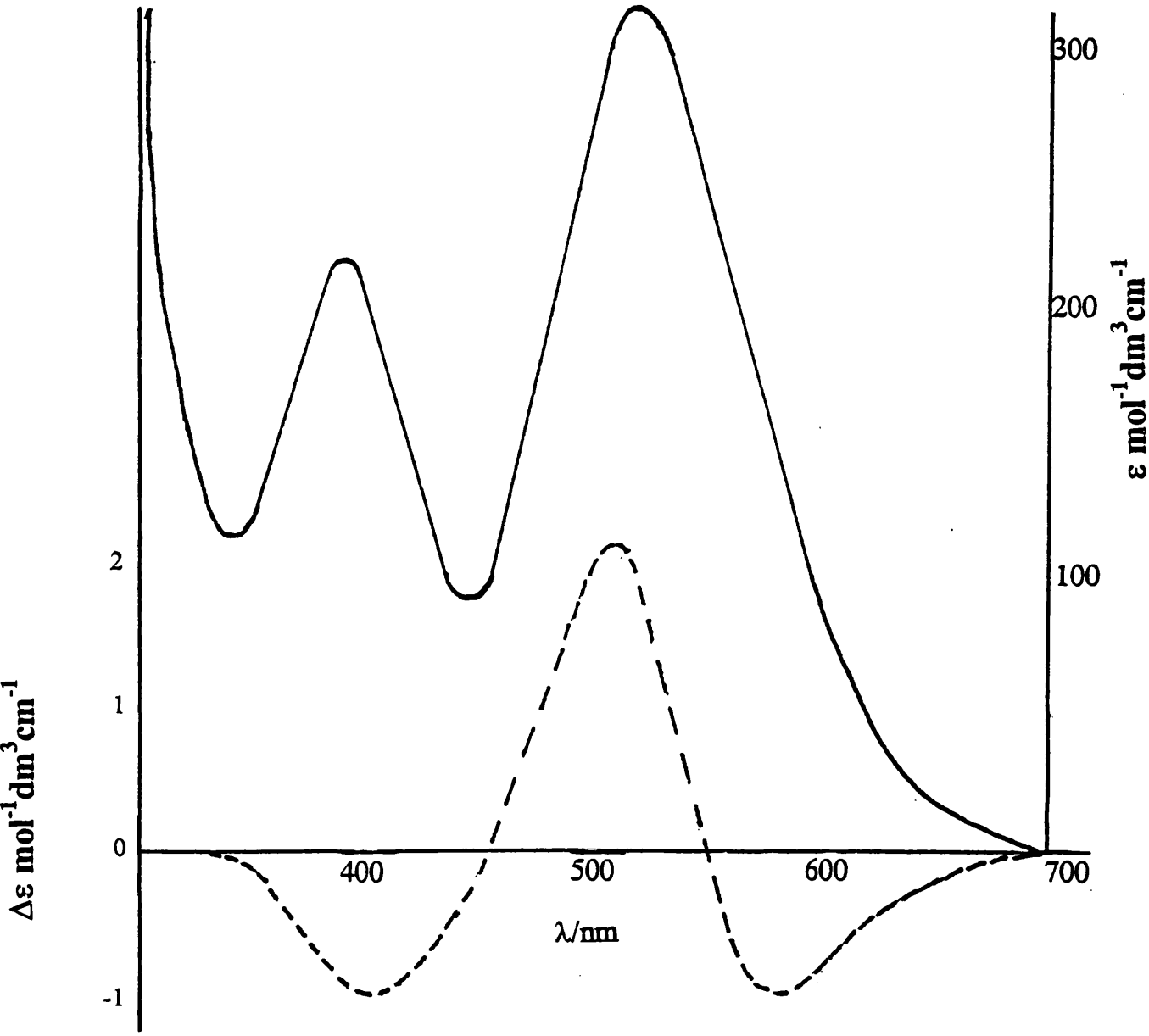

Fig. 3.7. *Absorption / CD spectra of [Cr (S)-MeTCTA].*

monomeric $[CrL^1H_3]^{3+}$ acid medium species. Again indicative that the trigonal twist, in the alcohol ligand monomer, is less than the 15° measured for the dimeric complex $[CrL^1H_3.L^1Cr]^{3+}$.

With bulky groups on each pendant arm, to prevent dimerisation the chromium complex of the ligand, L^2H_3, displays similar solution chemistry to $[CrL^1H_3.L^1Cr]^{3+}$. It is believed that in neutral solution (i.e. MeCN) a fully protonated species $[CrL^2H_3]^{3+}$ is unlikely, existing instead in mono $[CrL^2H]^+$ or di $[CrL^2H_2]^{2+}$ protonated forms, since the absorption spectra show the $^4A_{2g}\rightarrow{}^4T_{2g}$ band position to increase in energy on going from acidic to neutral to basic media. This increase is consistent with the change in donor properties from all alcohol through a mixture (alcohol/alkoxide) to an all alkoxide ligator. It is at the fully protonated monomer stage that the non bulky $[CrL^1H_3]^{3+}$ is able to dimerise, effectively spreading the charge over two chromium centres. The 10Dq values for the acidic and basic forms with L^2H_3 are slightly less (by 200-300cm^{-1}) than those with L^1H_3, highlighting the steric effects of the isopropyl groups over methyl groups on the overall binding efficiency of the ligand. There is a reduction in the metal-ligand bonding overlap and hence the ligand field splitting observed.

The three bands in the CD spectra are of opposite sign to transitions found with L^1H_3. Suggesting the overall twist is of the opposite sense i.e. $\omega<0$, thus highlighting the effect a small change in ligand design can have on the twist of

ligators around a particular metal centre. Like the previous two examples $\Delta\varepsilon$ values for the acidic species are greater than in the basic complex. Assigned once again to the difference in trigonal twist about the chromium ion, the steric interactions amongst the hydroxyl protons increase the distortion around the metal atom.

References.

(1) K.Wieghardt, W.Schmidt, R. van Eldik, B.Nuber and J.Weiss, *Inorg. Chem.*, 1980, **19**, 2922.

(2) P.Andersen, A.Dossing and S.Larsen, *Acta. Chem. Scand.*, 1990, **44**, 455.

(3) K.Wieghardt, W.Schmidt, H.Endres and C.R.Wolfe, *Chem. Ber.*, 1979, **112**, 2837.

(4) K.Wieghardt, U.Bossek, P.Chaudhuri, W.Herrmann, B.C.Menke and J.Weiss, *Inorg. Chem.*, 1982, **21**, 4308.

(5) U.Bossek, K.Wieghardt, B.Nuber and J.Weiss, *Angew. Chem. Int. Ed. Engl.*, 1990, **29**, 1055.

(6) M.W.Perkovic and J.F.Endicott, *J. Phys. Chem.*, 1990, **94**, 1217.

(7) K.Wieghardt, E.Schoffmann, B.Nuber and J.Weiss, *Inorg. Chem.*, 1986, **25**, 4877.

(8) I.A.Fallis, L.J.Farrugia, N.M.Macdonald and R.D.Peacock, *J. Chem. Soc., Dalton Trans.*, 1993, 2759.

(9) A.A.Belal, L.J.Farrugia, R.D.Peacock and J.Robb, *J. Chem. Soc., Dalton Trans.*, 1989, 931.

(10) R.D.Peacock and B.Stewart, *Coord. Chem. Rev.*, 1982, **46**, 129.

(11) R.Kuroda and Y.Saito, *Bull. Chem. Soc. Jpn.*, 1976, **49**, 433.

(12) J.Robb, *Ph.D. Thesis*, University of Glasgow, 1987.

CHAPTER 4

MANGANESE COMPLEXES WITH L^1H_3 AND L^2H_3.

4.1 MANGANESE CHEMISTRY.

The chemistry of manganese and its numerous complexes has been investigated for many years, especially in light of this metal's importance in bio-inorganic chemistry (**1**). Manganese forms the basic active centre in several metalloproteins and in most of these cases two or more manganese atoms are present in each subunit of these enzymes. Special emphasis has been paid to the coordination chemistry of manganese with mixed N and O donor complexes which mimic the active site chemistry. The macrocyclic chemistry of manganese is less well established, in particular those incorporating nitrogen-alcohol donation. Manganese is known to exist in oxidation states ranging from -3 to +7 (**2**). Of these the +2, +3 and +4 states are of the most relevance to this work. The +2 oxidation level is probably the most common, being fairly resistant to oxidation (except under basic conditions). The +3 state is known to disproportionate depending upon the pH to give Mn(II) and Mn(IV), additionally, as a result of its ground state configuration (d^4) it is liable to Jahn Teller distortions.

Finally the Mn(IV) ion is commonly associated with the compound MnO_2; however, suitable ligands such as Schiff bases, bipyridyls or alkoxides are able to stabilise this ion under neutral conditions.

4.2 PREPARATION OF MIXED VALENCE DIMER.

The synthesis of the manganese complex with L^1H_3 was found to be pH sensitive. The ethanolic solution containing the ligand and $MnCl_2$ was found to darken progressively on increasing the pH; indicating oxidation to Mn(IV) was taking place. Under strongly alkaline conditions (pH=12) no material could be crystallised out of solution. By adjusting the pH to 8 (i.e. mildly basic medium) the dimeric cation $[Mn(II)L^1H_3.L^1Mn(IV)]^{3+}$ was produced. On addition of solid ammonium hexafluorophosphate a brown-red powder precipitated out which, after analysis, was assigned the structure $[Mn(II)L^1H_3.L^1Mn(IV)][PF_6]_3$. A small amount of this material was used for variable temperature magnetic moment measurements; the remainder was recrystallised from acetonitrile for the purposes of X-ray crystallography.

4.2.1 STRUCTURAL ANALYSIS.

From the elemental analysis data the stoichiometry of this compound was assigned a dimeric cation with an overall 3+ charge in order to balance the three $[PF_6]^-$ counterions. Assigning the oxidation states of the metal centres was slightly more difficult. The crystal structure and atom labelling scheme of $[Mn(II)L^1H_3.L^1Mn(IV)][PF_6]_3$ is presented in figure 4.1.

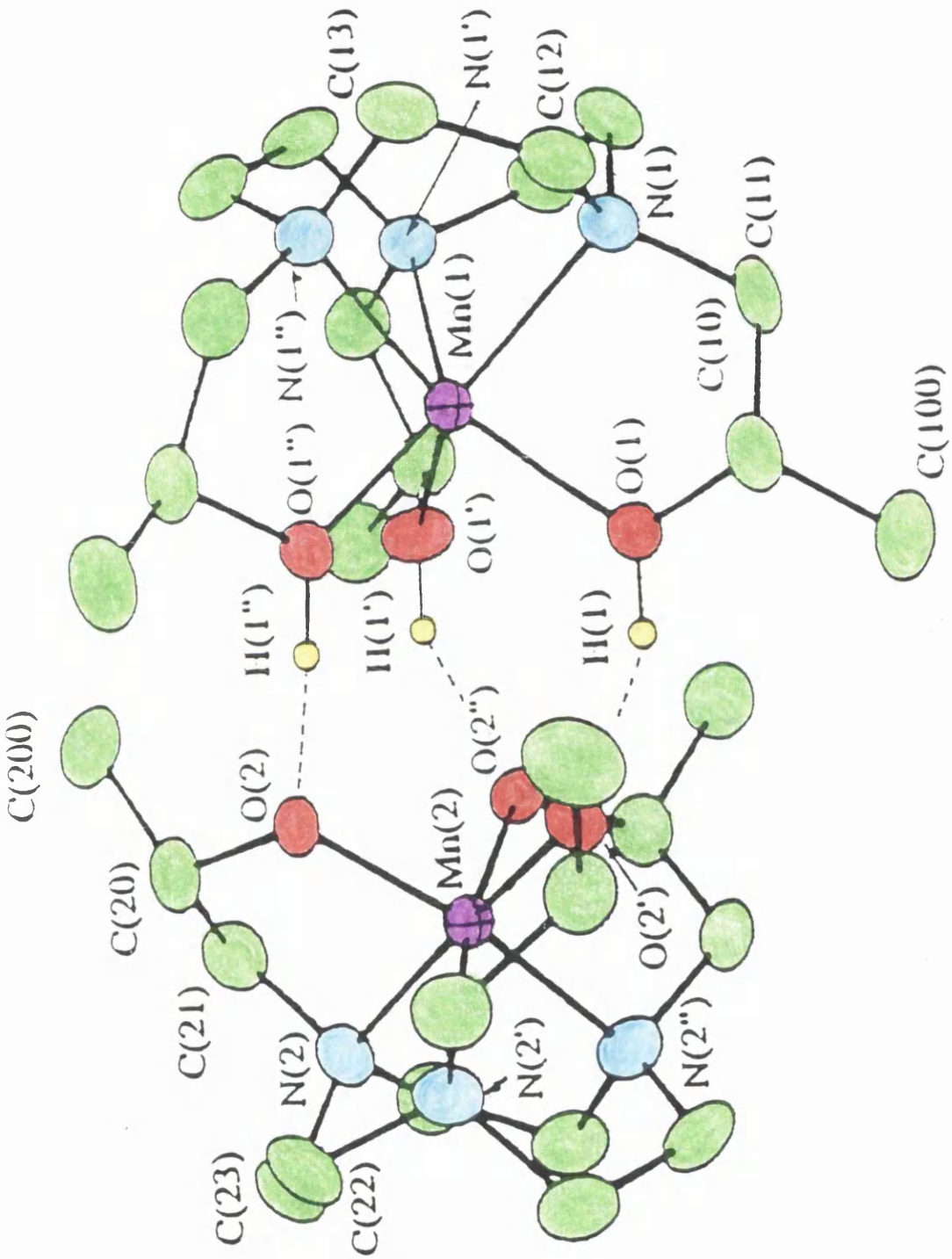

Fig. 4.1. *Crystal structure of* $[Mn(II)L^1H_3L^1Mn(IV)]^{3+}$ *cation.*

The complex cation consists a dimer, with two metal centres and two ligands, connected by hydrogen bonding. The asymmetric nature of these hydrogen bridges arises from the different ligating properties of the two ligand units. One half is protonated (alcohol donation) whilst the other is deprotonated (alkoxide donors) i.e. L^1H_3 and $[L^1]^{3-}$ respectively. A small amount of residual electron density was found in the difference map, which may have been a further non-bridging proton, disordered about three possible sites either side of the dimer. This added complication indicated a ligand set charge of 2- and a total metal charge of 5+. Therefore the permutation of possible oxidation states were : Mn(II)Mn(III); Mn(III)Mn(III) and Mn(II)Mn(IV). The presence of a Mn(I) centre was discounted due to the fact a "hard" donor i.e. L^1H_3 would be extremely unlikely to form a stable complex with such a "soft" centre.

The view down the primary axis (C_3) (figures 4.2, 4.3) shows the different geometries of the two halves, in effect, confirming that the two metal centres were different. A selection of bond lengths and angles is presented in table 4.1. The deprotonated component has a twist angle (ϕ) of 10.9° and is almost octahedral. It is unlikely that L^1H_3 would form a perfect octahedral complex since the pendant arms are too short to allow such a coordination geometry. This is supported by the observed geometry about each Co(III) ion in the complex $[Co(III)L^1H_3.L^1Co(III)]^{3+}$ (**3**). The average twist in this case is $\phi=10.7°$, in spite of the low spin d^6 Co(III) centre having maximum LFSE ($^{-12}/_5\Delta_o$).

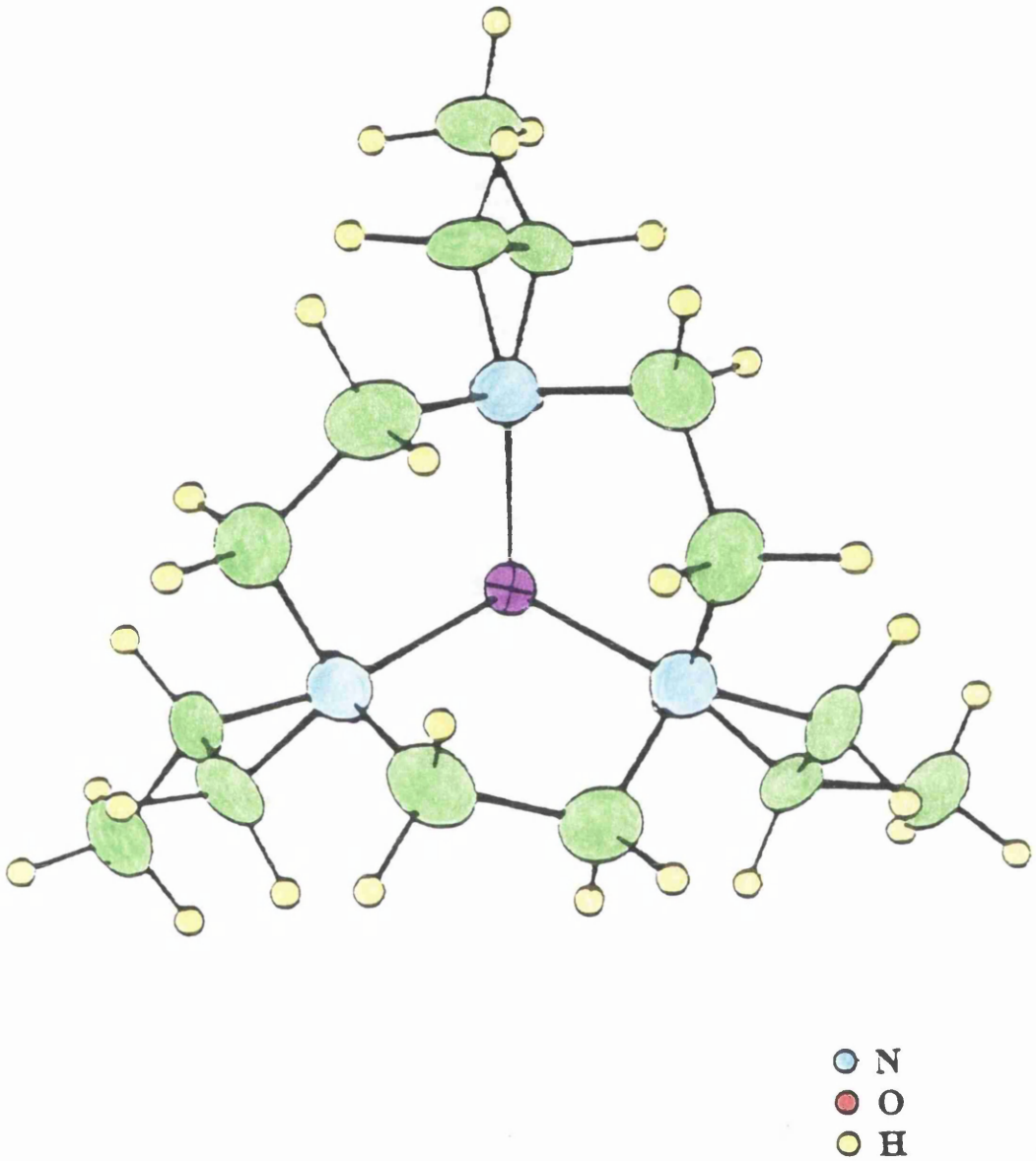

Fig. 4.2. *View along C_3 axis of $[Mn(II)L^1H_3]^{2+}$ component.*

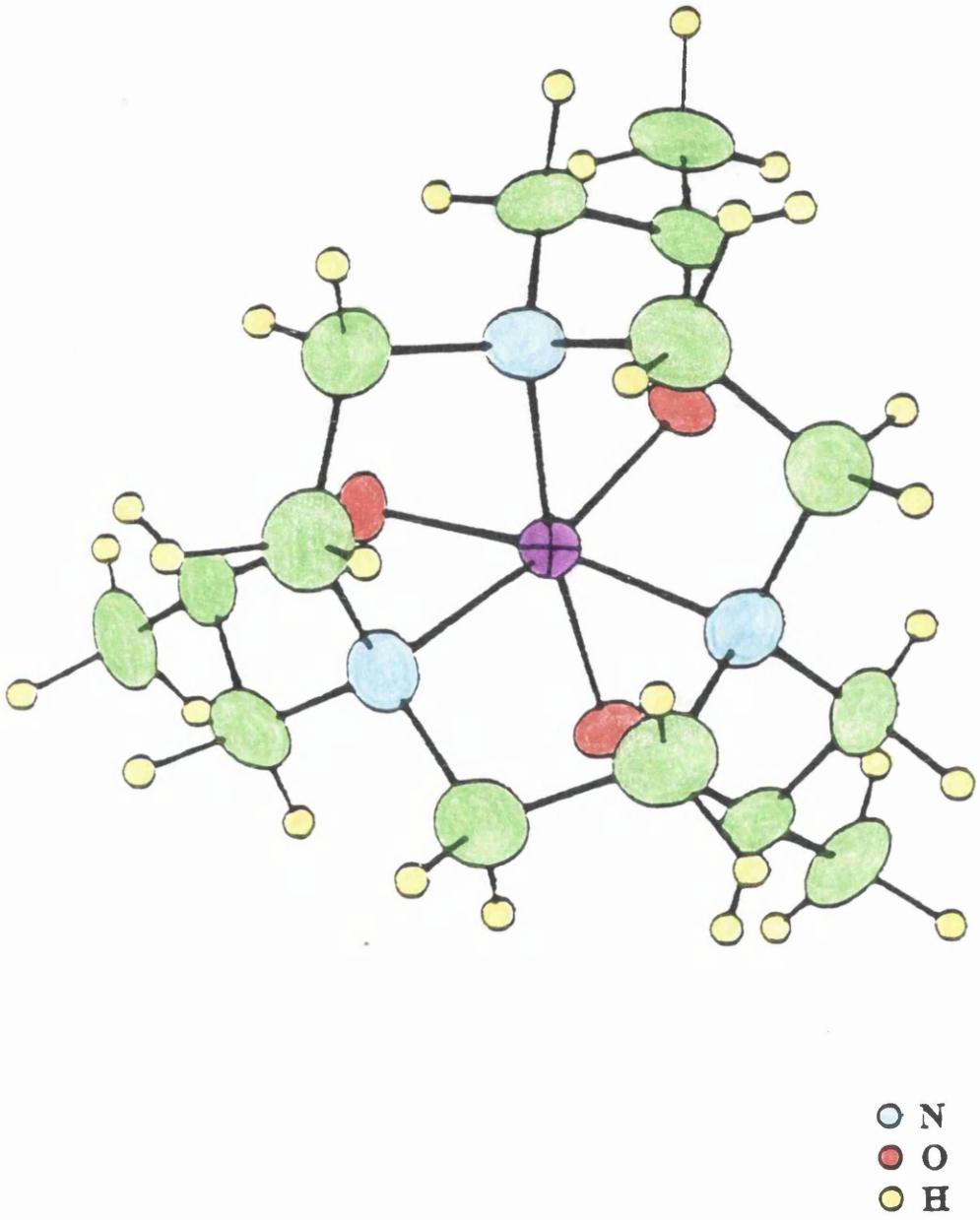

Fig. 4.3. *View along C_3 axis of $[Mn(IV)L^1]^+$ component*

Mn(1)-N(1)	2.251(5)	Mn(2)-N92)	2.051(5)
Mn(1)-O(1)	2.142(4)	Mn(2)-O(1)	1.857(4)
	0.906(4)	O(2)-H(1)	1.841(3)
N(1)-Mn(1)-N(1)'	78.6(2)	N(2)-Mn(2)-N(2)'	84.5(2)
O(1)-Mn(1)-O(1)'	91.8(2)	O(2)-Mn(2)-O(2)'	96.2(2)
N(1)-Mn(1)-O(1)	77.0(2)	N(2)-Mn(2)-O(2)	96.0(2)

Table 4.1. *Selected bond lengths (Å) and bond angles (deg) for* $[Mn(II)L^1H_3.L^1Mn(IV)]^{3+}$.

Both Mn(III) and Mn(IV) would be expected to exhibit octahedral symmetry although Mn(III) [d^4] would require a significant Jahn Teller distortion. In the crystal structure the metal atoms of the O_h unit lie along a three fold axis and all the M-O and M-N bond lengths would be expected to be essentially identical, thus indicating the absence of Mn(III) - this half is a Mn(IV) centre. The protonated ligand diplays almost perfect trigonal prismatic geometry (ϕ=60°) this rules out a metal centre which would require a significant amount of LFSE (i.e. Mn(III) or Mn(IV)). By examining the metal-ligand bond lengths of the protonated species, this centre may be confirmed as being Mn(II). This is supported by the fact that this component remains protonated, Mn(II) has a tendency to be acid stable. The alcohol donors will tend to deprotonate with Mn(III) and Mn(IV) complexes; the presence of these stronger Lewis acids results in the coordinated alcohol group becoming more acidic and

hence deprotonated. Therefore the complex is a Mn(II)-Mn(IV) dimer with an overall metal-metal separation of 4.653Å.

The exocyclic chelate rings of the two units have a δ conformation for the Mn(II) half and λ for the Mn(IV) side.

The trigonal prismatic geometry of the Mn(II) unit results in this conformation inversion; the chirality of the octahedral Mn(IV) side defined by the twist of ligators about the metal centre is Δ and hence the absolute configuration is Δ(λδ).

One unusual feature of this complex is the relative difference between the Mn-O distances and the Mn-N bond lengths of the two halves of the dimer. In the case of the Mn(II) side the Mn-O bonds are shorter than the Mn-N bonds by 0.11Å, with the Mn(IV) unit the Mn-O distances are 0.19Å shorter than the Mn-N bond lengths. The overall values for the bond lengths are smaller for the Mn(IV) centre (ionic radius 0.53Å) than for the Mn(II) ion (ionic radius 0.83Å) as expected. This however does not account for the Mn-O bond being much shorter than the Mn-N one in the case of Mn(IV) compared with Mn(II).

The Mn(IV) atom (t_{2g}^3), with its empty e_g set allows a closer approach by the pendant arm donor as a result of the reduced electronic repulsion thus facilitating a better bonding interaction. Additionally the ligating groups are alkoxide donors and as such are superior π donors than the alcohol groups of the Mn(II) component. This leads to a greater degree of pπ donation to the half

filled t_{2g}^3 set of Mn(IV) and therefore a degree of double bond character with resultant bond shortening. The nitrogen donors with no equivalent non-bonding lone pairs are unable to participate in such a π bonding interaction, hence the relative difference in Mn-N bonding in comparison with the Mn-O bonds.

4.2.2 ELECTRONIC SPECTROSCOPY.

Both the absorption and circular dichroism spectra of $[Mn(II)L^1H_3L^1Mn(IV)]^{3+}$ arise from the Mn(IV) part of the compound, the Mn(II) portion is high spin (d^5) and thus its ground state configuration has the ^6S term; any transitions occurring from this configuration are forbidden under the spin selection rule, they are also Laporte forbidden and as such will be very weak. The two high energy bands and a shoulder in the absorption spectrum (fig4.4) are assigned to charge transfer modes from their high extinction coefficients, $\varepsilon=9000 mol^{-1}dm^3cm^{-1}$. In the comparable case of Cr(III) compounds, also d^3, the spin allowed transition $^4A_{2g}\rightarrow{}^4T_{2g}$ has $\varepsilon=200 mol^{-1}dm^3cm^{-1}$; if the lowest band in the Mn(IV) case arose from d↔d transitions a similar extinction coefficient would also be expected. From the spectrum, the lower two bands have extinction coefficients of $1000 mol^{-1}dm^3cm^{-1}$ again attributed to charge transfer - a low energy charge transfer band is more likely than a high energy d↔d transition. Further verification of the origin of these bands is obtained

from the CD spectrum, being magnetic dipole allowed the $^4A_{2g} \rightarrow {}^4T_{2g}$ band should have a dissymmetry factor ($g=\Delta\varepsilon/\varepsilon$) of approximately 10^{-2}. The dissymmetry factors of the lower three bands are $5.0x10^{-4}$; $2.5x10^{-3}$ and $1.0x10^{-3}$ respectively. Again in comparison the isoelectronic Cr(III) species has a g factor value of $1x10^{-2}$, thus the lower energy Mn(IV) bands are attributed to charge transfer transitions.

In an attempt to verify the oxidation state by means of electronic spectroscopy a sample of $[Mn(II)L^1H_3L^1Mn(IV)]^{3+}$ was dissolved in acetonitrile and its spectrum obtained. The solvent was removed by slow evaporation to be replaced with a 1:4 solution of triethylamine in acetonitrile, the spectrum was recorded and the extinction coefficient doubled indicating that on basifying, the dimer deprotonates and the Mn(II) portion is oxidised to Mn(IV).

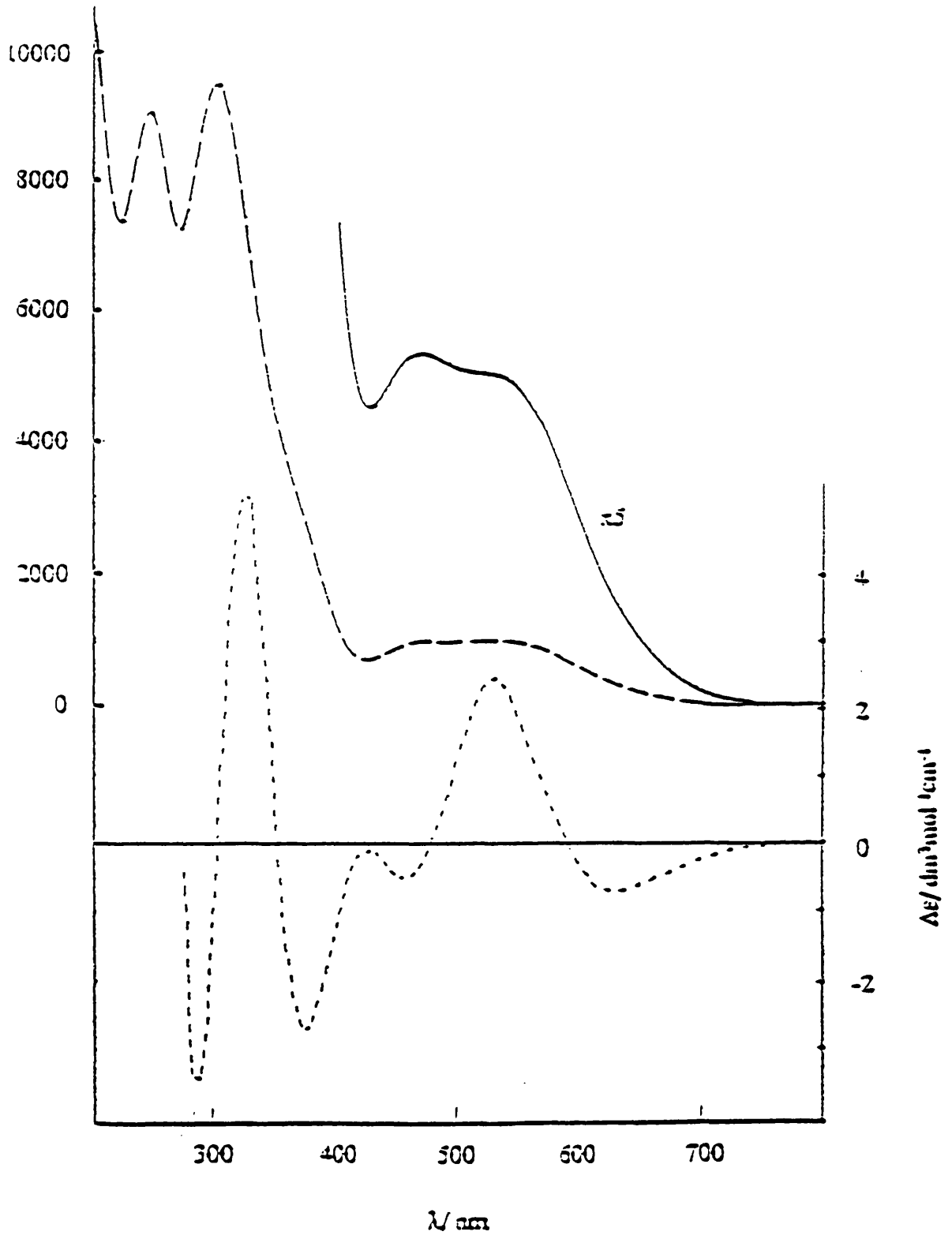

Fig. 4.4. *Absorption / CD spectra of* $[Mn(II)L^1H_3L^1Mn(IV)]^{3+}$.

4.2.3 MAGNETIC MOMENT MEASUREMENTS.

The temperature dependant magnetic moment and magnetic susceptibility of $[Mn(II)L^1H_3L^1Mn(IV)][PF_6]_3$ are shown in figure 4.5. The magnetic moment varies from $7.1\mu_B$ at 295K to $4.4\mu_B$ at 2K. This initial value is close to the spin only value for a Mn(II), Mn(IV) system: $(\mu_2^2 + \mu_2^2)^{½} = (5.92^2 + 3.87^2)^{½} = 7.07\mu_B$ and thus the assignment of Mn(II), Mn(IV) is entirely compatible with this. Since the Mn(II) centre has a ^6S ground state it will be expected to display almost entirely spin only behaviour ($5.93\mu_B$). Therefore the spin only value for Mn(IV) is $3.9\mu_B$ which compares favourably with other high spin d^4 species. With complete anti-parallel coupling (S=1 ground state) a moment of $2.83\mu_B$ would be expected, which is not achieved at 2K.

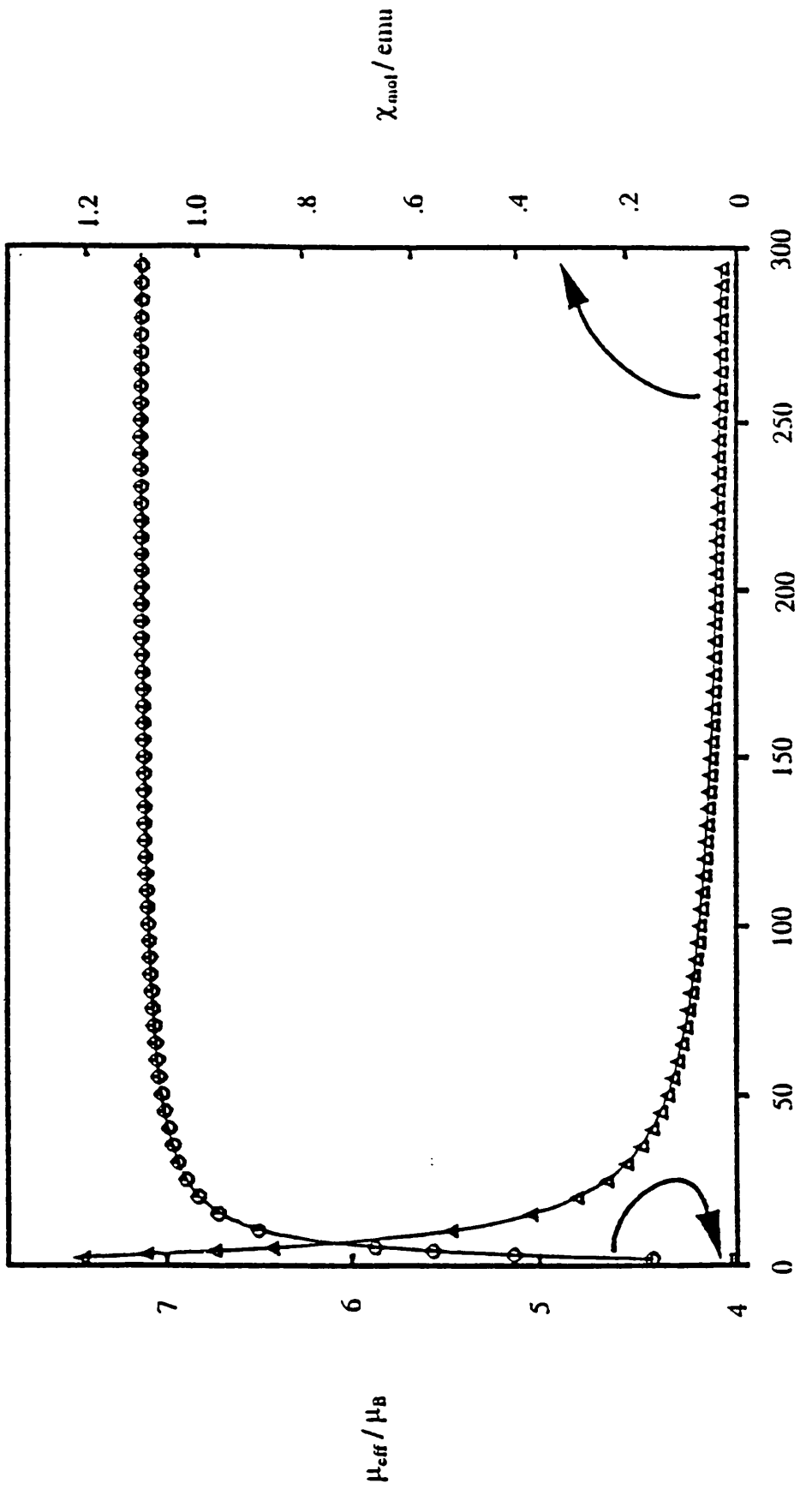

Fig. 4.5. *Magnetic moment, μ_B, and magnetic susceptibility, χ_{mol}/emu measurements for $[Mn(II)L^1H_3L^1Mn(IV)]^{3+}$.*

The Heisenberg-Dirac-van Vleck (HDVV) model for magnetic super-exchange (**4**) is used to interpret the temperature dependence of the magnetic susceptibility. The spin exchange Hamiltonian $H_{HDVV}=-2JS_1.S_2$ was used to fit the data; J is the spin super-exchange coupling constant, S_1 and S_2 are the total spin values of the metal centres $^5/_2$ and $^3/_2$ for Mn(II) and Mn(IV) respectively. In the final analysis of the data, terms for temperature-independent (field induced) paramagnetism or for paramagnetic contaminants were unnecessary to achieve an acceptable fit for the data, and gave $J=-0.66cm^{-1}$ with $g=2.06$. Anti-ferromagnetic super-exchange is implied from this negative J value and is to be expected from a coupling via an O-H-O bridge devoid of complete orthogonalities. This coupling constant lies within the range of values found for a number of dinuclear Cr(III) compounds (**5**). It should be noted, however, that the value of this coupling constant is very small. A 2J energy difference separates the parallel and anti-parallel states and with $83.59cm^{-1}/kJ$ this has a value of $15.79Jmol^{-1}$.

Use of the Boltzmann distribution shows that at room temperature both states are almost equally populated ($N_{parallel}/N_{anti\text{-}parallel}=N_p/N_a=0.9939$). Even at 17K $N_p/N_a=0.90$. Only at the last few data points does the upper state become significantly depopulated: $N_p/N_a=0.4$ (2K), 0.74 (6K), 0.83 (10K), 0.89 (15K), 0.91 (20K).

4.2.4 ELECTROCHEMISTRY

The cyclic voltammogram of $[Mn(II)L^1H_3L^1Mn(IV)]^{3+}$ was measured in acetonitrile (fig4.6), there is one fully reversible reduction at -0.06V (0.54V vs NHE), the other reduction at -0.64 (-0.06 vs NHE) is quasi reversible. A third wave, an oxidation at +1.07V (+1.65 vs NHE), is totally irreversible. The first reversible reduction is assigned to a $Mn^{II},Mn^{IV} \rightarrow Mn^{II},Mn^{III}$ process, by analogy with a similar Mn^{II},Mn^{III} dimeric compound prepared by Fallis (**6**), the expectation of obtaining a $Mn^{II/III}$ dimeric complex with L^1H_3 is not unrealistic. The quasi reversible process is assigned as follows $Mn^{II},Mn^{III} \rightarrow Mn^{II},Mn^{II}$. The existence of a Mn^{II} tris alcohol - Mn^{II} tris alkoxide species is, however, unlikely since Mn^{II} is a poor π acceptor and is also destabilised by basic conditions. A structure where both subunits enjoy alcohol/alkoxide donation is probably more likely.

The irreversible oxidation is assigned as a $Mn^{II},Mn^{IV} \rightarrow 2Mn^{IV}$ transformation, explained in terms of oxidation of the Mn^{II} species giving an increase in the acidity of the dimer leading to deprotonation and ultimately dissociation. The overall potential of this oxidation process is consistent with the Mn^{II} species being oxidised to Mn^{IV} by molecular oxygen. Due to this probable dissociation this process is chemically as well as electrochemically irreversible, unfortunately it is impossible to determine the fate of the bridging protons of the dimer.

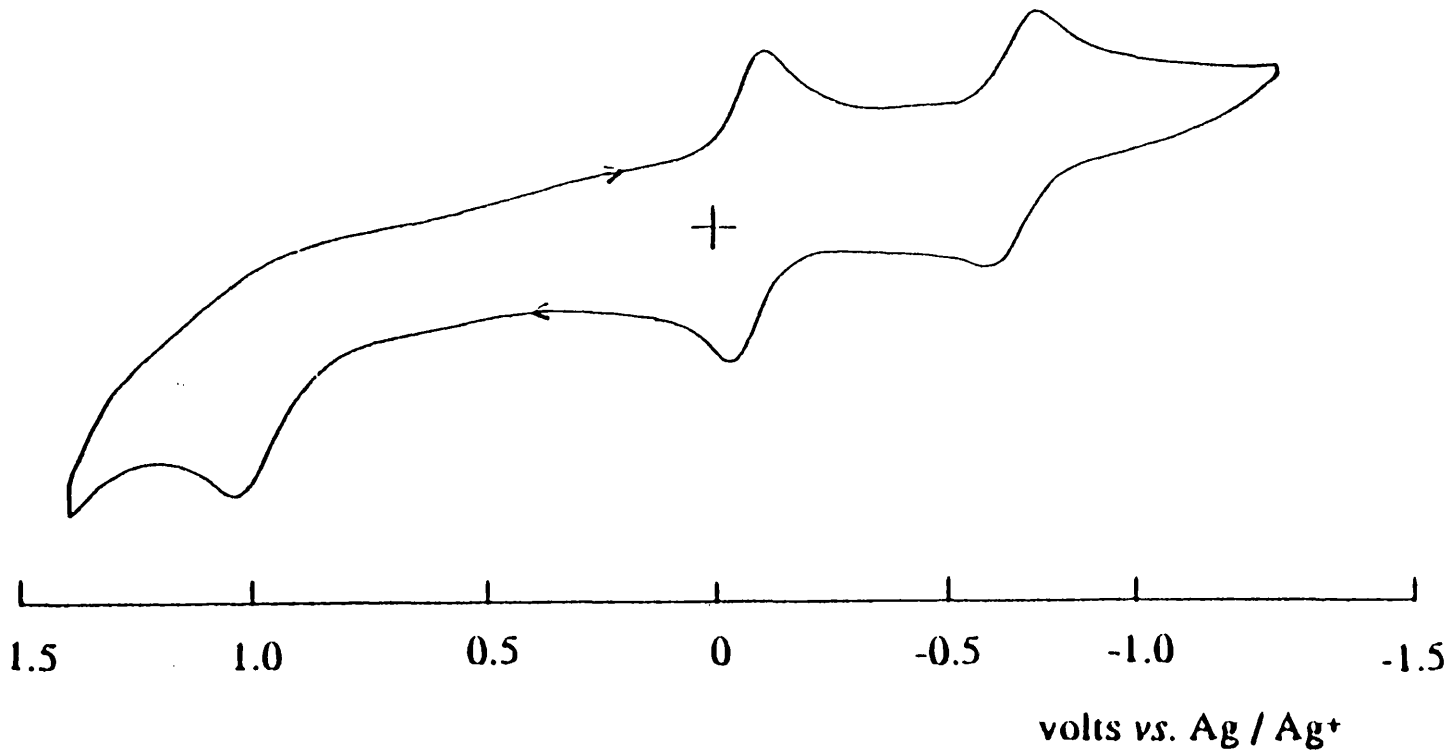

Fig. 4.6. *Cyclic voltammogram of* $[Mn(II)L^1H_3L^1Mn(IV)]^{3+}$ *in MeCN vs.* Ag/Ag^+ *(0.1mol* l^{-1} $AgNO_3$ *in MeCN).*

4.3 PREPARATION OF MONOMERIC COMPLEX.

Similar to $[Mn(II)L^1H_3L^1Mn(IV)]^{3+}$, the synthesis of the monomeric complex $[Mn(IV)L^2][PF_6].H_2O$ is pH dependent, (L^2H_3=N,N'N,''-tris[(2R)-2-hydroxy-3-methylbutyl]-1,4,7-triazacyclononane). The ligand L^2H_3 was prepared in an attempt to prevent the dimerisation process. On combining L^2H_3 with $MnCl_2$ the solution darkened appreciably without the addition of base; this is unusual for a Mn(II) species at pH7. Attempts to prevent this oxidation occurring, to try and obtain the Mn(II) complex were unsuccessful.

4.3.1 STRUCTURAL ANALYSIS.

The crystal structure and space-filling views of $[Mn(IV)L^2][PF_6].H_2O$ are displayed in figure 4.7 and figure 4.8 respectively. A monomeric cation is present with the Mn(IV) ion in an almost octahedral environment; the twist angle is 10.8°. The observed twist of pendant groups about the metal centre is of the Λ configuration. The chirality of the endocyclic and exocyclic chelate rings is δ and λ respectively. The overall chirality is thus Λ(δλ) which is opposite to that shown by the Mn(IV) half of $[Mn(II)L^1H_3L^1Mn(IV)]^{3+}$. This is a result of the differing chirality of the pendant arms L^1H_3 has the pendant groups of the (S)-configuration and those of L^2H_3 are of (R)-configuration.

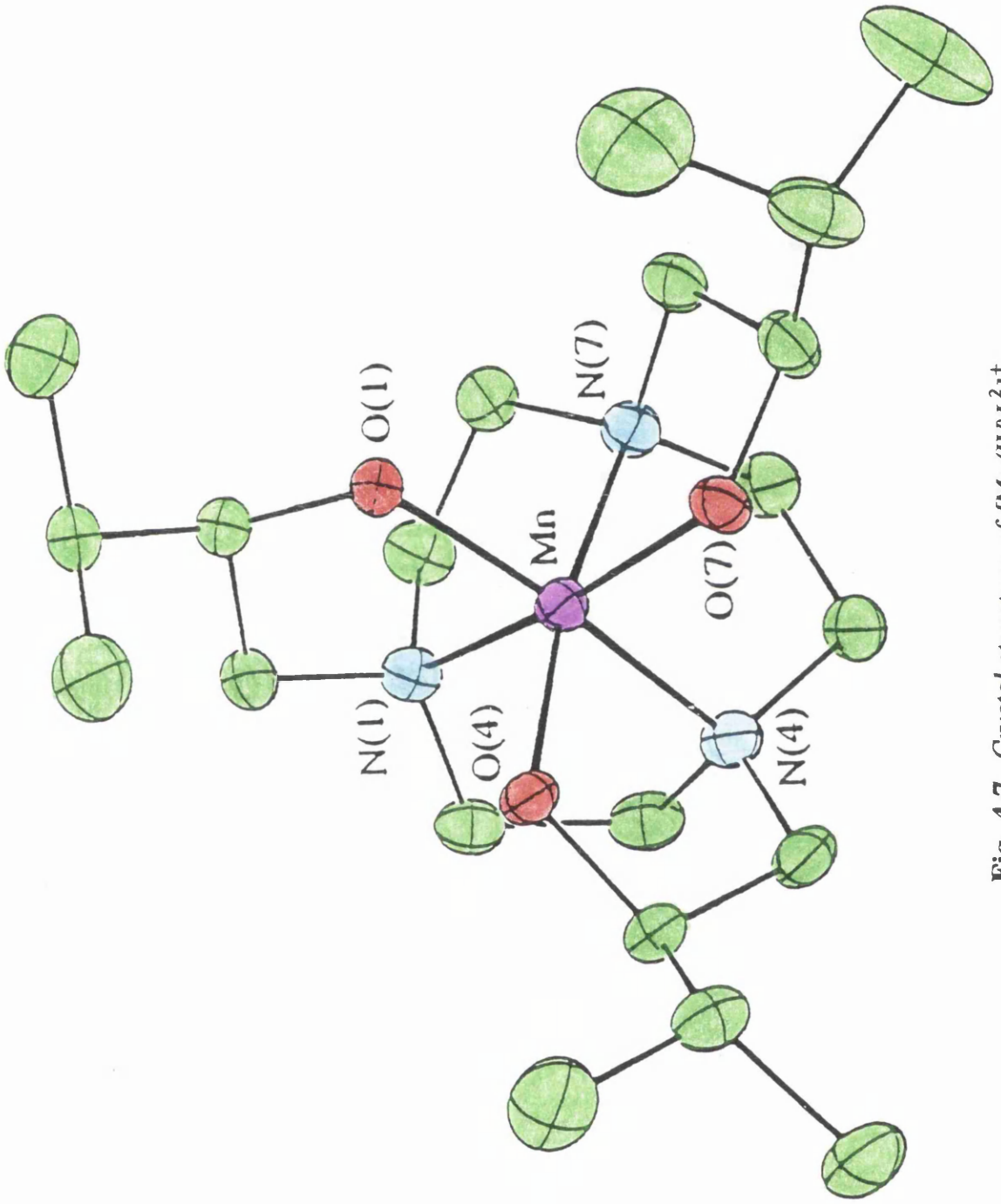

Fig. 4.7. *Crystal structure of* $[Mn(IV)L^2]^+$.

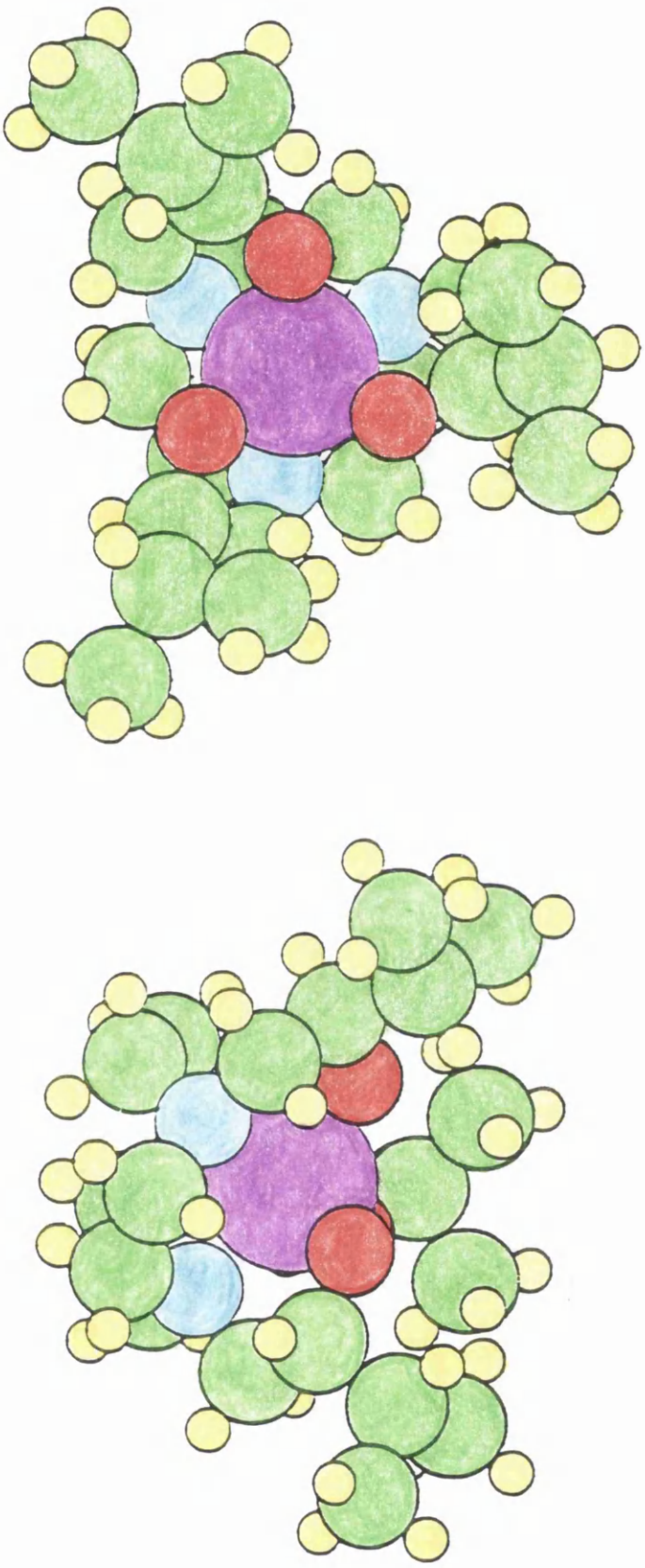

Fig. 4.8. *Space-filling views of* $[Mn(IV)L^2]^+$.

Examination of the bond lengths shows them to be almost identical to those of the Mn(IV) component in the mixed valence dimer. There is no apparent tetragonal elongation, justifying the assignment of a Mn(IV) oxidation state. A d^4 species [Mn(III)] would require a Jahn Teller distortion. The bond lengths and angles are presented in table 4.2. Like its Mn(IV) counterpart in the $[Mn(II)L^1H_3L^1Mn(IV)]^{3+}$ cation there is an observed difference in the metal-nitrogen and metal-oxygen bond lengths, the metal-oxygen distances are significantly shorter.

Mn-N(1)	2.052(3)	Mn-O(1)	1.819(3)
Mn-O(4)	2.049(3)	Mn-O(4)	1.826(3)
Mn-N(7)	2.044(3)	Mn-O(7)	1.831(3)
N(1)-Mn-N(4)	93.9(2)	N(1)-Mn-N(7)	84.8(2)
N(4)-Mn-N(7)	83.9(2)	N(1)-Mn-O(1)	84.2(2)
N(1)-Mn(1)-O(1)	84.1(2)	N(7)-Mn-O(7)	84.2(2)
O(4)-Mn-O(7)	97.7(1)	O(1)-Mn-O(7)	96.3(1)
O(4)-Mn-O(7)	97.0(1)		

Table 4.2. *Selected bond lengths (Å) and bond angles (deg) for* $[Mn(IV)L^2]^+$.

A comparison may be drawn between the monomeric cations $[Mn(IV)L^2]^+$ and $[Mn(IV)L^3]^+$ where L^3H_3=N,N',N''-tris[2-hydroxyethyl]-1,4,7-triazacyclononane (**7**). Both structures are very similar, however the intermolecular properties of the two vary quite considerably. In the case of

$[Mn(IV)L^3]^+$ each molecule is weakly hydrogen bonded to an adjacent molecule between the O,O',O'' face of one and the methylene residues of an other. For $[Mn(IV)L^2]^+$ the steric hindrance about the O,O',O'' face prevents any such bonding effects, in fact examination of the space-filling diagram highlights the steric congestion which also prevents the water molecule of crystallisation from hydrogen bonding to the alkoxide groups.

4.3.2 ELECTRONIC SPECTROSCOPY.

The absorption and CD spectra of $[Mn(IV)L^2][PF_6].H_2O$ are shown in figure 4.9. The absorption spectrum is quite similar to that of $[Mn(II)L^1H_3L^1Mn(IV)][PF_6]_3$ with the exception of an additional weak shoulder at 350nm. The extinction coefficients of the bands are also of a greater magnitude ($\varepsilon = 1000 mol^{-1}lcm^{-1}$ or more) suggesting that they arise from charge transfer processes. The CD spectrum,however,is quite different L^2H_3 is of the opposite configuration to L^1H_3 thus the lowest energy bands, in the visible region, of both complexes are split into two components of opposite sign.

The higher energy band in $[Mn(IV)L^2]^+$ (shoulder at 480nm) is split into two differently signed components whilst the corresponding band in $[Mn(II)L^1H_3L^1Mn(IV)]^{3+}$ remains unisignate. Finally both species have single component bands before the intense UV charge transfer bands.

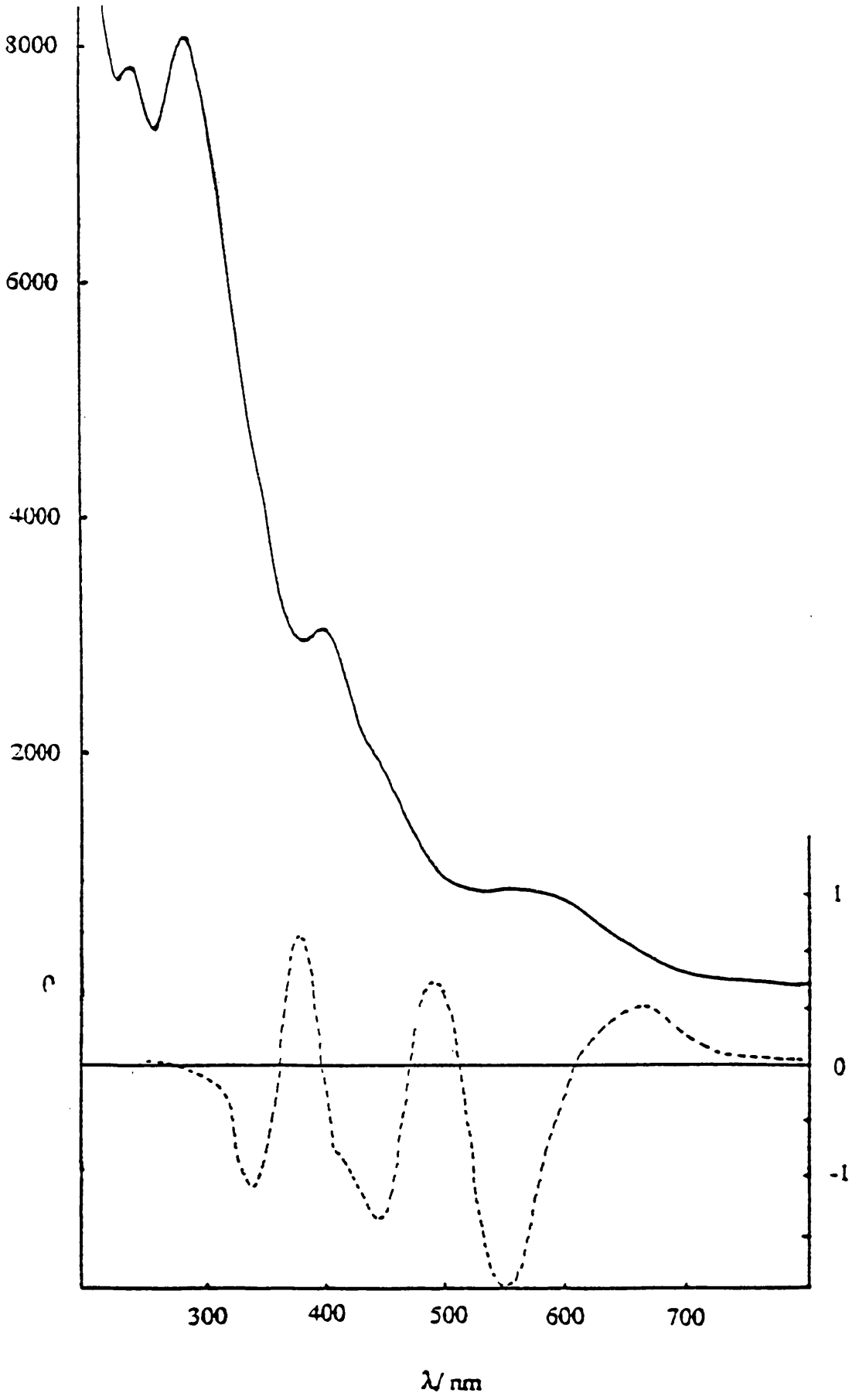

Fig. 4.9. *Absorption / CD spectra of* $[Mn(IV)L^2]^+$.

The difference in the positions of the respective bands in the absorption spectra of $[Mn(II)L^1H_3L^1Mn\ (IV)]^{3+}$ and $[Mn(IV)L^2]^+$ indicates the slight variation in donor properties of the oxygen ligators in each case. With $[Mn(II)L^1H_3L^1Mn(IV)]^{3+}$ the alkoxide groups are hydrogen bonded to the alcohol groups of the other half of the dimer which accordingly reduces their π-basicity; no such interactions occur in the $[Mn(IV)L^2]^+$ complex. Thus the two highest transitions are at slightly higher energy for $[Mn(IV)L^2]^+$. They are assigned as ligand (σ) to metal (e_g, t_{2g}) transitions with donation to the t_{2g} set taking place at higher energy. The remaining, lower energy, transitions are possibly ligand (p^π) to metal (d^π) in origin, since for the less π-basic species (i.e. $[Mn(IV)L^1]^+$) these transitions occur at higher energy than in the $[Mn(IV)L^2]^+$ case.

4.3.3 E.P.R. SPECTROSCOPY.

The EPR spectrum of $[Mn(IV)L^2][PF_6].H_2O$ (fig4.10) was obtained by Dr. L. Yellowlees (Edinburgh) as a frozen (77K) acetonitrile solution. The two components, g values 3.674 and 1.922 are consistent for a d^3 ion with axial symmetry in a strong ligand field (8) thus confirming the Mn(IV) assignment. No hyperfine coupling to ^{55}Mn was observed in the room temperature spectrum.

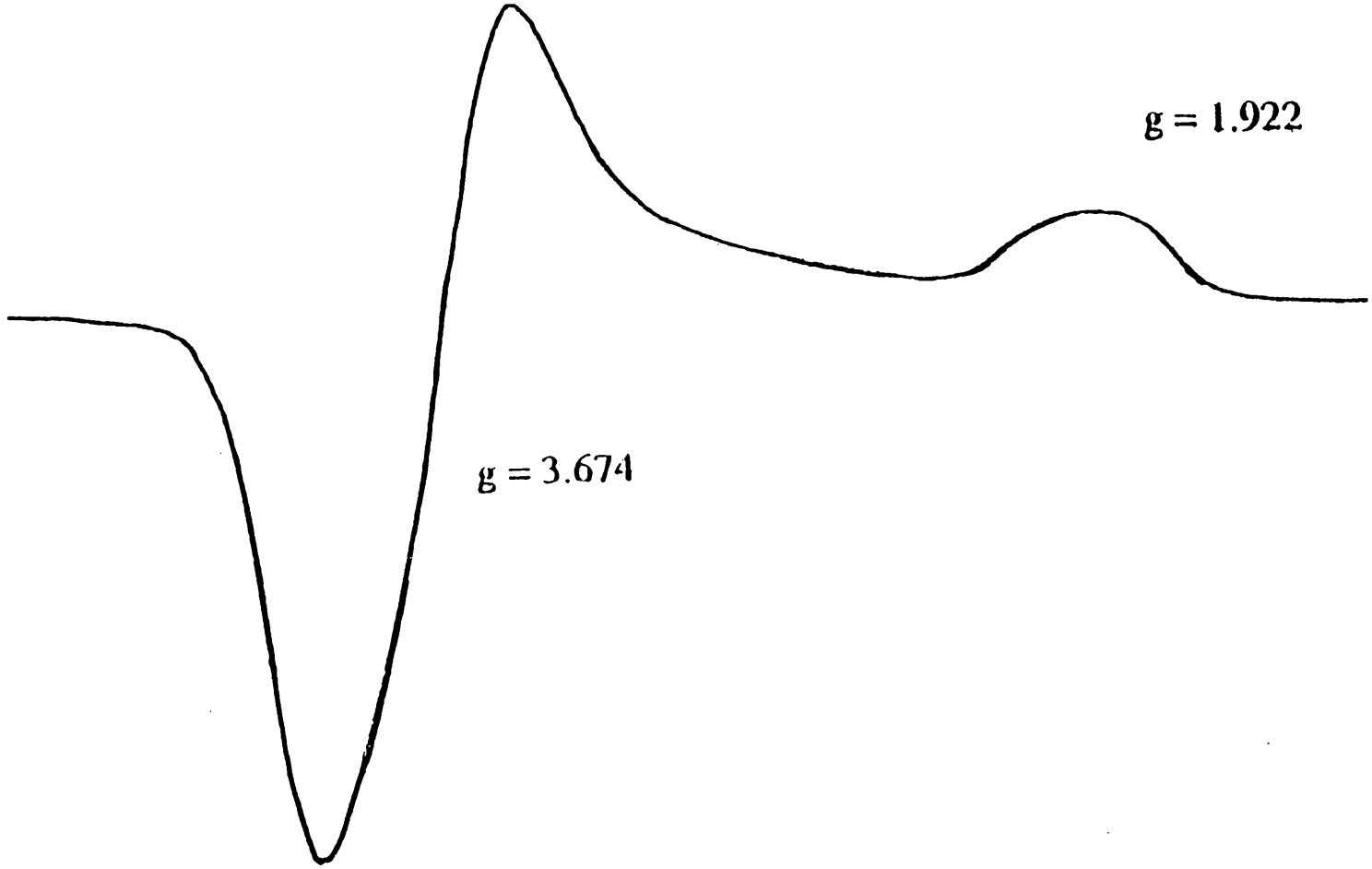

Fig. 4.10. *EPR spectrum of* $[Mn(IV)L^2][PF_6].H_2O$.

4.3.4 ELECTROCHEMISTRY

The cyclic voltammogram (fig4.11) was obtained in acetonitrile, 4Å molecular sieves were used to absorb the water of crystallisation. Two irreversible reductions are displayed at -0.58V and -0.79V (both vs Ag/Ag^{+}). No oxidation waves are observed. The first reduction at -0.58V is assigned as Mn(IV)→Mn(III) and the second (-0.79V) is believed to be a Mn(III)→Mn(II) process. These potentials are unusually high when compared with the isoelectronic Mn(IV) species of $[Mn(II)L^{1}H_{3}L^{1}Mn\ (IV)]^{3+}$; it is possible that the steric bulk of L^{2} prevents efficient complex-electrode interaction. Although it must be noted that even fully encapsulated metal ions (e.g. in sepulchrate complexes) display redox activity at lower potentials.

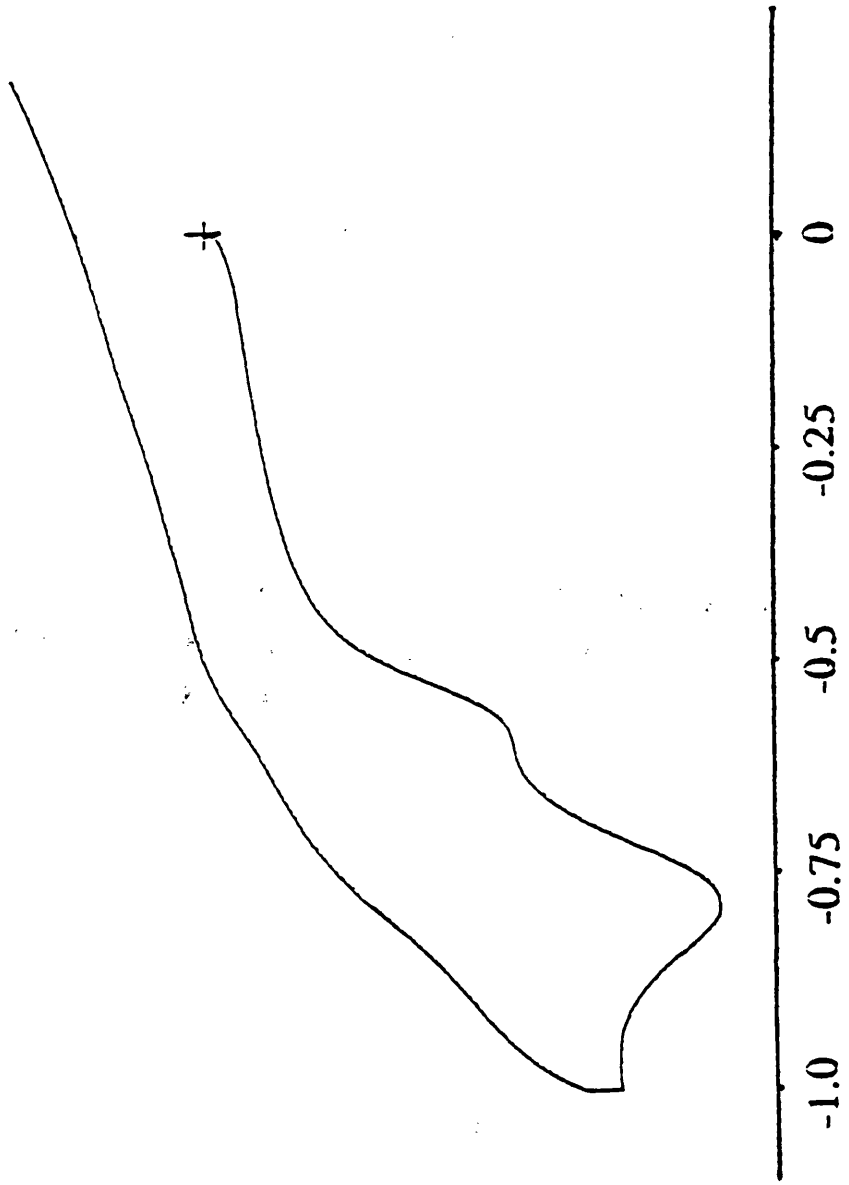

Fig. 4.11. *Cyclic voltammogram of $[Mn(IV)L^2]^+$ in MeCN vs. Ag/Ag^+ ($0.1 mol l^{-1}$ $AgNO_3$ in MeCN).*

References.

(1) K.Wieghardt, *Angew. Chem. Int. Ed. Engl.*, 1989, **28**, 1153.

(2) F.A.Cotton and G.Wilkinson, *Advanced Inorganic Chemistry (5th.Ed.)*, Wiley-Interscience, **1988**, p.698.

(3) A.A.Belal, L.J.Farrugia, R.D.Peacock and J.Robb, *J. Chem. Soc., Dalton Trans.*, 1989, 931.

(4) M.Gerloch, Prog. *Inorg. Chem.*, 1979, **26**, 1.

(5) U.Bossek, K.Wieghardt, B.Nuber and J.Weiss, *Angew. Chem. Int. Ed. Engl.*, 1990, **29**, 1055.

(6) I.A.Fallis, *Ph.D. Thesis*, University of Glasgow, 1992.

(7) A.A.Belal, P.Chaudhuri, I.Fallis, L.J.Farrugia, R.Hartung, N.M.Macdonald, B.Nuber, R.D.Peacock, J.Weiss and K.Wieghardt, *Inorg. Chem.*, 1991, **30**, 4397.

(8) S.Dutta, P.Basu and A.Chakravorty, *Inorg. Chem.*, 1991, **30**, 4031.

CHAPTER 5

ZINC - VANADIUM COMPLEX WITH L^1H_3.

5.1.1 VANADIUM CHEMISTRY.

The chemistry of vanadium in aqueous solution, especially of the higher (+4, +5) oxidation states is dominated by oxo ions such as $[V0]^{2+}$ and $[VO_2]^{+}$. In general, oxidation states of less than +3 are too reducing to form stable complexes under neutral conditions. Non-oxo vanadium species i.e. non-vanadyl ions are rare, unless stabilised by a suitable ligand. The investigation of vanadium and its complexes is an area of rapid expansion, as their value to bioinorganic chemistry and role in some biological processes becomes more widely recognised. Vanadium is now known to be present at the active site of various enzymes (**1**). In many naturally occurring vanadium containing compounds, the metal is present in its non-vanadyl (bare) state. There are, however, very few examples of synthetic non-oxo complexes recorded, they comprise catecholate (**2**), carboxylate (**3**) and phenolate (**4, 5**) ligands containing a mixed N,O donor set in the majority of cases.

One of the first published examples of a "bare" vanadium complex was $[V(S_2C_2Ph_2)_3]$ (**6**), in which the vanadium was found to be in a trigonal prismatic environment.

An all nitrogen donor (VN_6) complex, incorporating a sepulchrate or cage structure was prepared by Sargeson and co-workers (**7**). The resulting compound was extremely stable over a wide pH range (1-10), with the metal ion (V(IV)) encapsulated in a pseudo trigonal prismatic geometry (fig5.1), the

twist angle (ϕ) was measured at 36°. Electrochemical studies gave two reduction waves at -0.42V and -0.69V (vs Ag/AgCl) corresponding to the V^{V}/V^{IV} and V^{IV}/V^{III} redox couples respectively.

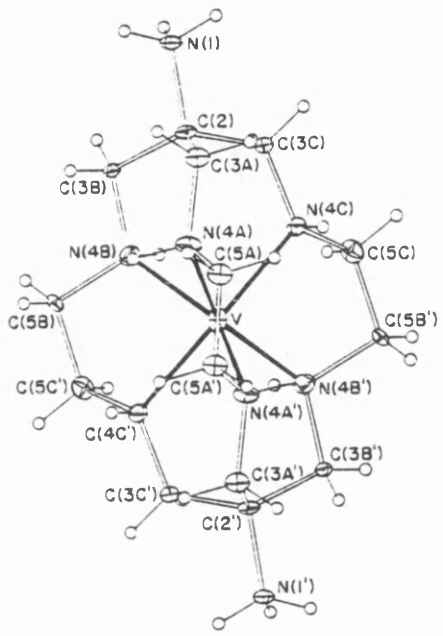

Fig 5.1. *Crystal Structure of [V(IV){di(amH)$_2$sar-2H}]$^{4+}$.*

Wieghardt and co-workers (**8**) prepared a V(III) dimeric complex with 1,4,7-trimethyl TACN. The crystal structure showed each metal centre in a pseudo octahedral environment, with the two halves, of the dimer, held together via a μ-oxo and two μ-acetate bridges. On aerial oxidation this compound was found to form a vanadyl V(IV) complex.

Phenolate donor ligands are of great interest because of their relevance to tyrosinate residues found in enzymes such as transferrin (**9**). One such model

ligand is tris phenolate pendant arm substituted TACN synthesised by Auerbach *et al.* (**4**). The resulting bare V(IV) complex was obtained via oxidation of the V(III) species; crystal structure analysis showed the metal centre to be in a pseudo-octahedral environment, however, no twist angle (ϕ) was reported. The average metal-ligand bond lengths were V-N 2.168Å and V-O 1.827Å indicating a degree of π bonding character in the V-O bond. Investigation of this complex using cyclic voltammetry displayed three reversible, one electron, waves at +0.38V (V^{V}/V^{IV}), -0.50V (V^{IV}/V^{III}) and -2.41V (V^{III}/V^{II}) all these $E_{½}$ values are with respect to the internal Fc^{+}/Fc reference couple. The three observed bands in the electronic spectrum occurred at 553nm, 430nm and 266nm, in addition a shoulder was seen at 310nm, indicating a fairly distorted geometry, with possibly tetragonal as well as trigonal distortion to lift the degeneracy of the $^{2}T_{2g}$ and $^{2}E_{g}$ levels. The molar extinction coefficients of all three bands indicated at least one (the highest energy transition) if not all three arose from metal-ligand charge transfer (CT) modes. A similar phenolate system (**5**) also isolated a non-vanadyl V(IV) complex; the observed reduction potentials in this case were at +0.16V (V^{V}/V^{IV}) and, -0.84V (V^{IV}/V^{III}) again vs Fc^{+}/Fc. The electronic absorption bands were very intense and assigned to vanadium phenolate charge transfer although in this case only two transitions at 512nm and 400nm were observed. From the crystal structure the observed metal-ligand bonding contacts at V-N(average) 2.183Å and V-O(average)

1.874Å were not as short as in the previous macrocyclic case, although the relative difference in V-N and V-O distances was maintained.

Interest in alkoxide donation is also increasing mainly because of their relevance to the deprotonated alcohol groups found in serine and threonine residues. A recent paper (**10**) investigated the complexation behaviour of hydroxyalkyl salicyli -deneamine systems (fig5.2). These potentially tridentate NO_2 donors formed stable complexes with oxo cations of V(IV) which underwent oxidation in solution to the corresponding V(V) species, unfortunately no "bare" vanadium compounds were synthesised, suggesting that this ligand type is unable to stabilise non-vanadyl derivatives.

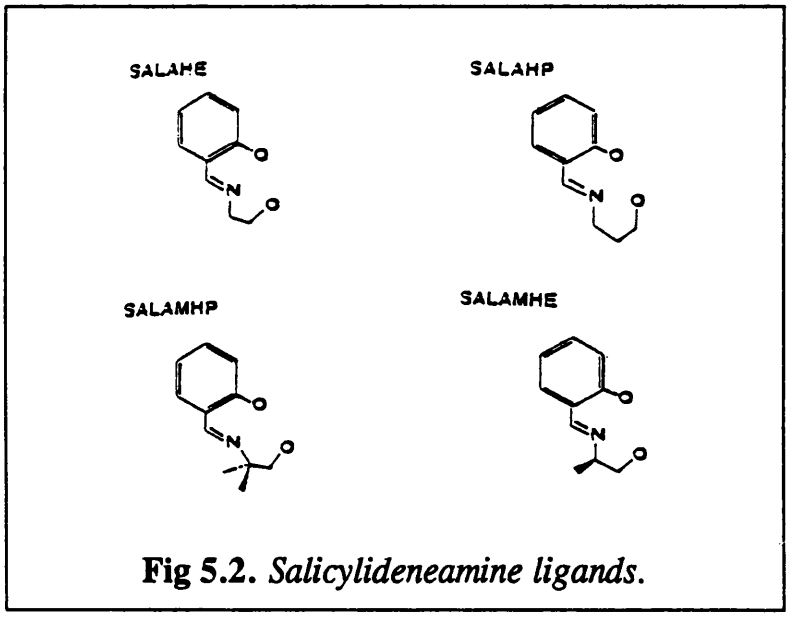

Fig 5.2. *Salicylideneamine ligands.*

5.1.2 ZINC CHEMISTRY.

The chemistry of zinc complexes is mainly associated with its +2 oxidation state. Strictly speaking, Zn(II), because of its $3d^{10}$ electronic configuration is classed as a group IIB metal rather than a transition metal. It commonly forms complexes with coordination numbers of 4 or 5; hexadentate coordination compounds are less common.

In biological terms, Zn(II) is extremely important since it plays an essential role at the active centre of a great many enzymes (**11**).

Zinc has been found to form extremely stable complexes with TACN and its derivatives (**12**), and in particular the coordination of zinc with amine-alcohol donors is currently of great interest due to their relevance in the coordination sites in many biological molecules.

5.2 SYNTHESIS OF COMPLEX.

The synthesis of the mixed metal cation $[Zn(II)L^1H_3.L^1V(IV)]^{3+}$ (fig5.3) involved initially the reduction of an aqueous vanadyl chloride solution with zinc granules. The resulting green solution $\{V(III)_{aq}\}$ was combined with the ligand and on treating the greyish mixture with solid ammonium hexafluorophosphate, a mixture of yellow and purple solids precipitated out.

Washing with acetone dissolved out the yellow material (believed to be the corresponding V(V) complex) leaving the purple solid which was successfully recrystallised from acetonitrile to form crystallographic quality crystals.

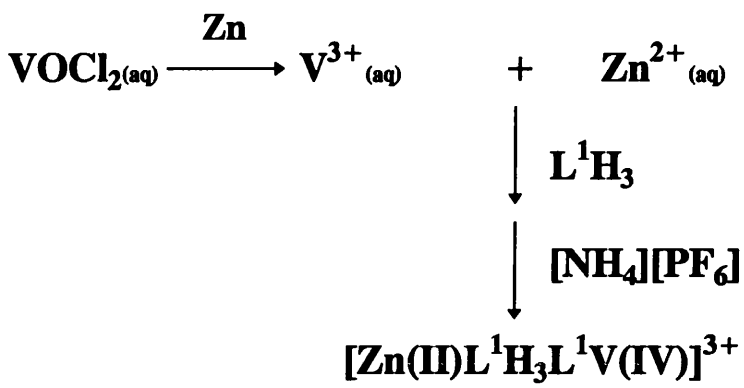

Fig 5.3. *Complexation scheme.*

5.3 STRUCTURAL ANALYSIS.

The crystal structure and atom labelling scheme of $[Zn(II)L^1H_3.L^1V(IV)]^{3+}$ is presented in figure 5.4. The dimeric structure is maintained through hydrogen bonding between the alcohol ligators of the Zn(II) unit and the alkoxide groups of the V(IV) side. A list of bond lengths and angles is presented in table 5.1. The view down the main C_3 axis (figures 5.5, 5.6) immediately shows the different geometry about each metal ion. This dissimilarity can be explained on the basis of the relative stereochemical requirements of the two metal centres. The V(IV) ion is in a distorted octahedral environment with a twist angle of

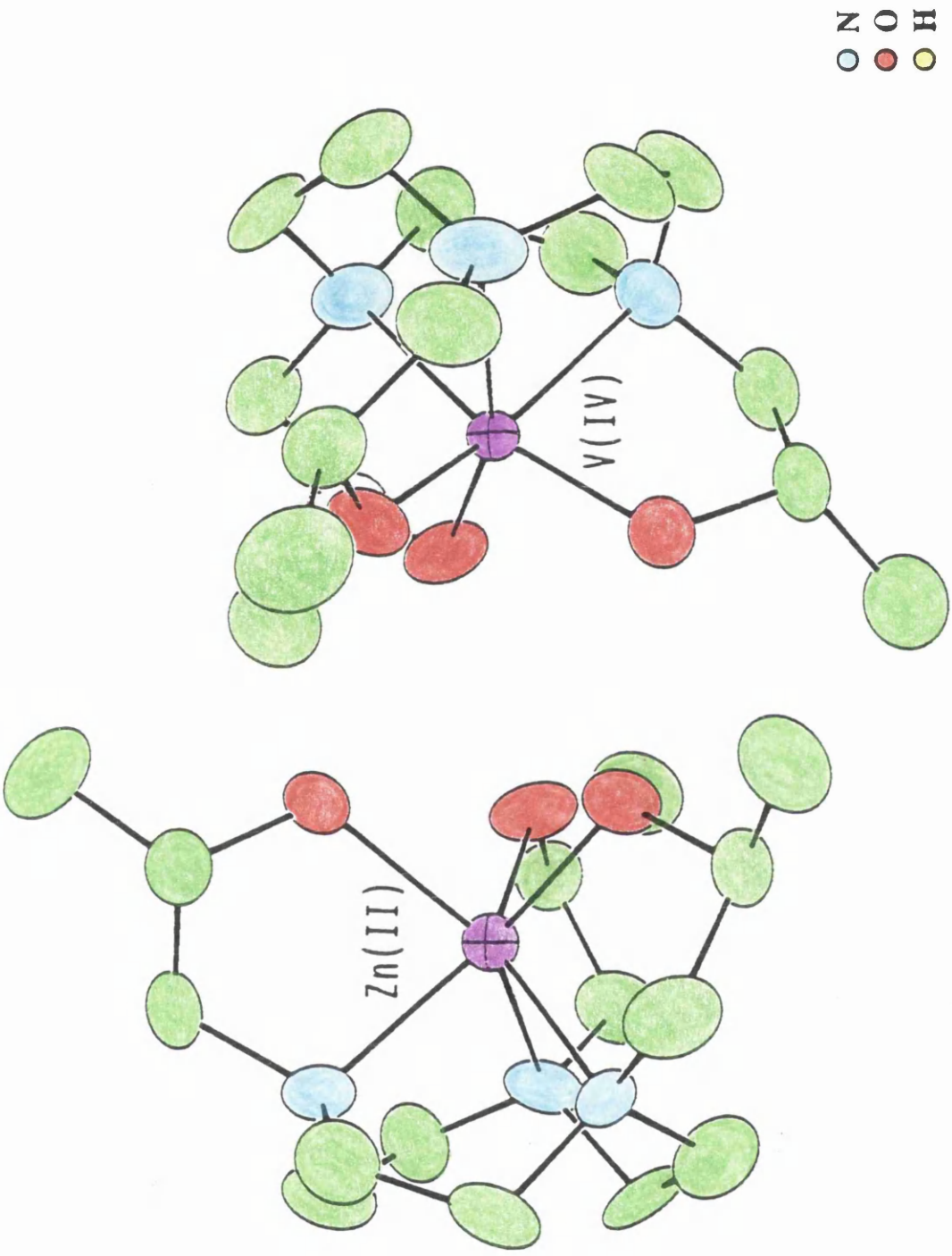

Fig. 5.4. *Crystal structure of* $[Zn(II)L^1H_3L^1V(IV)]^{3+}$ *cation.*

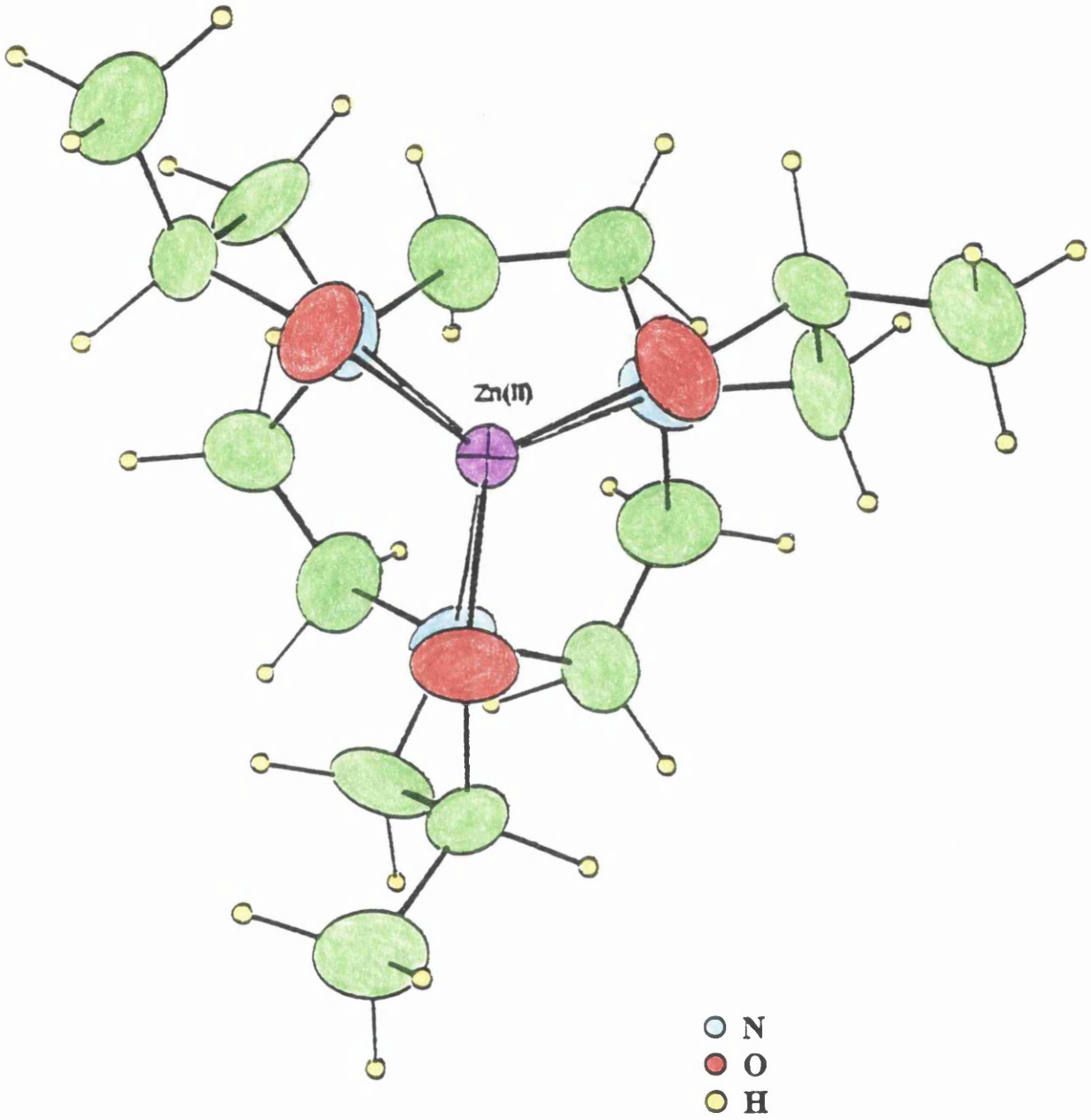

Fig. 5.5. *View along C_3 axis of $[Zn(II)L^1H_3]^{2+}$.*

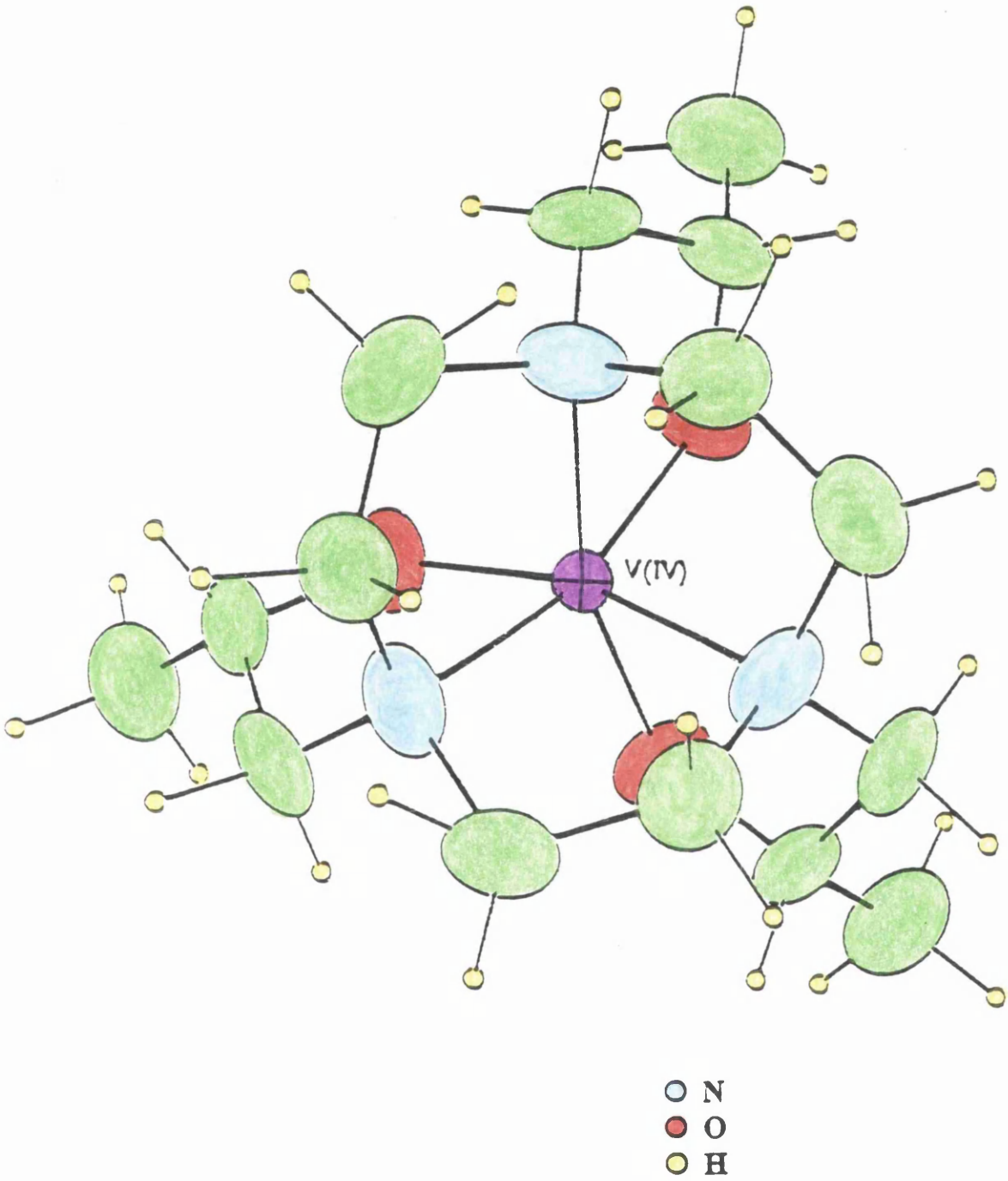

Fig. 5.6. *View along C_3 axis of $[V(IV)L^1]^+$.*

20.2°. The d^1 configuration of this metal confers a small degree of LFSE (i.e. only a small preference for octahedral coordination) and, as a result, the magnitude of trigonal twist is fairly large. On the other hand the Zn(II) centre (d^{10}) is expected to show absolutely no preference for octahedral symmetry, hence the ligand's requirement for trigonal prismatic coordination is satisfied, with a twist angle of 55.5°. There are a few examples of trigonal prismatic coordination to a Zn(II) centre, however, this is the first observed for a saturated ligand system.

Zn-N(1)	2.146(10)	V-N(2)	2.177(13)
Zn-O(1)	2.110(9)	V-O(2)	1.872(9)
N(1)-Zn-N(1)	81.6(4)	N(2)-V-N(2)	81.5(5)
N(1)-Zn-O(1)	78.5(4)	N(2)-V-O(2)	79.6
O(1)-Zn-O(1)	86.9(4)	O(2)-V-O(2)	97.5(5)

Table 5.1. *Selected bond lengths (Å) and bond angles (deg) for* $[Zn(II)L^1H_3.L^1V(IV)]^{3+}$.

The configurational symmetry about each metal ion is also different. In both cases the exocyclic chelate rings, formed by the hydroxy propyl arms, have the same δ conformation. As a result of the different stereochemistries in each subunit, the endocyclic rings are of differing signs. In the V(IV) side the λ

conformation is present, on the other hand the Zn(II) half diplays the opposite δ symmetry. The overall absolute configurations are therefore Δ(λδ) for the $[V(IV)L^1]^+$ moiety; this is the same as in Cr(III) and Co(III) complexes with L^1H_3. That of the $[Zn(II)L^1H_3]^{2+}$ unit is assigned Λ(δδ) which is similar to the other trigonal prismatic species, $[Mn(II)L^1H_3]^{2+}$, of the mixed valence manganese dimer.

It is not clear why a mixed metal species is formed. A V(III) dimer is unlikely due to the probable oxidation of this species in aqueous solution to V(IV). A V(IV) dimer is unrealistic, the presence of a high oxidation state ion (i.e. good Lewis acid) increases the lability of the hydroxyl protons - leading to pendant arm deprotonation (i.e. the formation of alkoxide ligators). A dimeric structure requires a degree of hydrogen bonding to effect stabilisation; this is not possible if both halves are deprotonated. Disproportionation of V(III) to V(II) and V(IV) is a possibility, however, a V(II) ion in aqueous media would be too reducing to form a stable complex, even with a ligand like L^1H_3. The presence of Zn(II) ions in the initial solution must be a factor in dimeric complex formation. The overall reaction therefore is not simple, however, a putative mechanism may be put forward. The initial V(III) species present, undergo oxidation on combining with L^1H_3 in aqueous solution; simultaneously the Zn(II) metal ions also react with L^1H_3. The $[V(IV)L^1H_3]^{4+}$ unit undergoes deprotonation to alkoxide ligation yielding $[V(IV)L^1]^+$, this unit is stabilised in solution by hydrogen

bonding with the $[Zn(II)L^1H_3]^{2+}$ moiety, giving the complex $[Zn(II)L^1H_3.L^1V(IV)]^{3+}$.

Reactions using modified conditions were performed in an attempt to isolate a pure divanadium complex. In order to prevent aerial oxidation the process was carried out under an N_2 atmosphere; again the final compound analysed as above. Additionally different reductants* were utilised in the initial reduction process, unfortunately no products could be isolated from the resulting solutions; it seems likely that the presence of Zn(II), however small, is a contributory factor in the complexation process.

* sodium disulphite ($Na_2S_2O_5$), phosphinic acid (H_3PO_2), magnesium turnings, SO_2 gas and Na_2S (sodium sulphide).

5.4 N.M.R. SPECTROSCOPY.

In an attempt to study the oxidation/reduction process spectroscopically, some n.m.r. data was obtained for the $[Zn(II)L^1H_3.L^1V(IV)][PF_6]_3$. It was reasoned that the change from a slightly paramagnetic V(IV) d^1 centre to a d^0 configuration, V(V), could be followed using nmr spectroscopy. The complex was dissolved in deutero-dimethyl formamide giving a light purple solution; in spite of the d^1 centre, a fairly well resolved ^{13}C n.m.r. spectrum was obtained.

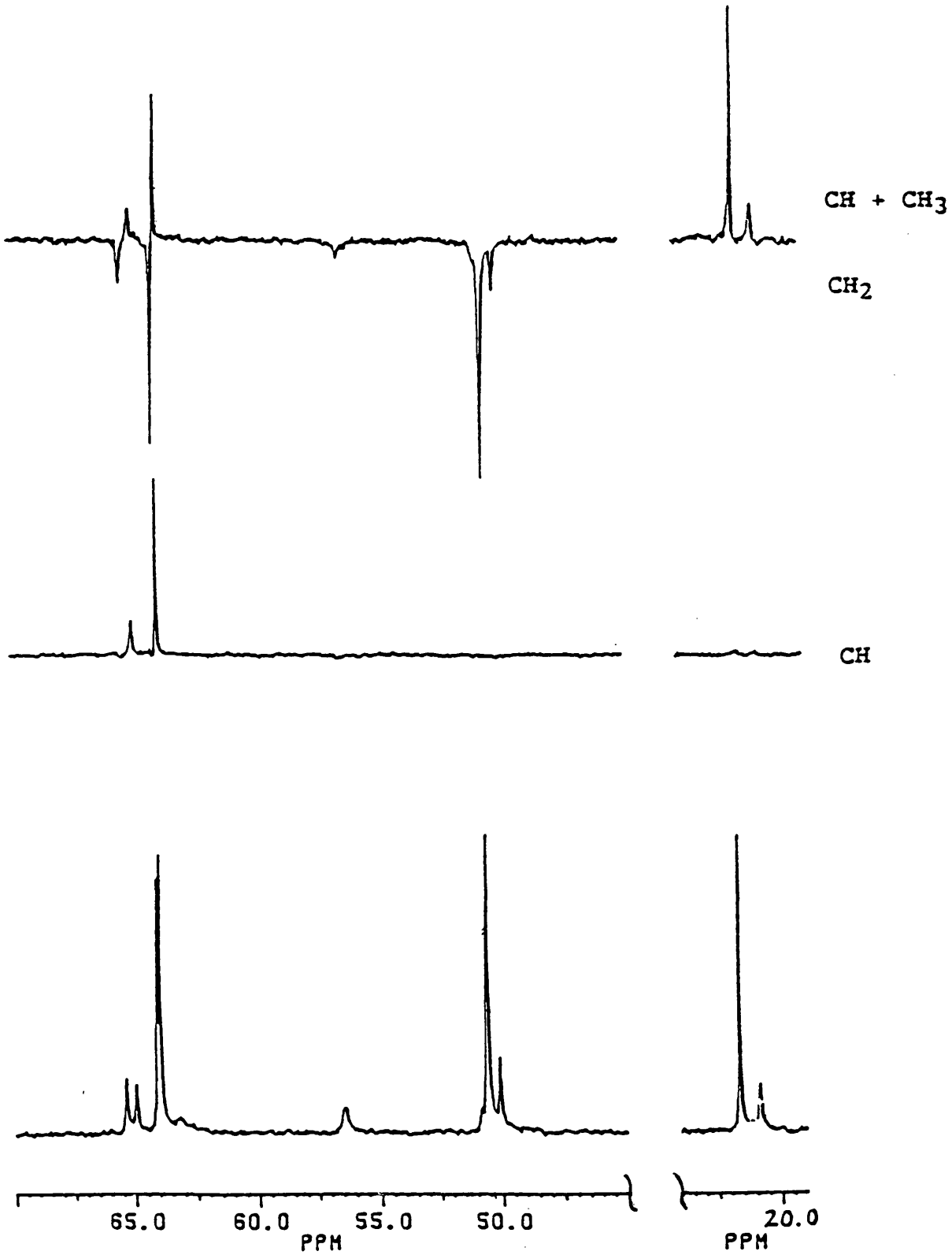

Fig. 5.7. *^{13}C n.m.r. spectrum of $[Zn(II)L^1H_3L^1V(IV)]^{3+}$ in d_7- DMF.*

The ^{13}C DEPT sequence (fig5.7) displays sharp signals due to the diamagnetic $[Zn(II)L^1H_3)]^{2+}$ component with weaker broader resonances of the paramagnetic $[V(IV)L^1]^+$ unit. The following assignments have been made (Table 5.2).

^{13}C DEPT SEQUENCE			
carbon type	$[Zn(II)L^1H_3]^{2+}$	$[V(IV)L^1]^+$	
(a) $\underline{C}H_3$	21.6ppm	20.82ppm	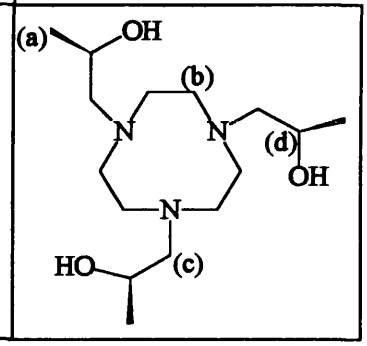
b) $\underline{C}H_2$ (ring)	50.58ppm	50.06ppm	
(c) $\underline{C}H_2$ (arm)	64.01ppm	65.35ppm	
(d) $\underline{C}H$	63.92ppm	64.94ppm	

Table 5.2. ^{13}C NMR data.

The ^1H n.m.r. spectrum (fig5.8) shows both the unshifted diamagnetic signals of the Zn(II) subunit and the shifted broader resonances of the V(IV) half. The methyl ($\underline{C}H_3$) signals (coupled to C-H) can be clearly observed at 1.28ppm {Zn(II) side} and 1.29ppm {V(IV) side}. Unfortunately assignment of the methylene signals is extremely difficult, due to the overlapping nature of the resonances; it is merely possible to suggest that the complex multiplet at 2.85-3.4ppm is in the expected region for $C\underline{H}_2$ protons. The methine ($C\underline{H}$) peaks occur at 4.22ppm $\{[Zn(II)L^1H_3]^{2+}\}$ and at 4.35ppm $\{[V(IV)L^1]^+\}$. The broadened singlet observed at +22ppm is thought to be due to the bridging protons. The same

signal found in the analogous Co(III) complex, $[Co(III)L^1H_3L^1Co(III)][PF]_6$, occurred at +14.6ppm (**13**), the influence of the V(IV) centre would be expected to move this signal downfield, although a shift of almost 8ppm is larger than anticipated.

The sample was oxidised using $[NO][PF_6]$ to produce a yellow solution; the ^1H n.m.r. spectrum of this sample was obtained (fig5.9). The spectrum displayed a doublet for the methyl protons of equal intensity; all other signals corresponded to the methylene and methine protons of each unit. There was no shift of methine signals, line broadening or weakening in intensity, suggesting the paramagnetism present in the purple complex had been removed. Unfortunately no low field signals, consistent with bridging protons, was observed suggesting that the dimeric nature of the complex breaks down on oxidation of the V(IV) component.

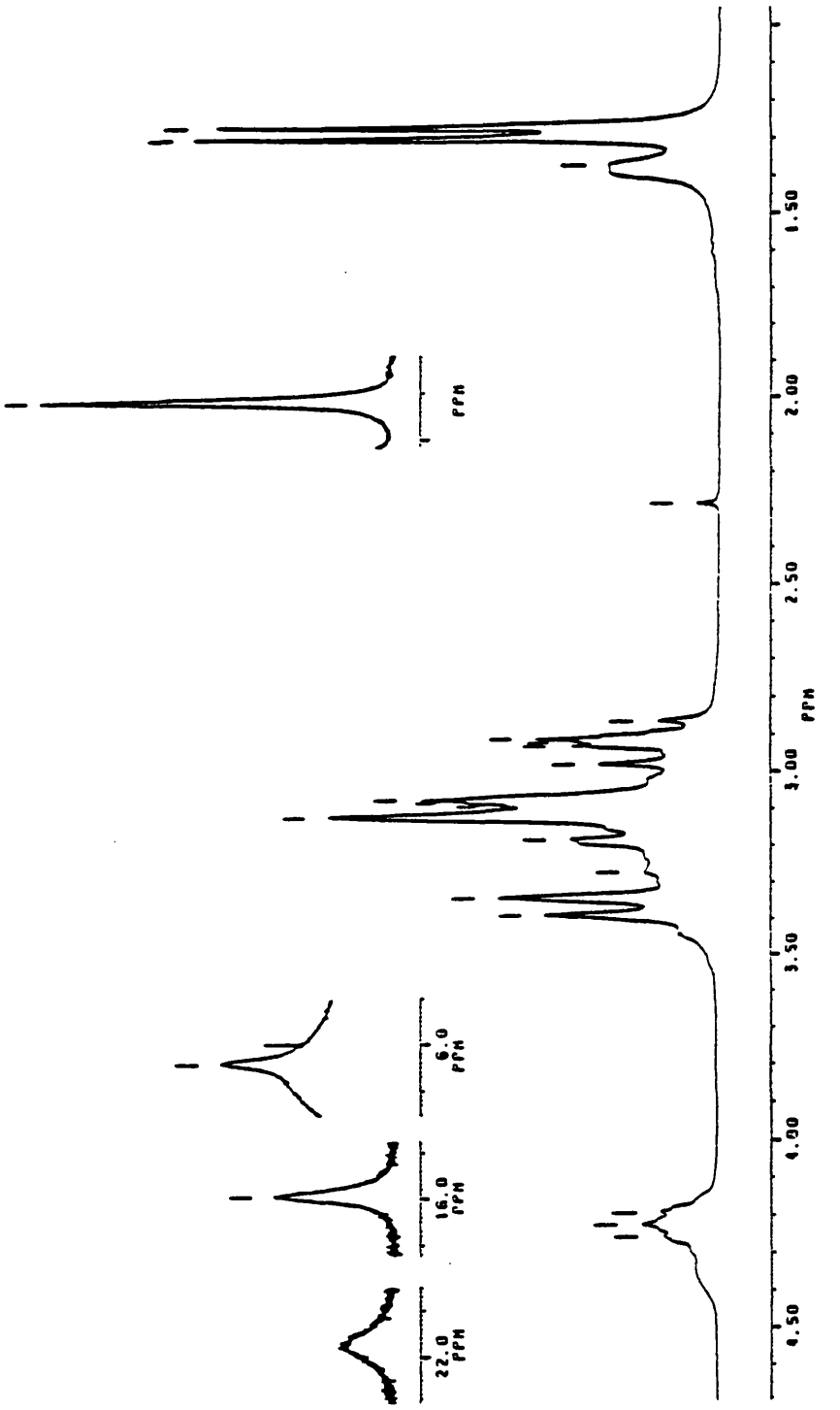

Fig. 5.8. *^1H n.m.r. spectrum of $[Zn(II)L^1H_3L^1V(IV)]^{3+}$ in d_7- DMF.*

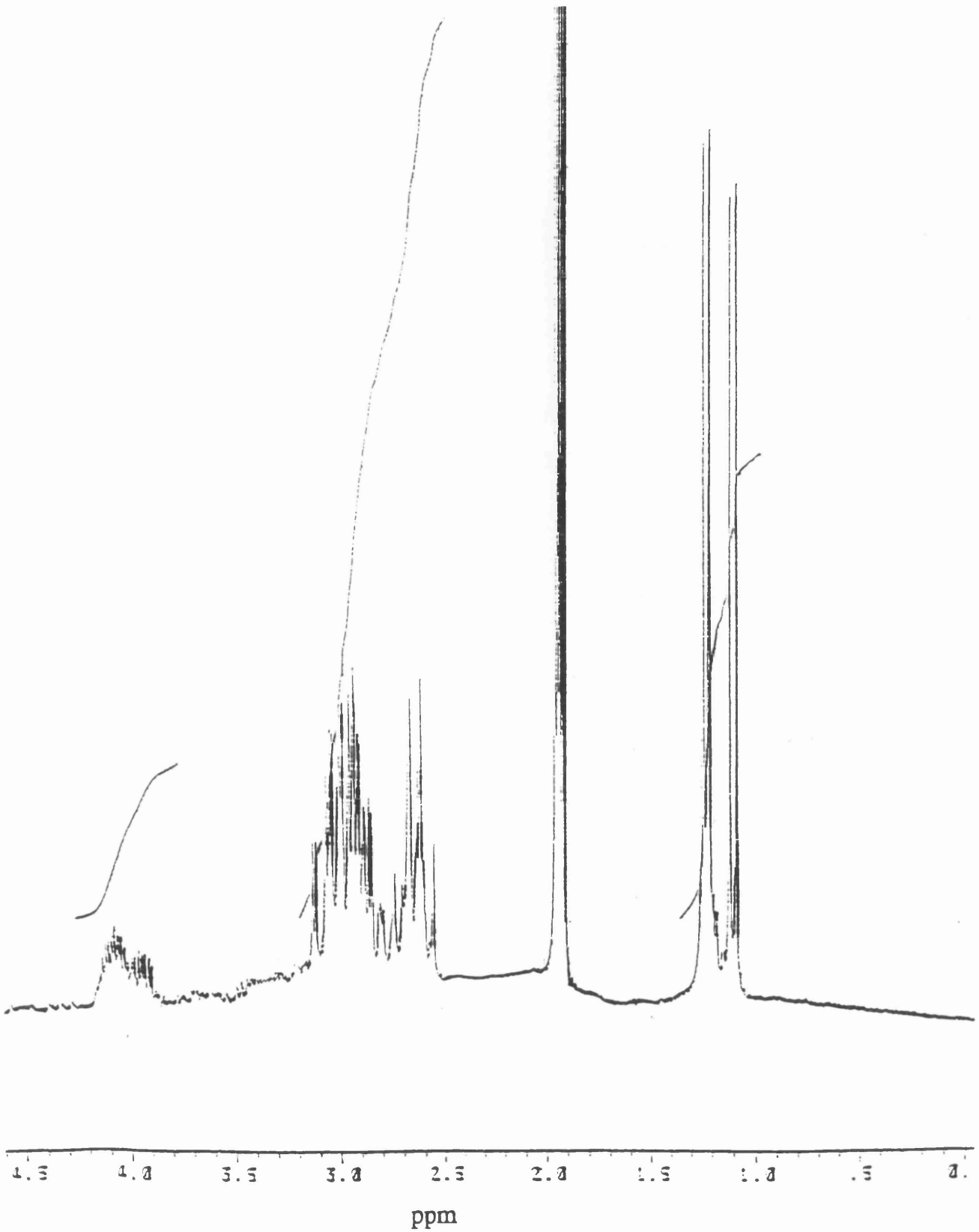

Fig. 5.9. *^1H n.m.r. spectrum of oxidation product run in d_3-MeCN.*

5.5 ELECTRONIC SPECTROSCOPY.

In general the absorption spectra of vanadium(IV) complexes are simple. In octahedral symmetry the ground state (^2D) is split into $^2T_{2g}$ and ^2E_g levels; the transition from $^2T_{2g} \rightarrow {}^2E_g$ occurs in the visible region. As the symmetry about the V(IV) centre is reduced the triplet ground state degeneracy is removed, forming $^2A_1$ and ^2E levels. A second peak or shoulder to this main band may be observed from the splitting of the excited ^2E state by a Jahn Teller mechanism.

It is characteristic of many bare vanadium(IV) complexes with phenolate or catecholate ligands to be very intense in colour (blue or violet) due to ligand-metal charge transfer bands in their visible spectra (ε=2000-10,000$mol^{-1}dm^3cm^{-1}$). The presence of a high oxidation state metal centre facilitates these charge transfer modes, in general they occur from 20,000cm^{-1} upwards.

In the case of $[Zn(II)L^1H_3.L^1V(IV)]^{3+}$ the complex is pale lilac in colour which is due to a single absorption band ($^2T_{2g} \rightarrow {}^2E_g$) of V(IV) at 540nm ($\varepsilon$=60$mol^{-1}dm^3cm^{-1}$). This absorption is partially overlapped by the tail of a charge transfer transition (λ_{max}=330nm; ε=1560$mol^{-1}dm^3cm^{-1}$), the spectrum is shown in figure 5.10.

The circular dichroism spectrum (fig5.10) of this visible transition is of a single sign, the positive rotational strength is fully consistent with a negative twist of ligators about the metal ion as displayed by the $[V(IV)L^1]^+$ half.

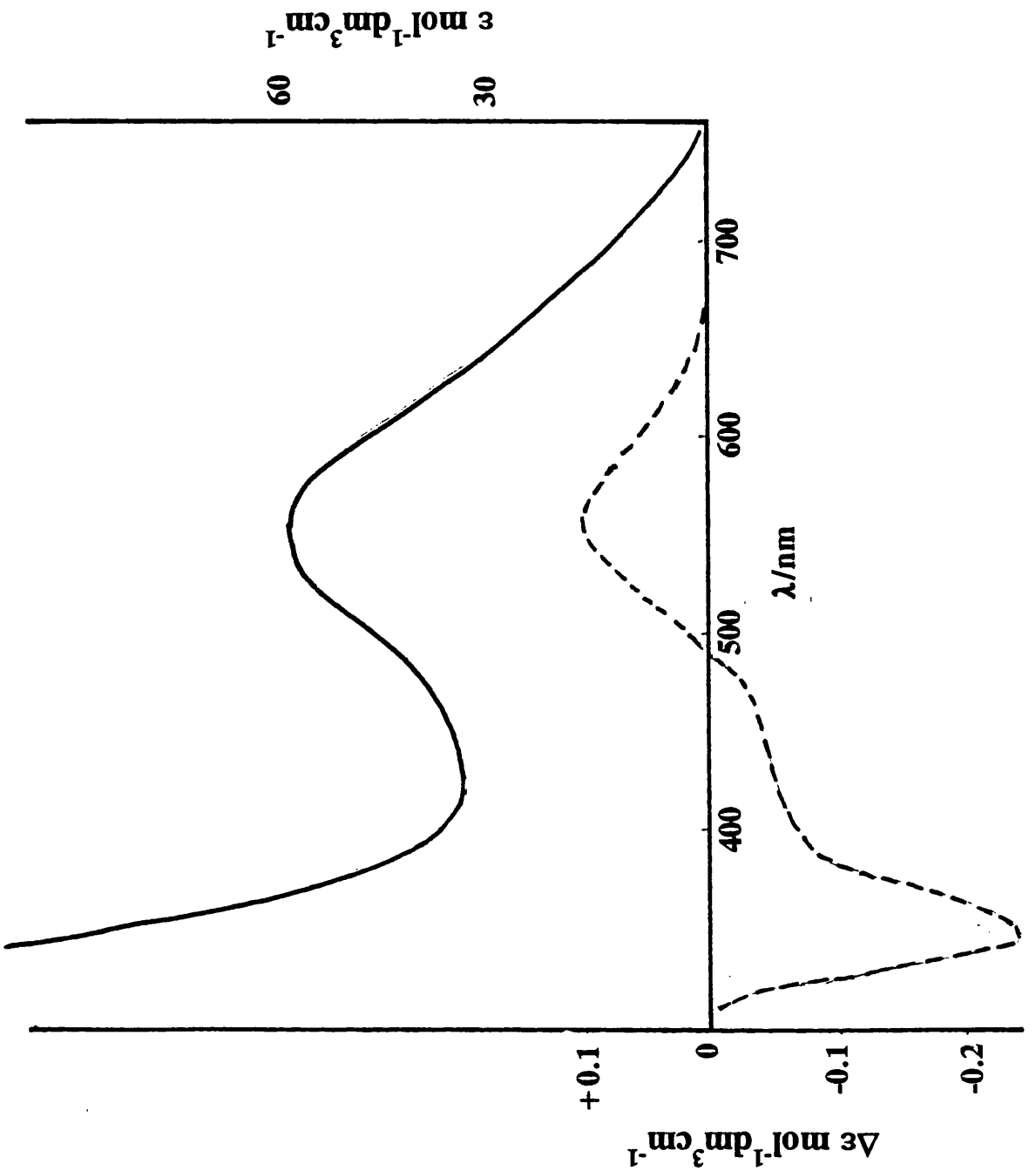

Fig. 5.10. *Absorption / CD spectra of* $[Zn(II)L^1H_3L^1V(IV)]^{3+}$ *in MeCN.*

The dissymmetry factor (g) pertaining to this band is of the order $8x10^{-3}$ confirming that the transition type is d↔d and is also magnetic dipole allowed; it must be therefore assigned to the $^2A_1$ or ^2E ($^2T_{2g}$) → ^2E (^2E_g) transition. This is entirely consistent with a d^1 ion in almost C_3 symmetry. There is no sign of a second transition at lower energy corresponding to the intra configurational $^2A_1$ ↔ ^2E ($^2T_{2g}$) transition. This is most probably masked by the vibrational spectrum which strongly suggests that the $^2A_1$ ↔ ^2E trigonal splitting is quite small.

The absorption spectrum of the oxidation product (yellow material) believed to be a V(V) containing complex, displayed only an intense charge transfer type band at λ_{max}=400nm (ε=1890$mol^{-1}dm^3cm^{-1}$) the relatively low energy of this band indicates the ease of a CT transition to a metal with unoccupied d-orbitals.

5.6 ELECTROCHEMISTRY.

The cyclic voltammogram measured in dimethyl formamide of the $[Zn(II)L^1H_3.L^1V(IV)]^{3+}$ cation (fig5.11) shows a single reversible redox wave at +0.105V vs Fc/Fc^+ which is assigned to the V^{IV}/V^V couple. This value is indicative of V(IV) being oxidised to vanadium(V) by molecular oxygen (E_o=+1.23V). In comparison with other complexes that incorporate the

vanadium(IV) non-oxo ion the metal centre in $[V(IV)L^1]^+$ is far easier to oxidise to the higher +5 oxidation state.

The corresponding V^{IV}/V^V couples for catecholate or phenolate type complexes are +0.18V and +0.38V respectively. In fact the stabilisation of this $[V(IV)L^1]^+$ species may be attributed to the hydrogen bonding with the $[Zn(II)L^1H_3]^{2+}$ unit. It has proved impossible to obtain a V(IV) species unless zinc is used in the initial reduction. Any protonation of the dimer apparently results in oxidation to a V(V) species, on acidification the purple solution containing $[Zn(II)L^1H_3.L^1V(IV)]^{3+}$ turns yellow almost immediately. Interestingly the reduction to a V(III) species diplays an irreversible wave at -1V vs Fc/Fc^+ suggesting chemical as well as electrochemical irreversibility.

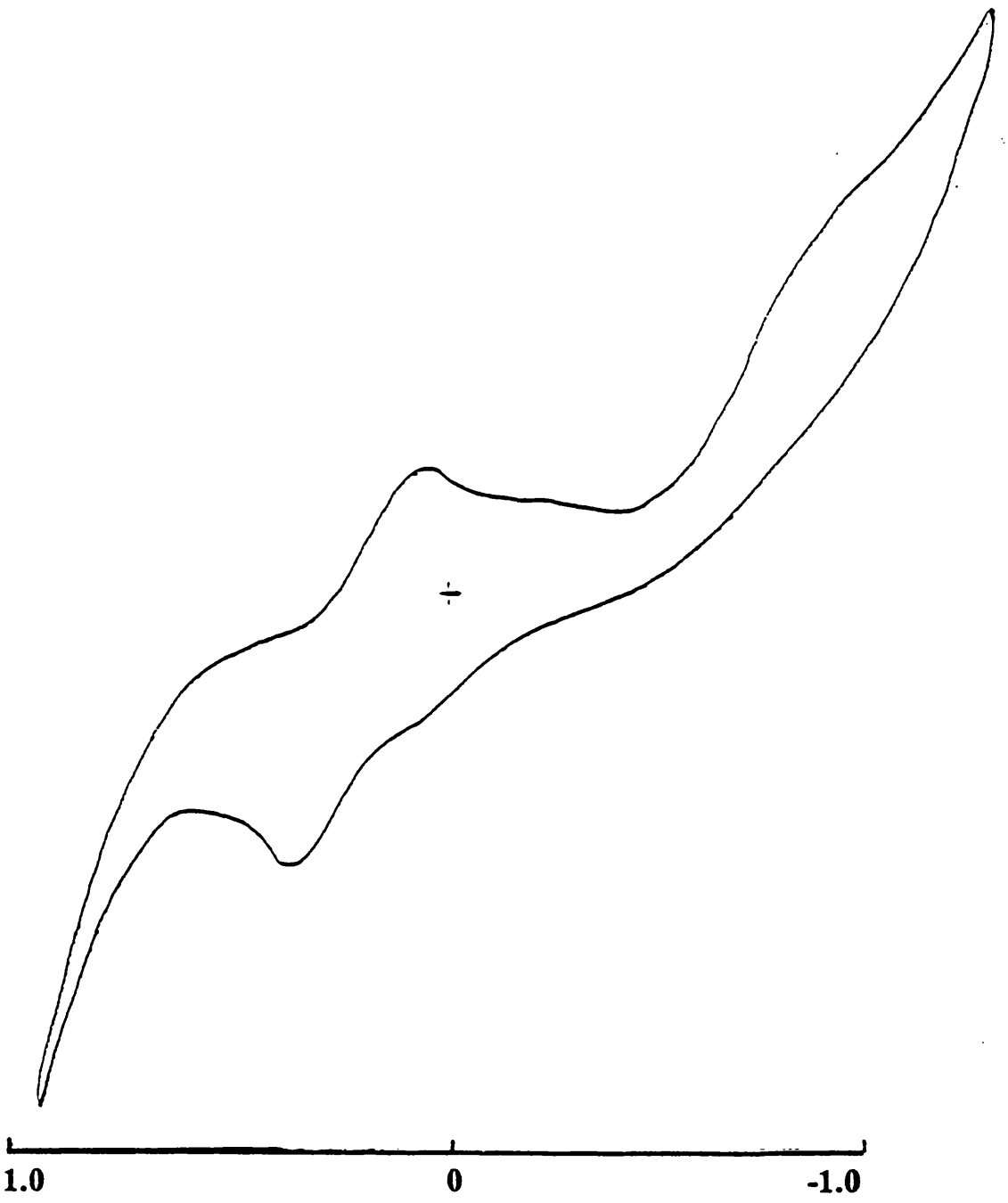

Fig. 5.11. *Cyclic voltammogram of* $Zn(II)L^1H_3L^1V(IV)]^{3+}$ *in DMF vs.* Fc/Fc^+.

References.

(1) D.Rehder, *Angew. Chem. Int. Ed. Engl.*, 1991, **30**, 148.

(2a) T.A.Kabanos, A.M.Z.Slawin, D.J.Williams and J.D.Woollins, *J. Chem. Soc., Chem. Commun.*, 1990, 193.

(2b) T.A.Kabanos, A.J.P.White, D.J.Williams and J.D.Woollins, *J. Chem. Soc., Chem. Commun.*, 1992, 17.

(3) M.A.A.F. de C.T.Carrondo, M.T.L.S.Duarte, J.C.Pessoa, J.A.L.Silva, J.J.R.F. da Silva, M.C.T.A.Vaz and L.J.Vilas-Boas, *J. Chem. Soc., Chem. Commun.*, 1988, 1158.

(4) U. Auerbach, B.S.P.C.Della Vedova, K.Wieghardt, B.Nuber and J.Weiss, *J. Chem. Soc., Chem. Commun.*, 1990, 1004.

(5) A.Neves, A.S.Ceccato, I.Vencato, Y.P.Mascarenhas and C.Erasmus-Buhr, *J. Chem. Soc., Chem. Commun.*, 1992, 652.

(6) R.Eisenberg, E.I.Stiefel, R.C.Rosenberg and H.B.Gray, *J. Am. Chem. Soc.*, 1966, **88**, 2874.

(7) P.Comba, L.M.Engelhardt, J.MacB.Harrowfield, G.A.Lawrance, L.L.Martin, A.M.Sargeson and A.H.White, *J. Chem. Soc., Chem. Commun.*, 1985, 174.

(8) K.Wieghardt, M.Koppen, B.Nuber and J.Weiss, *J. Chem. Soc., Chem. Commun.*, 1986, 1530.

(9) N.D.Chasteen, J.K.Grady and C.E.Holloway, *Inorg. Chem.*, 1986, **25**, 2754.

(10) C.J.Carrano, C.M.Nunn, R.Quan, J.A.Bonadies and V.L.Pecoraro, *Inorg. Chem.*, 1990, **29**, 944.

(11) E.Kimura, *Prog, Inorg. Chem.*, 1994, **41**, 443.

(12) P.Chaudhuri and K.Wieghardt, *Prog. Inorg. Chem.*, 1987, **35**, 329.

(13) A.A.Belal, L.J.Farrugia, R.D.Peacock and J.Robb, *J.Chem.Soc., Dalton Trans.*, 1989,931.

CHAPTER 6

REVIEW OF L^1H_3 COMPLEX CHEMISTRY.

6.1 COMPLEXES WITH L^1H_3: GEOMETRIC CONSIDERATIONS.

The ligand N,N',N''-tris{(2S)-2-hydroxy propyl}-1,4,7-triazacyclononane (L^1H_3) was first prepared by Robb and Peacock(**1**); it is in effect a hexadentate N_3O_3 donor. Similar ligands include TCTA (**2**) and THETACN (**3**); both are N_3O_3 systems; the former uses carboxylate oxygen functions while the latter, like L^1H_3, incorporates alcohol pendant groups. Both these ligands, when complexed to first row transition metal ions, display a wide range of coordination geometries which exhibit varying degrees of trigonal distortion.

Ligand complexes which are able to display such a range of chromophoric geometries are of great value and are emin ntly suitable for study by electronic spectroscopy.

On substituting a methyl group (i.e. introducing an asymmetric carbon centre) onto each pendant arm of the ligand THETACN, Robb and Peacock produced a compound [L^1H_3] which, after complexation, may be investigated using circular dichroism spectroscopy. This technique, in many cases, extracts more information about the chromophoric geometry surrounding the metal centre.

The synthesis of L^1H_3 utilised the ring opening mechanism of oxiranes to introduce a new functional group onto each nitrogen donor of the parent macrocycle. To obtain the required 100% optical purity of such a ligand, it was necessary to have a mechanism which was regio and stereospecific, to prevent

the formation of enantiomeric species and to ensure all the chiral centres were of the same configuration.

The reaction between TACN and (S)-propylene oxide (itself optically pure), was found to proceed via an S_N2 type mechanism under alkaline conditions. The nucleophilic nitrogen function of the ring attacked the less hindered carbon atom, resulting in cleavage of the epoxide ring. This process retained the stereochemistry at each chiral centre producing the pendant arm ligand, L^1H_3, in which all the arms were of the (S) configuration.

L^1H_3 was initially complexed with Co(III) and Ni(II), two metals which give rise to very characteristic electronic spectra. The Co(III) species was found to form a dimeric structure in which the two metal centres were in, essentially, the same geometric environment. A small trigonal distortion of 11° was measured; this was consistent with similar results obtained for the analogous ligand TCTA with which, metal ions having a significant amount of LFSE displayed only a small degree of trigonal twist. The electronic spectra obtained for this complex were found to be pH sensitive, suggesting that the dimeric structure dissociates in acid or alkaline solutions and is only maintained under neutral conditions.

The Ni(II) compound with L^1H_3 was found, from structural analysis (**4**), to be monomeric (fig6.1). The Ni(II) centre was in a trigonally distorted environment; initially a twist angle (ϕ) of 19° was reported. This was later revised to 17.5°. The monomeric nature of this complex is believed to be

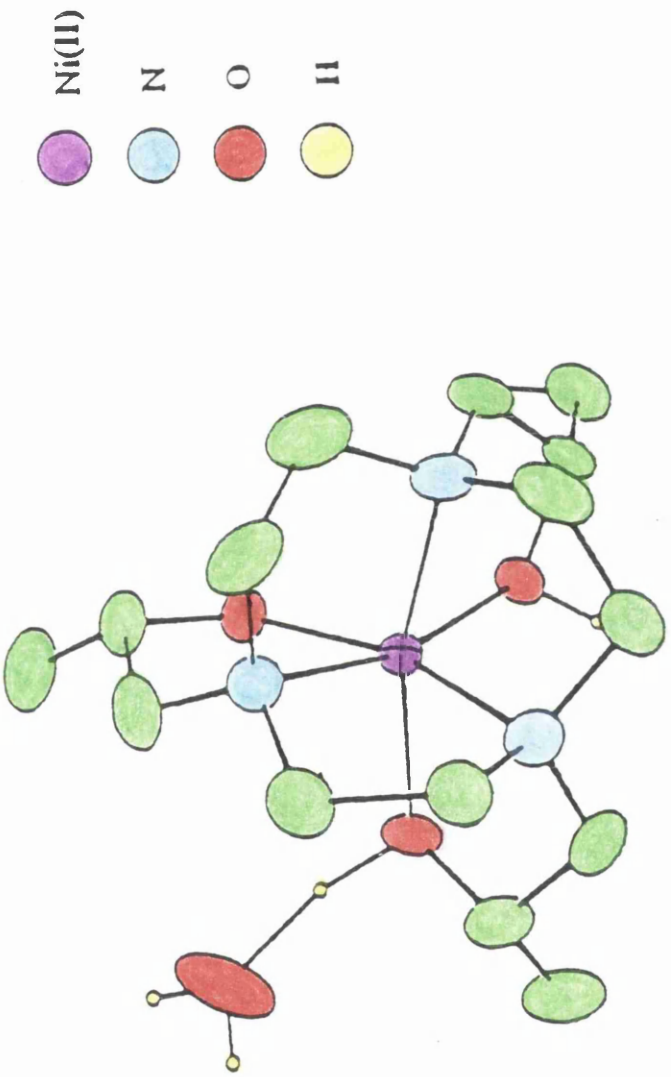

Fig. 6.1. *Crystal structure of* $[Ni(II)L^1H_3]^{2+}$ *cation.*

retained in solution, since the spectroscopic properties of [Ni(II) $L^1H_3]^{2+}$ were found to be pH independent over a wide range (1-12). Thus suggesting that the complex is extremely stable under varying conditions in aqueous solution,in effect the Ni(II) centre is well stabilised, being resistant to oxidation or reduction.

Hancock and co-workers (**5**) prepared a Ni(II) complex with TCTA; they oxidised the $[Ni(II)TCTA]^-$ complex by treating it with dilute nitric acid. A similar strategy was applied with $[Ni(II)L^1H_3]^{2+}$ which had no effect, implying that L^1H_3 would be unable to support a highly oxidising species such as Ni(III); its presence would inevitably lead to metal-ligand bond rupture.

The absorption spectrum of $[Ni(II)L^1H_3]^{2+}$ showed three distinct bands corresponding to the $^3A_{2g}\rightarrow{}^3T_{2g}(F)$; $^3A_{2g}\rightarrow{}^3T_{1g}(F)$ and $^3A_{2g}\rightarrow{}^3T_{1g}(P)$ transitions from low to high energy respectively. Spin-orbit coupling resulted in an extremely complex low energy band, the corresponding region in the CD spectrum displayed a multitude of peaks. An overall Δ_o value of 10,700cm^{-1} was determined from the observed spectrum.

An attempt was made to prepare a monomeric, divalent cobalt complex with L^1H_3, namely $[Co(II)L^1H_3]^{2+}$ (**6**).

During the synthesis of the Co(III) dimer, the initial Co(II) salt underwent rapid oxidation to Co(III) in aqueous solution. It was noted that this process occurred at a slower rate in ethanol. The preparation of $[Co(II)L^1H_3]^{2+}$ was therefore carried out under anaerobic conditions, in degassed absolute ethanol. The

electronic spectra of the resulting compound showed not only bands indicative of a Co(II) species, but also ones which were characteristic of Co(III).

On purely steric grounds Co(II) would be expected to be the preferred choice of the ligand, L^1H_3, since Co(II) with an ionic radius of 0.745Å in its high spin configuration should give a better size-match ratio than Co(III) which has been described as a hypersmall ion (0.545Å) (**7**). Additionally, the work of Gillum *et al.* (**8**) indicated that when electron repulsion parameters were included in calculating the difference in d orbital splitting between octahedral and trigonal prismatic symmetry, for a high spin d^7 ion, the loss of LFSE on going from O_h to TP is compensated, in part, by the reduction in interelectron repulsion. Accordingly, the preference of Co(II) for octahedral coordination is not as strong as might be expected. In other words Co(II) would be able to accommodate the ligand's desire for trigonal prismatic stereochemistry whereas Co(III) has a very strong preference towards octahedral geometry.

The oxidation of the Co(II) species is a consequence of the inherent stability conferred upon a complex by the greater LFSE of the Co(III) centre. Also the extraordinary flexibility of L^1H_3 plays a part, in that, it is able to accommodate Co(III) in preference to the, theoretically more favoured Co(II) ion.

The observed geometry at a particular metal centre arises from the competing forces of the stereochemical preferences of the metal ion and the geometrical requirements of the ligand.

From the crystal structures of the monomeric and dimeric complexes formed between L^1H_3 and first row transition metal ions, the following observations have been made. The Co(III) dimer has a trigonal twist of approximately 10.9°, away from octahedral geometry around each Co(III) ion. The Mn(IV) species has a twist of 10.3° whilst in the case of the Cr(III) complex the distortion increases to 15°. The measured twist about the Ni(II) centre in the monomeric $[Ni(II)L^1H_3]^{2+}$ unit is 17.5°. The largest deviation measured, for a so called octahedral centre, is in the case of V(IV) with a distortion of 20.2°.

These results have been rationalised in terms of the LFSE values of the various metal ions, since the ligand is essentially the same in all cases. The amount of LFSE required by a metal centre is a powerful driving force in determining the geometry about it. It has been shown (**8**) that metal ions can have a preference toward a particular geometry, in the case of a six coordinate species this preference is towards octahedral coordination. The converse, however, is not true, if a structure is distorted away from octahedral it may be stated that the preference for octahedral symmetry is small, not that the preference for trigonal distortion is large. In general, it is the geometrical requirements of the ligand which favour such a trigonal distortion. Where the LFSE of a metal ion is large the ion requires this to be kept at a maximum value. A decrease will almost certainly lead to a less stable compound. In the case of hexa-coordinated species, the geometry which maximises the degree of LFSE is octahedral. All distortions from O_h symmetry result in a decrease in the ligand field splitting

i.e. the 10Dq energy difference between the t_{2g} and e_g levels is reduced, hence a reduction of the overall LFSE is observed. For Co(III), in its low spin ground state configuration (t_{2g}^6), the LFSE value of $^{-12}/_5\Delta_0$ is the maximum possible available. In other words this metal ion has the maximum amount of LFSE which it requires to preserve and thus enhance the stability of any complexes it forms. The Co(III) ion will therefore have a very strong preference for octahedral coordination, this is reflected in the complex with L^1H_3 and its small trigonal distortion of 10.9°. It must be noted, however, that perfect octahedral symmetry has not been observed for any complexes with triazamacrocycles and pendant arms of the length found in L^1H_3. It is believed that to obtain octahedral coordination, with no trigonal distortion, the size of the macrocyclic ring and the length of the pendant arms would have to be increased in order to accommodate such a geometry.

As the overall LFSE of a particular metal ion reduces i.e. as its preference for octahedral stereochemistry diminishes, the observed trigonal twist increases. The three ions Mn(IV), Cr(III) and Ni(II) all have an LFSE measured at $^{-6}/_5\Delta_0$ (a fairly strong preference towards octahedral symmetry). They show trigonal distortions of 11°, 15° and 17.5° respectively. In these three cases since the magnitude of LFSE and ligand type are invariant the increase in twist on going from Mn(IV) to Cr(III) to Ni(II) may be a consequence of metal ion size [Mn(IV) 0.53Å; Cr(III) 0.615Å; Ni(II) 0.69Å]. The ligand, in order to

coordinate a larger metal centre necessarily has to distort. This takes the form of a twist about the main trigonal C_3 axis, with one set of ligators rotating round in relation to the other set. The size difference between Mn(IV) at 0.53Å and Ni(II) at 0.69Å is quite marked hence the large difference in observed twist angles (11°-17.5°).

In the case of V(IV) the ground state configuration of this ion is t_{2g}^1 it thus has a small degree of LFSE ($^{-2}/_5\Delta_o$). This metal would be expected to display only a very small preference for octahedral coordination. A mitigating factor for the relatively small observed twist (ϕ=20.2°) is presumably the small overall size of the ion, for V(IV) the ionic radius is 0.58Å.

The two species which display trigonal prismatic symmetry, i.e. an extremely large distortion away from octahedral coordination, are Zn(II) and Mn(II); both are fairly large ions, especially manganese, with effective ionic radii of 0.74Å and 0.83Å respectively. These ions both have a zero amount of LFSE, a consequence of their ground state configuration, Zn(II) is d^{10} and Mn(II) is high spin d^5; they should therefore be expected to exert no influence on the coordination geometry. The ligand L^1H_3 is believed, from model building, to prefer trigonal prismatic geometry in effect maximising the overall bonding interactions with the metal centre. The trigonal twist in the case of Zn(II) is 55.5° whilst for the Mn(II) species the geometry is an exact trigonal prism with ϕ=60°.

This is entirely consistent with the theory that greater trigonal distortions are required by L^1H_3 to comfortably coordinate larger metal ions.

The formation of dimeric complexes is rather unusual and initially, quite unexpected. In the early investigations it was presumed that L^1H_3 would form monomeric 1:1 type complexes with first row transition metals and indeed this is observed with divalent metal ions. One reason for dimer formation may be attributed to the presence of higher oxidation levels of +3 or more. Metal ions in these higher states are, as a consequence of their relatively small size and greater positive charge, very good and efficient Lewis acids. When such a metal coordinates to L^1H_3, the three hydroxyl groups experience this superior Lewis acidity. Electron donation from the oxygen donor to the metal centre is enhanced leading to an increase in the basicity of the alcohol protons. The overall process is synergic; the greater the extent of electron donation to the metal centre, the more labile these hydroxyl protons become. Therefore deprotonation occurs, leading to a series of alkoxide donors - these groups are extremely proficient π donors and are able to stabilise the high oxidation level of the metal ion.

Dimer formation is facilitated via a hydrogen bonding contact, between the alkoxide functions and any protonated subunits, in solution.

The alkoxide groups are quite basic and form very strong hydrogen bridges with any available protonated residues. In the case of $[Mn(IV)L^3]^+$ prepared by

Wieghardt and co-workers (9), the ligand is present in its deprotonated, alkoxide donor form. Dimer formation does not occur; presumably the reaction conditions are too oxidising for any protonated ligands to remain in solution. The crystal structure (fig6.2) indicates the Mn(IV) tris alkoxide unit is stabilised through a contact with the methylene residues of a crystallographically adjacent molecule. This behaviour highlights the need of the alkoxide groups to form a bonding contact, however weak, with any available proton containing groups.

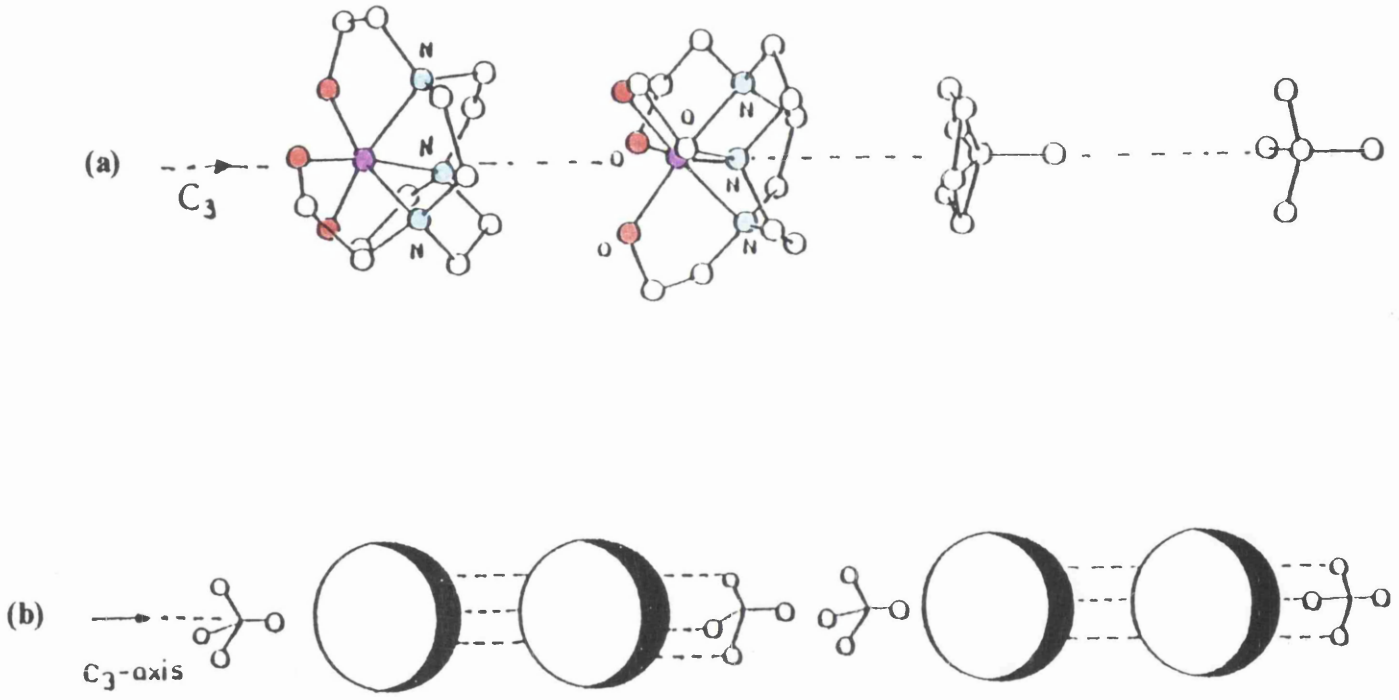

Fig. 6.2. *(a) crystal packing of anions and cations in $[Mn(IV)L^3][ClO_4]$ (b) schematic representations; cations = large spheres, dotted lines are possible C-H - - - O contacts.*

6.2 BONDING TRENDS.

On investigating the structures of the complexes prepared with L^1H_3, an interesting phenomenon has emerged, in respect of the variation of metal-nitrogen and metal-oxygen bond lengths. The observed differences are outwith the values expected for the various metal ions of the first row transition series. In general a metal-oxygen single bond would be expected to be slightly shorter than its metal-nitrogen counterpart, purely on the basis of their respective ionic radii - nitrogen (1.46Å), oxygen (1.36-1.35Å). The overall interaction between the metal and oxygen atom, however, is complicated by the lone pairs present on the oxygen, which are available for π-bonding. These p^{π} orbitals have the correct symmetry to overlap with the t_{2g} set of the metal. In the case of L^1H_3 the oxygen atoms comprise either alcohol or alkoxide groups the latter being superior π donors due to their extra available lone pairs. Since the ligating groups of L^1H_3 are essentially π donating and the p^{π} orbitals are of lower energy than the metal t_{2g} set, the qualitative π-bonding molecular orbital diagram (fig6.3) is applicable.

The overall process involved is a ligand to metal electron donation; π-bonding within the first row metals is quite rare, the main examples involving π acid

ligands such as CO or ligands with delocalised π systems i.e. benzene and cyclopentadienyl.

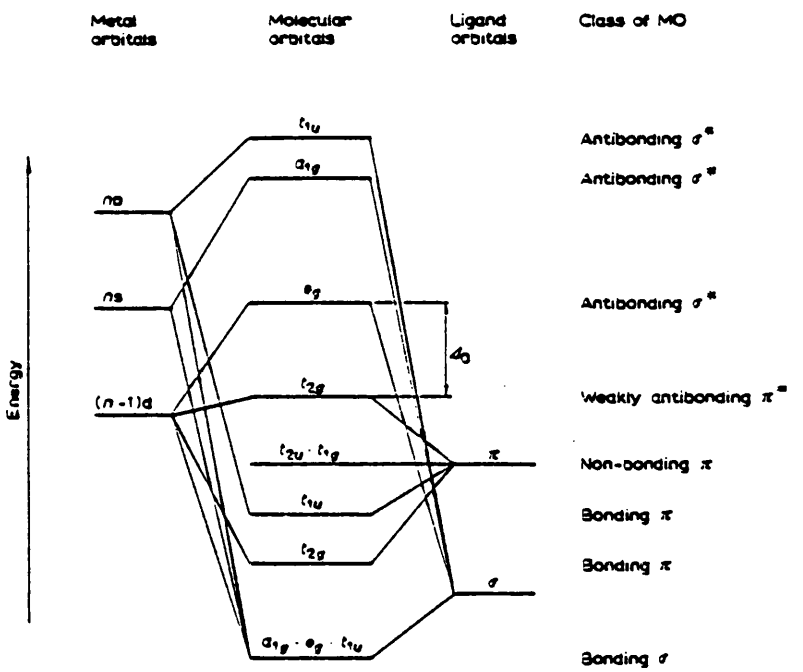

Fig. 6.3. *π-bonding Molecular orbital diagram.*

The donor type is very important when examining metal-oxygen bond lengths; generally alkoxide ligators are better π-donors than alcohol ligators, thus they should display a greater degree of p^{π}-d^{π} bonding. In addition the effective ionic radius of an oxygen group, depends upon its coordination number. An alkoxide

oxygen with a coordination number of two has a radius of 1.35Å whilst for an alcohol oxygen (coordination number = 3) the radius is 1.36Å.

With the ligand L^1H_3 the tertiary nitrogen functions have no lone pairs available for π-bonding. Therefore the metal-nitrogen bonds are expected to show only single (σ) bond character.

The crystallographically determined metal-nitrogen and metal-oxygen bond lengths of the various complexes with L^1H_3 are presented in table 6.1. Where the pendant arms are fully deprotonated (i.e. alkoxide donors) the ligand is denoted as L^1 and for alcohol ligators the ligand is assigned as L^1H_3.

When the t_{2g} set is fully occupied (i.e. t_{2g}^6) as in the case of Co(III), Ni(II) and Zn(II), the relative difference between the metal-nitrogen and metal-oxygen bond lengths is not significant.

With the Mn(II) component of the complex cation $[Mn(II)L^1H_3.L^1Mn(IV)]^{3+}$ the metal-oxygen bonds are shorter than the metal-nitrogen ones by almost 0.11Å; a similar value is observed for the Cr(III) dimer. Both these ions can be regarded as being bound to essentially alcohol donors. For the Mn(IV) half of the manganese dimer, which also has three t_{2g} electrons, the difference {i.e. (M-N)-(M-O)} increases to 0.19Å.

Finally, for the V(IV) ion which is t_{2g}^1 the metal-nitrogen and metal-oxygen distances differ by an extremely significant 0.305Å.

Complex	M-N (Å)	M-O (Å)	Configuration	Ref.
$[Zn(II)L^1H_3]^{2+}$	2.146	2.110	$t_{2g}^6e_g^4$	this work
$[Co(III)L^1H_3]^{3+}$	1.954	1.939	t_{2g}^6	10
$[Ni(II)L^1H_3]^{2+}$	2.064	2.084	$t_{2g}^6e_g^2$	4
$[Co(III)L^1]^+$	1.944	1.939	t_{2g}^6	10
$[Mn(II)L^1H_3]^{2+}$	2.251	2.142	$t_{2g}^3e_g^2$	this work
$[Cr(III)L^1H_3.L^1Cr(III)]^{3+}$	2.071	1.970	t_{2g}^3	this work
$[Mn(IV)L^1]^+$	2.051	1.857	t_{2g}^3	this work
$[Mn(IV)L^2]^+$	2.048	1.825	t_{2g}^3	this work
$[V(IV)L^1]^+$	2.177	1.872	t_{2g}^1	this work

Table 6.1. ***Bond lengths in L^1H_3 and L^2H_3 complexes.***

Thus there is a strong correlation between the difference in metal-nitrogen and metal-oxygen bond lengths and the occupancy of the t_{2g} set; as the number of t_{2g} electrons decreases the value of (M-N)-(M-O) increases i.e. becomes more positive.

Initially, the evidence for a shortening of the metal-oxygen distances, in other words a p^{π}-d^{π} bonding interaction, seems quite straightforward. A more detailed analysis, however, is required before any firm conclusions can be drawn.

It is possible, in the case of simple covalent bonds such as single σ bonds to obtain a measure of the bond length by simply adding the effective ionic radii of the respective atoms, in order to gain an approximate value for a single bond between the relevant species. The values of all the ionic radii used were obtained from the data compiled by R.D. Shannon (**12**).

The ionic radii of various metal ions employed in this investigation are presented in table 6.2.

Metal Ion	Ionic Radius (Å)
V(IV)	0.58
Cr(III)	0.615
Mn(II)	0.83
Mn(IV)	0.53
Co(III)	0.545
Ni(II)	0.69
Zn(II)	0.745

Table 6.2. *Effective ionic radii.*

The calculated (theoretical) metal-nitrogen and metal-oxygen bond lengths are listed in table 6.3. The values are a summation of the ionic radii of the individual species.

Metal Ion	$(M\text{-}N)_{calc.}$ [Å]	$(M\text{-}O)_{calc.}$ [Å]	Donor Type
V(IV)	2.04	1.93	alkoxide
Cr(III)	2.08	1.98/1.97	alcohol/alkoxide
Mn(II)	2.29	2.19	alcohol
Mn(IV)	1.99	1.88	alkoxide
Co(III)	2.01	1.91/1.90	alcohol/alkoxide
Ni(II)	2.15	2.05	alcohol
Zn(II)	2.21	2.11	alcohol

Table 6.3. *Calculated bond lengths.*

By dealing with the donor type (alkoxide and alcohol) in turn, a comparison may be made in the respective metal-oxygen bond lengths. In the case of alkoxide donors a distinct variation is observed, in conjunction with t_{2g} site occupancy (table 6.4).

Metal Ion	$(M\text{-}O)_{calc.}$ [Å]	$(M\text{-}O)_{exp.}$ [Å]	Difference [Å]	Electronic Configuration
V(IV)	1.93	1.87	+0.06	t_{2g}^{1}
Cr(III)	1.97	1.97	0.00	t_{2g}^{3}
Mn(IV)	1.88	1.86	+0.02	t_{2g}^{3}
Co(III)	1.90	1.94	-0.04	t_{2g}^{6}

Table 6.4. *M-O distances with alkoxide ligators.*

For alcohol ligation, the same treatment of figures leads to quite dissimilar results. In all cases the experimental values are the same as or even greater than the calculated values,except in the case of Mn(II). This, however, may be a consequence of the trigonal prismatic symmetry displayed by the $[Mn(II)L^1H_3]^{2+}$ unit. Overall, no real bond shortening is taking place and no direct correlation exists between the $(M\text{-}O)_{exp.}$ bond lengths and the number of t_{2g} electrons.

Metal Ion	$(M\text{-}O)_{calc.}$ [Å]	$(M\text{-}O)_{exp.}$ [Å]	Difference [Å]	Electronic Configuration
Cr(III)	1.98	1.97	+0.01	t_{2g}^3
Mn(II)	2.19	2.14	+0.05	$t_{2g}^3e_g^2$
Co(III)	1.91	1.94	-0.03	t_{2g}^6
Ni(III)	2.05	2.08	-0.03	$t_{2g}^6e_g^2$
Zn(II)	2.11	2.11	0.00	$t_{2g}^6e_g^4$

Table 6.5. *M-O distances with alcohol ligators.*

Surprisingly, the metal-nitrogen bond lengths have been observed to vary in relation to the metal-oxygen bond lengths. As the metal-oxygen bond length decreases a concomitant lengthening of the metal-nitrogen bond is observed; this effect becomes quite marked especially in the case of V(IV). The data is summarised in tables 6.6 and 6.7.

Metal Ion	$(M\text{-}N)_{calc.}$ [Å]	$(M\text{-}N)_{exp.}$ [Å]	Difference [Å]
V(IV)	2.04	2.18	-0.12
Cr(III)	2.08	2.07	+0.01
Mn(II)	2.29	2.25	+0.04
Mn(IV)	1.99	2.05	-0.06
Co(III)	2.01	1.95	+0.06
Ni(II)	2.15	2.06	+0.09
Zn(II)	2.21	2.15	+0.06

Table 6.6. *M-N bond lengths.*

Metal Ion	$(M\text{-}N)_{exp.}$ [Å]	$(M\text{-}O)_{exp.}$ [Å]	Difference [Å]
V(IV)	2.18	1.87	+0.31
Cr(III)	2.07	1.97	+0.10
Mn(II)	2.25	2.14	+0.11
Mn(IV)	2.05	1.86	+0.19
Co(III)	1.95	1.94	+0.05
Ni(II)	2.06	2.08	-0.02
Zn(II)	2.15	2.11	-0.04

Table 6.7. *Comparison of M-N and M-O distances.*

Thus from the data, it can be ascertained that there is a link between the $(M\text{-}O)_{exp}$ bond lengths and the number of t_{2g} electrons when alkoxide donors are present. In addition it has been observed that as the magnitude of metal-oxygen bond shortening increases, the metal-nitrogen distances lengthen (in comparison to their calculated values).

It is clear, therefore, that a metal-oxygen π-bonding interaction is occurring; the degree of π-bonding is in direct correlation to the t_{2g} site occupancy. Concurrently an increase in metal-nitrogen bond lengths is seen, reaching a maximum when the amount of M=O bond character is at a maximum.

Studies by Auerbach *et al.* (**13**) into the transition metal complexes formed with a tris phenolate substituted TACN, L'', (where L''=N,N',N''-tris{5-*tert*-butyl-2-hydroxybenzyl}-1,4,7-triazacyclononane), revealed very similar results.

The aromatic nature of the benzene ring and the highly electron withdrawing hydroxyl functions, conspire to produce very efficient π-donor pendant groups. These phenolate arms are superior π-donors to the alkoxide groups of L^1H_3, thus the extent of π-bonding is more pronounced.

The general tends, however, compare extremely favourably with this work.

In the case of $[V(IV)L'']^+$ (d^1) and $[Ti(IV)L'']^+$ (d^0) the authors observed a considerable degree of metal-oxygen bond shortening by 0.10Å and 0.13Å respectively. A lengthening of the metal-nitrogen distances was also seen 0.13Å

$[V(IV)L'']^+$ and 0.16Å $[Ti(IV)L'']^+$. The overall differences $\{(M\text{-}N)_{exp}\text{-}(M\text{-}O)_{exp}\}$ were measured at 0.34Å and 0.40Å, respectively.

It seems likely that the amount of $p^{\pi}\text{-}d^{\pi}(t_{2g})$ overlap results in a significant degree of M=O bond character. The increase in covalency of these metal-oxygen bonds, leads to a weakening in the metal-nitrogen bonding. Hence the observed increase in metal-nitrogen distances. Auerbach *et al.* invoked a pseudo trans-influence in which they argued that the magnitude of $p^{\pi}\text{-}d^{\pi}$ bonding (i.e. a measure of the degree of M=O bond character) would be expected to exert an influence on the trans metal-nitrogen distances. Thus the species which is capable of stronger covalent bonding (i.e. alkoxide or phenolate oxygen) will necessarily acquire the highest degree of metal hybridisation, thereby exerting an influence on the bonding to weaker covalent bonding species (e.g. tertiary nitrogen donors).

References.

(1) J.Robb and R.D.Peacock, *Inorg. Chim. Acta.*, 1986, **121**, L15.

(2) T.Arishima, K.Hamada and S.Takamoto, *Nippon Kagaku Kaishi*, 1973, 1119.

(3) B.A.Sayer, J.P.Michael and R.D.Hancock, *Inorg. Chim. Acta.*, 1983, **77**, L63.

(4) L.J.Farrugia and R.D.Peacock, *Acta. Crystallogr. Sect. C.*, 1991, **47**, 1312.

(5) M.J. van der Merwe, J.C.A.Boeyens and R.D.Hancock, *Inorg. Chem.*, 1983, **22**, 3490.

(6) I.A.Fallis, *Ph.D. Thesis*, University of Glasgow, 1992.

(7) R.D.Hancock, *Prog. Inorg. Chem.*, 1989, **37**, 187.

(8) W.O.Gillum, R.A.D.Wentworth and R.F.Childers, *Inorg. Chem.*, 1970, **9**, 1825.

(9) A.A.Belal, P.Chaudhuri, I.Fallis, L.J.Farrugia, R.Hartung, N.M.Macdonald, R.D.Peacock, B.Nuber, J.Weiss and K.Wieghardt, *Inorg. Chem.*, 1991, **30**, 4397.

(10) A.A.Belal, L.J.Farrugia, R.D.Peacock and J.Robb, *J. Chem. Soc., Dalton Trans.*, 1989, 931.

(11) I.A.Fallis, L.J.Farrugia, N.M.Macdonald and R.D.Peacock, *J. Chem. Soc., Dalton Trans.*, 1993, 2759.

(12) R.D.Shannon, *Acta. Crystallogr.*, 1976, **A32**, 751.

(13) U.Auerbach, T.Weyhermuller, K.Wieghardt, B.Nuber, E.Bill, C.Butzlaff and A.X,Trautwein, *Inorg. Chem.*, 1993, **32**, 508.

CHAPTER 7

COMPLEXES WITH L^4H_2.

7.1 INTRODUCTION

With the aim of studying a potentially pentadentate system which, in theory, would be able to support geometries that were beyond the "flexibility" of TACN based N-substituted macrocycles, a ligand based upon the 9-aneN_2O ring has been prepared. The pendant groups incorporate chiral isopropyl substituted alcohol arms.

The synthesis of the parent macrocycle proved to be less than straightforward with various cyclisation and detosylation strategies being employed. The ring forming process, a variation on the Richman-Atkins theme, as used by Beveridge *et al.* (**1**) was finally utilised as was the reductive alkaline detosylation process outlined by Wieghardt and co-workers (**2**). The yields, however, were still relatively low.

The introduction of pendant groups followed the same general route as for L^1H_3. The alcohol functions were introduced by a ring cleavage mechanism of the desired oxirane. The ligand was analysed by ^1H and ^{13}C n.m.r. spectroscopy.

7.2 SYNTHESIS OF NICKEL COMPLEX.

The preparation of this compound was carried out in methanol by reacting a 1:1 ratio of $[Ni(H_2O)_6][SO_4]$ and L^4H_2, (where L^4H_2=N,N'-di(2S-hydroxy-3-methylbutyl)-1-oxa-4,7-diazacyclononane). To the resulting blue solution was added solid ammonium hexafluorophosphate giving a pale blue precipitate. Elemental analysis of this solid indicated the presence of L^4H_2 and nickel as a 1:1 complex and to two $[PF_6]^-$ units as counterions. The infra-red spectrum measured as a solid KBr disc displayed bands characteristic of $[PF_6]^-$ at 837cm^{-1}. Bands corresponding to C-N, C-O and C-O-C modes were also observed. At ≈ 3250cm^{-1} a broad band characteristic with H_2O was seen, this was lower in energy than would be expected for free H_2O suggesting that the water molecule is in some way coordinated to the metal centre.

Thus, so far, the data indicates that a pentacoordinate or more probably a hexacoordinate Ni(II) complex is present with two hexafluorophosphate units to balance the overall +2 charge. Therefore a tentative formulation of the complex may be written $[NiL^4H_2.H_2O][PF_6]_2$.

7.2.1 ELECTRONIC SPECTROSCOPY.

As outlined in section 1.8, the absorption spectrum of a given octahedral Ni(II) species is very characteristic. Three main bands are displayed $^3A_{2g}\rightarrow{}^3T_{1g}(P)$; $^3A_{2g}\rightarrow{}^3T_{1g}(F)$ and $^3A_{2g}\rightarrow{}^3T_{2g}(F)$ in order of decreasing energy.

A feature of many nickel (II) species is spin-orbit coupling associated with the $^3T_{1g}(F)$ band and an adjacent spin-forbidden $^3A_{2g}\rightarrow{}^1E_g$ transition. This effect is clearly observed in the spectrum of $[Ni(II)(H_2O)_6]^{2+}$ (fig7.1), as a shoulder on the middle $^3A_{2g}\rightarrow{}^3T_{1g}(F)$ absorption. In some cases, it must be noted, the ^1E_g band lies at lower energy thus mixing with the $^3T_{2g}(F)$ band; the resulting shoulder is observed at the higher energy side of this low energy band.

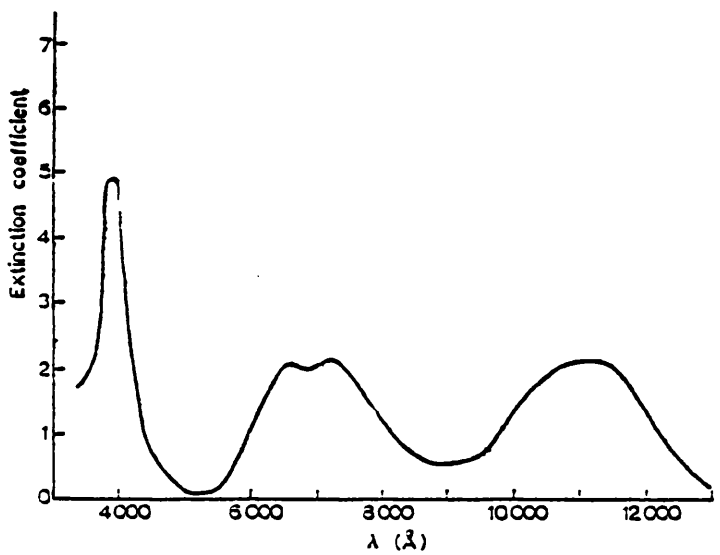

Fig 7.1. *Absorption spectrum of* $[Ni(II)(H_2O)_6]^{2+}$.

7.2.2 ABSORPTION AND CIRCULAR DICHROISM SPECTRA.

The absorption spectrum of $[Ni(II)L^4H_2(H_2O)][PF_6]_2$ is presented in figure 7.2. Octahedral labels will be used in interpreting the electronic spectra. The bands displayed are highly indicative of a structure based upon an octahedron as opposed to a five coordinate trigonal or square based pyramid or even a four coordinate tetrahedron. The low and middle energy bands are both highly unsymmetrical, in the case of the low energy transition this may, in part, be due to spin-orbit coupling with ^3F states. The intensity fall off to the lower energy side of the two bands is of a lower magnitude. There is a small peak/shoulder at approximately 760nm;it is possible this arises from spin-orbit coupling with the spin forbidden $^3A_{2g} \rightarrow {}^1E_g$ mode, although any such assignment is highly speculative.

The corresponding bands in the circular dichroism spectrum (fig7.3) are also quite unsymmetrical and the spectrum is quite complex. Examination of the CD spectrum suggests that it is the low symmetry of the compound which is the primary cause of the asymmetric absorption bands.

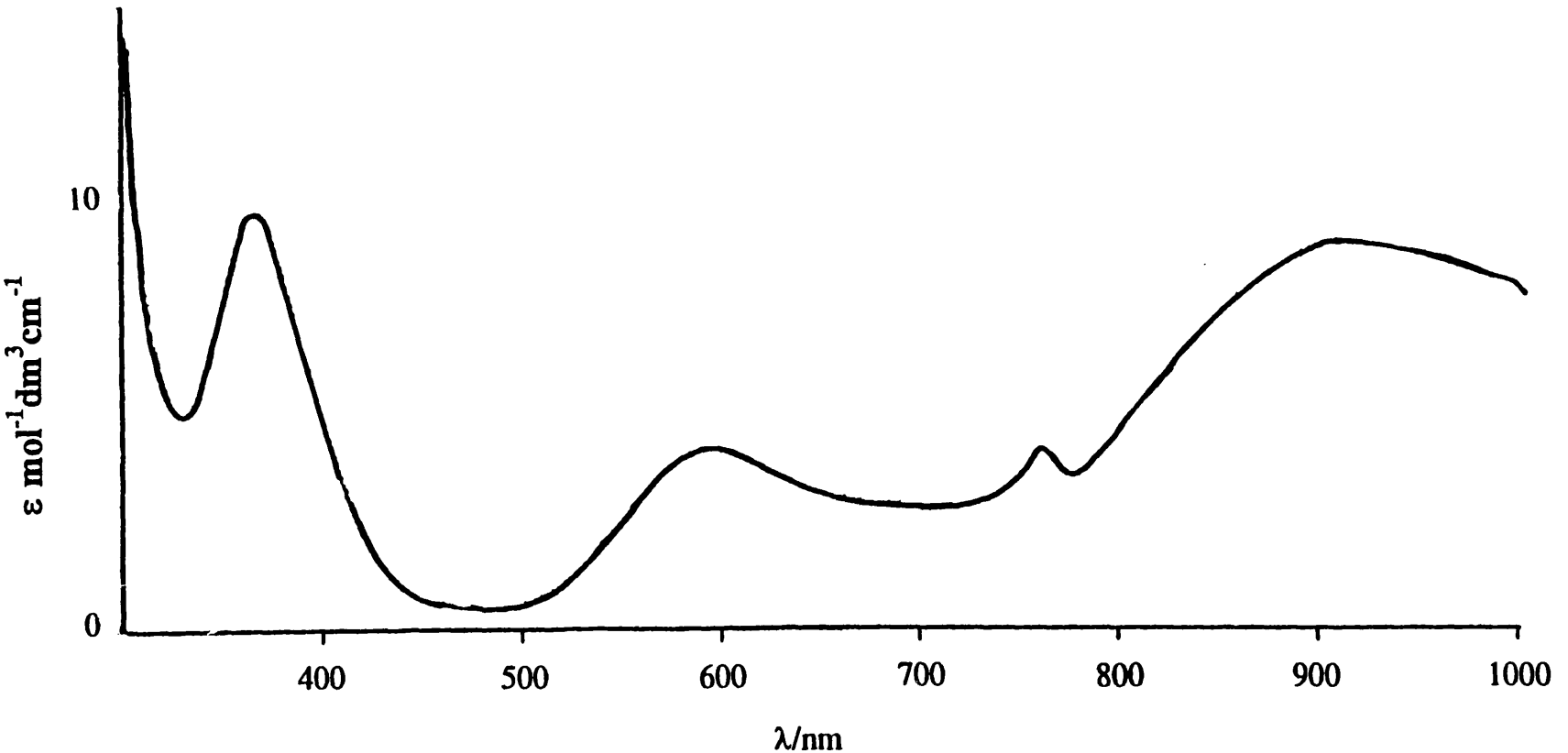

Fig. 7.2. *Absorption spectrum of* $[Ni(II)L^4H_2.(H_2O)]^{2+}$ *in methanol.*

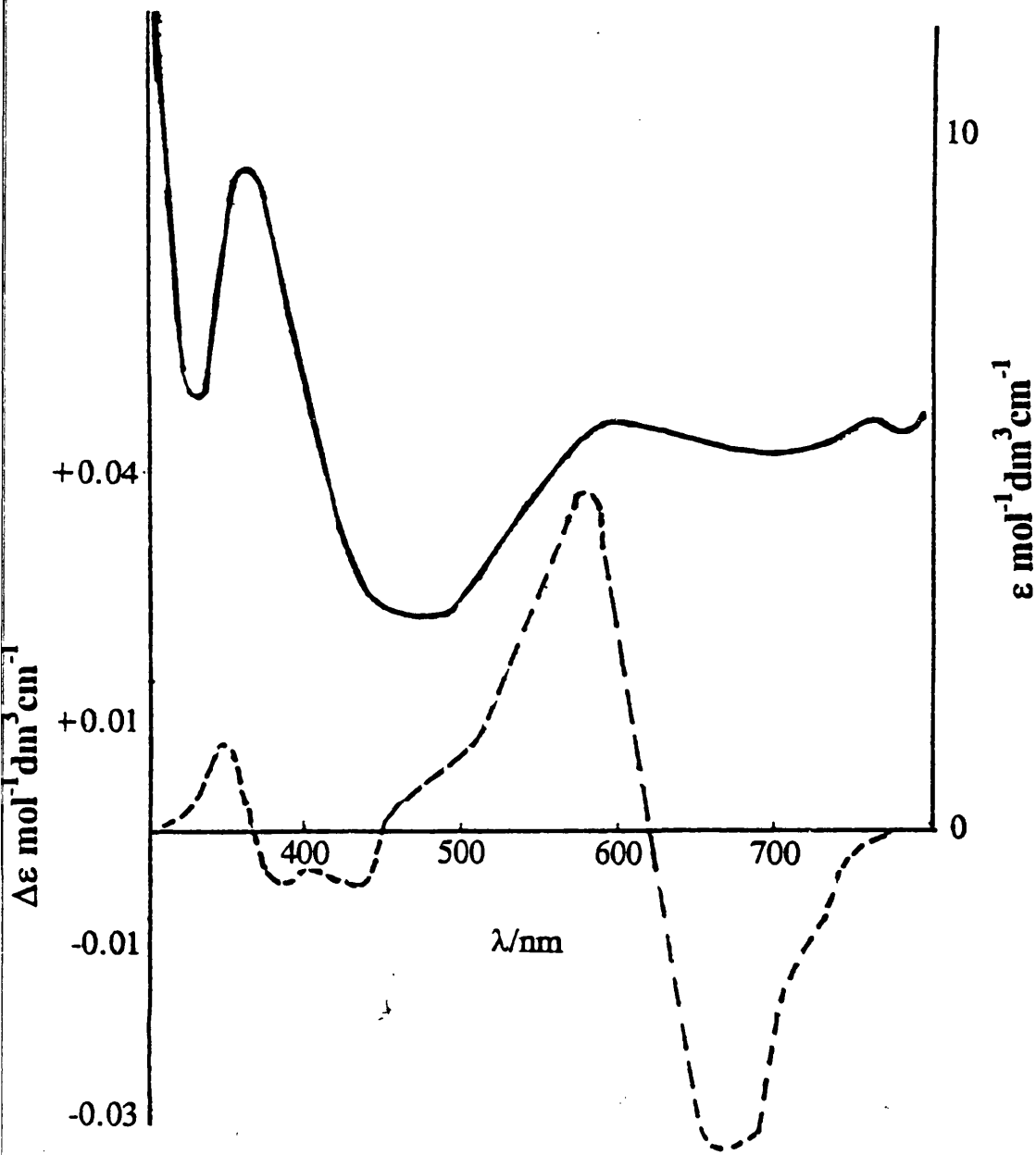

Fig. 7.3. *Absorption / CD spectra of* $[Ni(II)L^4H_2.(H_2O)]^{2+}$ *in methanol.*

7.2.3 COMPARISON WITH $[Ni(II)L^1H_3]^{2+}$ and $[Ni(II)L^5H_3]^{2+}$.

A weakly trigonally distorted Ni(II) complex such as $[Ni(II)L^1H_3]^{2+}$ displays a quite straightforward CD spectrum (fig7.4), the components of each band are of single sign and the asymmetry is resultant from the spin-orbit interactions. In the case of $[Ni(II)(L^4H_2)(H_2O)]^{2+}$ each band is made up of two or more separate components which suggests that the symmetry of this species is very low. On going from O_h to D_3 symmetry the T states lose their degeneracy by transforming into A and E components. Lowering the symmetry even further to C_3 increases the number of possible electronic transitions observed in the CD spectrum since those which are forbidden under D_3 geometry (i.e. $^3A_2 \rightarrow {}^3A_2$) are now allowed.

The circular dichroism spectrum of $[Ni(II)(L^4H_2)(H_2O)]^{2+}$ shows two components, for the middle $^3A_{2g} \rightarrow {}^3T_{1g}(O_h)$ absorption, of opposite sign - possibly $^3A \rightarrow {}^3A$ and $^3A \rightarrow {}^3E$ under C_3 symmetry. The highest energy band $^3A_{2g} \rightarrow {}^3T_{1g}(P)$ has three underlying modes; two are negatively signed and one is of positive sign. The chromophore about the Ni(II) ion consists of three nitrogen donors, two alcohol functions and a water molecule, thus constituting an N_3O_3 group which would be expected to have less symmetry than the N_3O_3 chromophore of L^1H_3. In essence the complexity of the CD spectrum indicates that the structure must have very low symmetry of point group C_3 or even C_2.

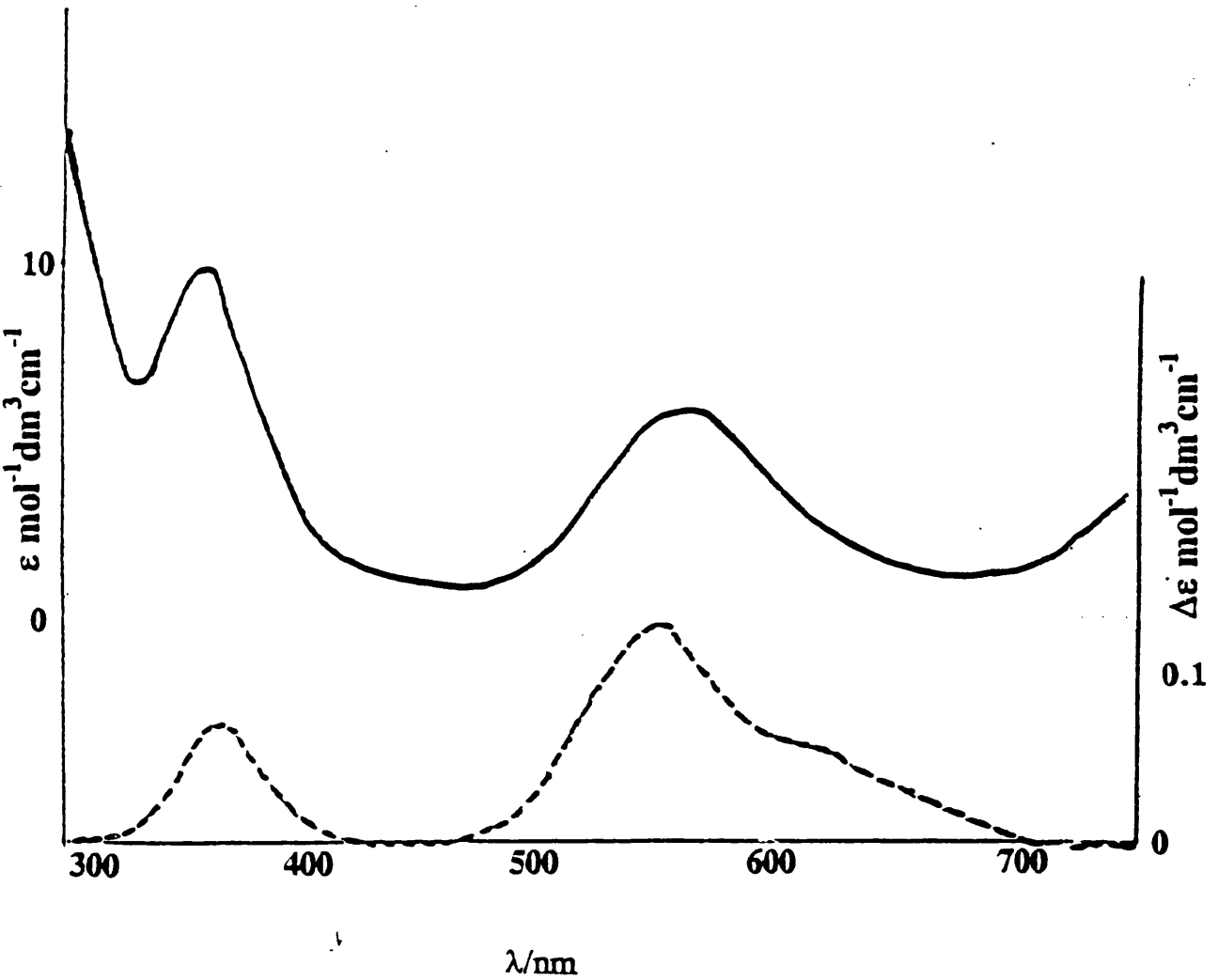

Fig. 7.4. *Absorption / CD spectra of* $[Ni(II)L^1H_3]^{2+}$ *in MeCN.*

Analysis of the electronic spectrum gives an approximate 10Dq value of 10,900cm^{-1} which highlights the different chromophore about the metal centre. This value is very close to that obtained for $[Ni(II)L^1H_3]^{2+}$ (10,770cm^{-1}), surprising given that L^1H_3 is hexadentate whilst L^4H_2 is pentadentate. One explanation is the slightly modified cavity of L^4H_2 most probably results in a better size-match fit giving a stronger ligand field with concomitant increase in the d-orbital splitting. Unsurprising, however, is the larger Racah B value (894cm^{-1} as opposed to 862cm^{-1}) calculated for $Ni(II)(L^4H_2)(H_2O)(PF_6)_2$ which is a result of the greater inductive effect of the pendant arm isopropyl groups. An increase in electron density at the pendant arm oxygen will increase both the σ and π donor properties of the ligand. Thus increasing the degree of inter electron repulsion hence the higher Racah B measurement. A similar result is observed with the complex $[Ni(II)L^5H_3]^{2+}$ (**3**) in which the ring size although very large produces a 10Dq value close to that observed for L^1H_3 and L^4H_2. A very trigonally distorted coordination geometry has been suggested for this compound.

In the case of this complex the observed absorption and CD spectra are fairly complicated (fig7.5), with the CD of the middle and highest energy transitions giving rise to two or more bisignate components. Accordingly, the symmetry of $[Ni(II)L^5H_3]^{2+}$ is believed to be very low.

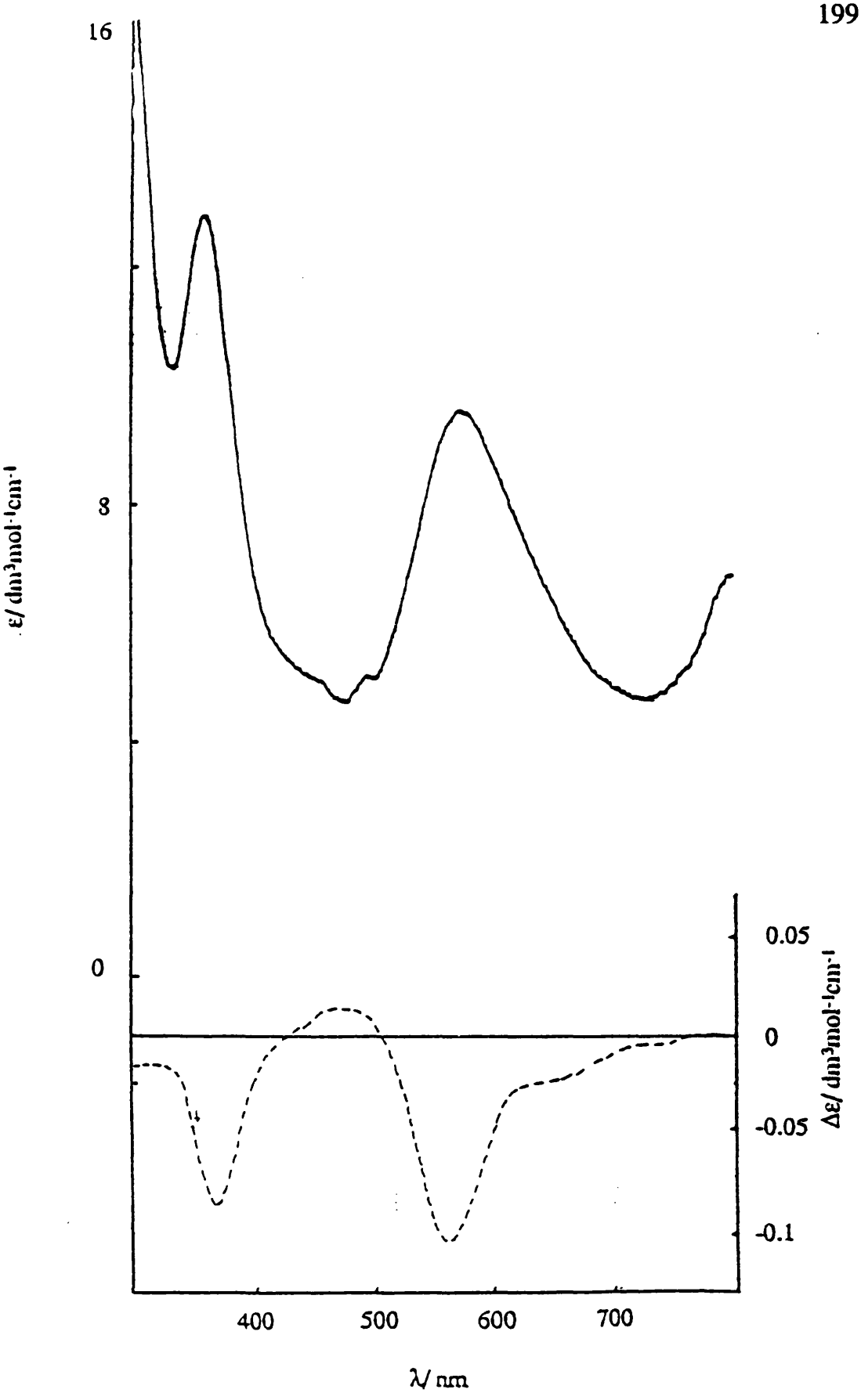

Fig. 7.5. *Absorption / CD spectra of* $[Ni(II)L^5H_3]^{2+}$ *in MeCN.*

7.3 SYNTHESIS OF COBALT COMPLEX.

The cobalt complex was prepared in a similar manner to the nickel compound, although in this case the reaction was carried out in absolute ethanol. The starting compound was $CoCl_2.6H_2O$; on addition of L^4H_2 and subsequent heating to promote the complexation process a deep violet colouration was observed. On removal of solvent the residue was taken up in acetonitrile and solid ammonium hexafluorophosphate added, giving a pink solid and pale purple solution. The purple solution, using absorption spectroscopy, displayed a mixture of bands some of which indicated the presence of tetrahedrally coordinated starting material; this solution was found not to be optically active. A small portion of pink solid was taken for elemental analysis; the resultant data indicated a monomeric complex was present again with two $[PF_6]^-$ counterions. The infra-red displayed bands characteristic of $[PF_6]^-$ units, coordinated water (ν=839cm^{-1} and 3305,1609cm^{-1} respectively) and the ligand L^4H_2.

Again this data suggests a five or six coordinate complex is formed between Co(II) and L^4H_2.

7.3.1 ELECTRONIC SPECTROSCOPY.

In the case of many hexa coordinated Co(II) complexes (d^7, high spin) three transitions are expected in their absorption spectra. At low energy a band pertaining to the $^4T_{1g} \rightarrow {}^4T_{2g}(F)$ transition and at higher energy, an absorption corresponding to $^4T_{1g} \rightarrow {}^4T_{1g}(P)$. The third transition $^4T_{1g} \rightarrow {}^4A_{2g}(F)$ is normally associated with a weak band or shoulder on the lower side of the $^4T_{1g} \rightarrow {}^4T_{1g}(P)$ absorption.

On reducing the symmetry from $O_h \rightarrow$T.P. the triplet states lose their degeneracy. The spectra of Co(II) complexes, however, often lack resolution to display an increase in the number of transitions.

The intensity of bands in the absorption spectra of Co(II) species is usually low, with extinction coefficients of the order 1-20 $mol^{-1}dm^3cm^{-1}$ (**4**). The complex $[Co(II)L^4H_2(H_2O)][PF_6]_2$ is no exception with observed ε values in the range 2-7 $mol^{-1}dm^3cm^{-1}$.

7.3.2 ABSORPTION AND CIRCULAR DICHROISM SPECTRA.

In the absorption spectrum (fig7.6) two bands are displayed, one at 492nm assigned to the $^4T_{1g} \rightarrow {}^4T_{1g}(P)$ transition and one at 1070nm which is characteristic of the low energy $^4T_{1g} \rightarrow {}^4T_{2g}(F)$ process.

The high energy band is quite unsymmetrical with a slight shoulder to low energy which may result from the $^4T_{1g} \rightarrow {}^4A_{2g}(F)$ two electron process. In the presence of quite strong ligand fields this transition is very close in energy to $^4T_{1g} \rightarrow {}^4T_{1g}(P)$.

The CD spectrum (fig7.6) shows two asymmetric bands at 530nm (-ve) and 420nm (+ve) corresponding to the high energy absorption transition. No assignments of these bands, however, will be made. With no structural data on the complex any assignment would be, at best, highly speculative. Suffice to say that the g-factors of the order 10^{-3} indicate the absorption to be d$\leftrightarrow$d in origin and the symmetry of the complex is low.

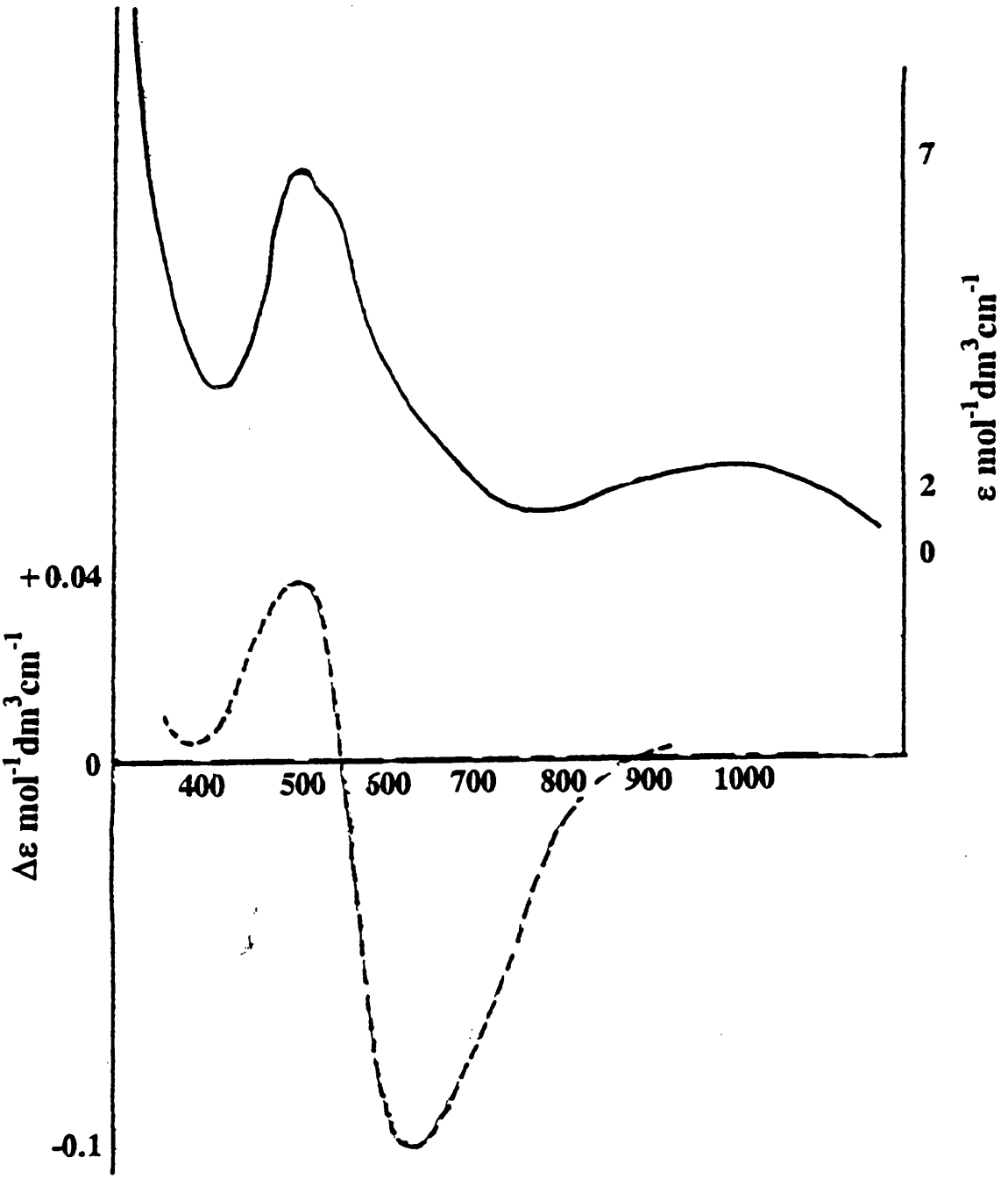

Fig. 7.6. *Absorption / CD spectra of Co(II)$L^4H_2(H_2O)$ in ethanol.*

7.3.3 COMPARISON WITH $[Co(II)L^5H_3]^{2+}$ and $[Co(py)_3tach]^{2+}$.

Similar electronic spectra have been observed for other six coordinate Co(II) complexes which are severely trigonally distorted.

$[Co(II)L^5H_3]^{2+}$ **(3)** displays a distorted trigonal prismatic geometry about the metal centre. The positions of the low and high energy bands at 1082nm and 494nm respectively. This suggests that the ligand field in the complex with L^4H_2 is of a similar magnitude to L^5H_3 surprising since the former is pentadentate and the latter hexadentate. The flexible L^4H_2 ring is obviously well suited to coordinating larger metal ions.

The trigonal prismatic complex $[Co(py)_3tach]^{2+}$ **(5)** gave bands at 1180nm $^4T_{1g}\rightarrow{}^4T_{2g}$ and 495nm, $^4T_{1g}\rightarrow{}^4T_{1g}(P)$ with a weak band/shoulder at 524nm $^4T_{1g}\rightarrow{}^4A_{2g}(F)$. It seems likely that the geometry about the Co(II) centre in $[Co(II)L^4H_2.H_2O]^{2+}$ is six coordinate with a high degree of trigonal distortion. A penta-coordinated complex i.e. $[Co(II)L^4H_2]^{2+}$ would be expected to give rise to more bands in the absorption spectrum and each transition would be of greater intensity than in the case of six coordinate species.

7.4 SYNTHESIS OF COPPER COMPLEX.

The synthesis of this complex was performed in ethanol by reacting a 1:1 ratio of $CuSO_4.5H_2O$ and L^4H_2. The complex was obtained as the corresponding nitrate salt on the addition of excess sodium nitrate. Elemental analysis suggested that a complex of the form $CuL^4H_2.(NO_3)_2$ was present. The infra-red spectrum displayed bands corresponding to the nitrate ions and also C-N, C-O and C-O-C modes of the ligand.

7.4.1 ELECTRONIC SPECTROSCOPY.

The electronic configuration of Cu(II), $t_{2g}^6e_g^3$, is such that the six coordinate complexes it forms tend to deviate from octahedral symmetry. The ligand field is not stabilised significantly under O_h geometry, leading to the formation of distorted species. Most Cu(II) species give rise to a single band in the visible region assigned to the $^2T_{2g}\rightarrow{}^2E_g(O_h)$ transition at approximately 700nm. Due to the geometrical distortions however this band is generally unsymmetrical and quite often has a shoulder.

7.4.2 ABSORPTION AND CIRCULAR DICHROISM SPECTRA.

The absorption spectrum of Cu(II)$L^4H_2.(NO_3)_2$ (fig7.7) displays an asymmetric broad band at ~610nm. The extinction coefficient measured at 36 $mol^{-1}dm^3cm^{-1}$ is quite typical for a Cu(II) ion in a trigonally distorted environment a weak band at 1150nm (ε=8 $mol^{-1}dm^3cm^{-1}$), was also seen. The high energy of the upper band suggests that the d orbital splitting (i.e. $d_{yz,xz} \rightarrow d_{x^2-y^2}$) is large. It is possible that the ligand cavity to metal size match is very good in this case.

The CD spectrum (fig7.7) shows a bisignate couplet corresponding to the high energy transition again suggesting that the overall symmetry of this Cu(II) complex is low.

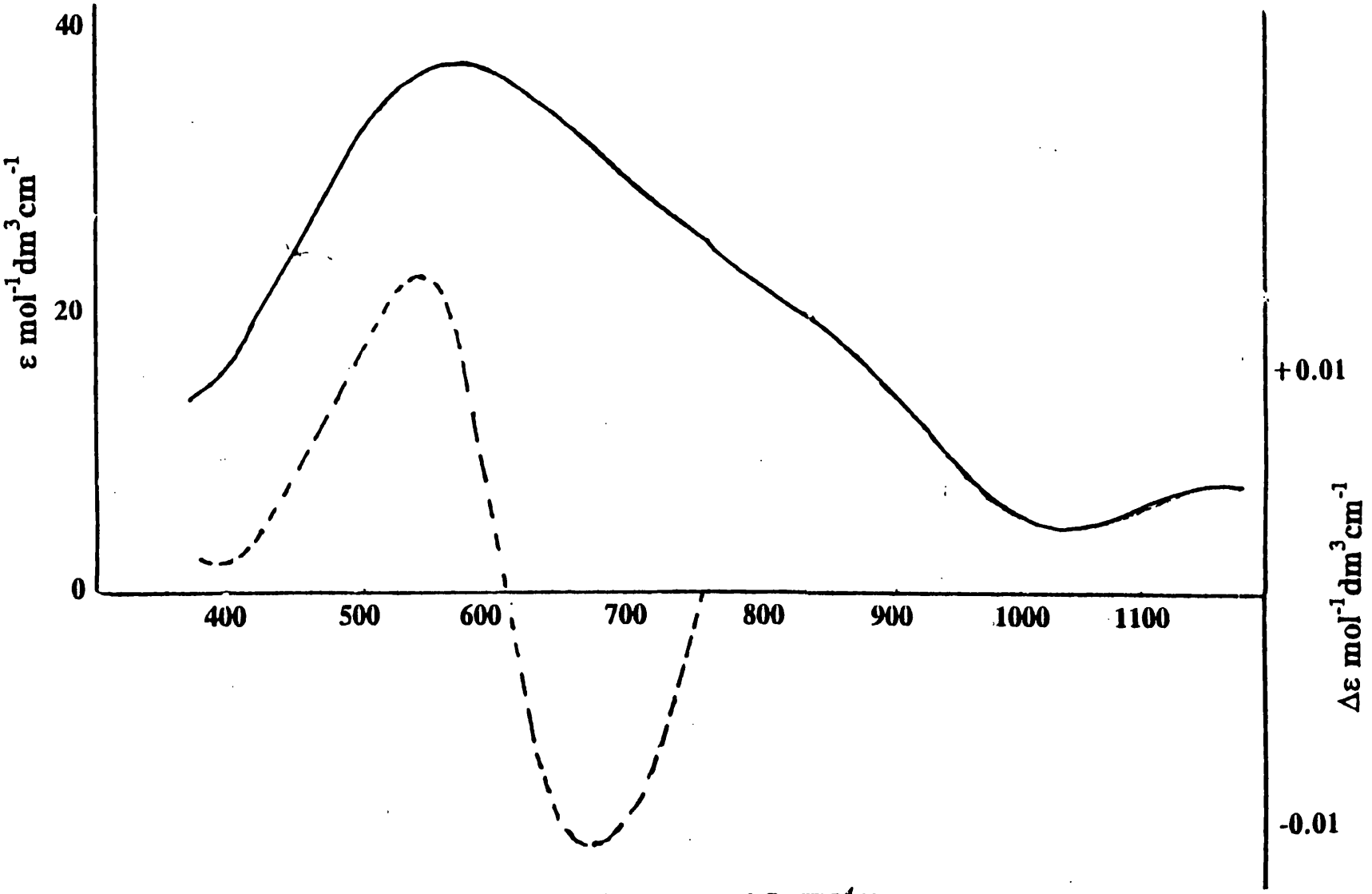

Fig. 7.7. *Absorption / CD spectra of Cu(II)$L^4H_2(NO_3)_2$.*

7.4.3 COMPARISON WITH $[Cu(II)(TACN)_2]^{2+}$.

The electronic spectrum of $[Cu(II)(9\text{-ane}N_3)_2]^{2+}$ bears a strong similarity to that of $Cu(II)L^4H_2(NO_3)_2$. It has two bands at 1230nm and 620nm (**6**). The structure of this compound was believed to show a degree of trigonal distortion. It is a characteristic of six coordinate trigonally distorted compounds to display two bands in the visible and near IR region in their electronic spectrum (**4**).

It is tempting to suggest therefore, that $Cu(II)L^4H_2.(NO_3)_2$ is six coordinate on examination of its electronic spectrum, although it must be noted that five coordinate complexes can have trigonal symmetry and their spectra may resemble those of six coordinate species (**7**).

References.

(1) K.A.Beveridge, A.McAuley and C.Xu, *Inorg. Chem.*, 1991, **30**, 2074.

(2) D.Reinen, A.Ozarowski, B.Jakob, J.Pebler, H.Stratemeier, K.Wieghardt and I.Tolksdorf, *Inorg. Chem.*, 1987, **26**, 4010.

(3) I.A.Fallis, *Ph.D. Thesis*, University of Glasgow, **1992**.

(4) A.B.P.Lever, *Inorganic Electronic Spectroscopy*, (2nd,Ed.); Elsevier, Amsterdam, **1984**.

(5) W.O.Gillum, R.A.D.Wentworth and R.F.Childers, *Inorg.Chem.*, 1970, **9**, 1825.

(6) R.Yang and L.J.Zompa, *Inorg. Chem.*, 1976, **15**, 1499.

(7) B.J.Hathaway and D.E.Billing, *Coord. Chem. Rev.*, 1970, **5**, 143.

CHAPTER 8

GENERAL CONCLUSIONS

The ligand L^1H_3 forms stable complexes with an extremely wide and diverse range of first row transition metal ions.

A remarkable degree of flexibility is shown. L^1H_3 is able to coordinate both small (Mn(IV), 0.53Å) and large (Mn(II), 0.83Å) ions alike.

The geometry of each complex is dictated primarily by the metal ion. Octahedral coordination is displayed when the LFSE requirements are high. With no LFSE, the intramolecular forces of L^1H_3 determine the overall geometry.

Two distinct structural types have been observed with the complexes of L^1H_3.

Monomeric species are formed with divalent metal ions.

In the presence of higher oxidation states, the alcohol pendant groups deprotonate yielding alkoxide donors. These basic groups readily stabilise Mn(III) or Mn(IV) ions and they form hydrogen bonding contacts with protonated subunits giving a dimeric complex.

The dimeric complexes comprise $[Cr(III)L^1H_3L^1Cr(III)]^{3+}$, $[Mn(II)L^1H_3L^1Mn(IV)]^{3+}$ and $[Zn(II)L^1H_3L^1V(IV)]^{3+}$.

The mixed valence and mixed metal compounds show different geometries about each metal centre.

The two examples of trigonal prismatic coordination, namely, $[Zn(II)L^1H_3]^{2+}$ and $[Mn(II)L^1H_3]^{2+}$ are rare for a saturated ligand system.

Many of the previously reported examples have involved unsaturated, highly rigid ligands.

This geometry is believed to be a consequence of several factors. Both metal ions have no preference towards octahedral coordination, they are both large ions and the trigonal prismatic geometry is stabilised by hydrogen bonding within the dimeric structure. No monomeric trigonal prismatic species with L^1H_3 have been isolated.

There is evidence of a π-bonding interaction between the p^{π} and d^{π} (t_{2g}) orbitals on the oxygen donors and metal respectively.

A degree of metal-oxygen bond shortening is displayed when the pendant groups comprise alkoxide donors.

The magnitude of M=O bond character varies in relation to the number of t_{2g} electrons.

In the case of V(IV) d^1, the metal-oxygen bonds are significantly shorter than expected (or can be accounted for by experimental error).

Increasing the occupancy of the t_{2g} set, raises the number of electrons in the π^* levels, reducing the extent of π-bonding. For Co(III), t_{2g}^6, no M=O bond character is observed, the metal-oxygen bonds in this case are essentially single.

Interestingly, the metal-nitrogen distances have been seen to lengthen in correlation to the increase in M=O bond character.

The modified ring system in L^4H_2 has been found to form stable complexes with Co(II), Ni(II) and Co(II). The pendant arms in this case are sterically bulky in order to prevent any dimerisation processes.

The spectroscopic results of these monomeric complexes suggest that the structures of the compounds are trigonally distorted and six coordinate. A degree of tetragonal distortion may be present in the Cu(II) case. The ligand fields are all strong as evidenced by the band positions, indicating that the cavity of L^4H_2 is well suited to coordinating large metal ions.